

# Pythagorean-Hodograph B-Spline Curves

Gudrun Albrecht<sup>a,\*</sup>, Carolina Vittoria Beccari<sup>b</sup>, Jean-Charles Canonne<sup>a</sup>, Lucia Romani<sup>c</sup>

<sup>a</sup>Univ Lille Nord de France, UVHC, LAMAV, FR CNRS 2956, F-59313 Valenciennes, France.

<sup>b</sup>Department of Mathematics, University of Bologna, P.zza Porta San Donato 5, 40127 Bologna, Italy

<sup>c</sup>Department of Mathematics and Applications, University of Milano-Bicocca, Via R. Cozzi 55, 20125 Milano, Italy

---

## Abstract

We introduce the new class of planar Pythagorean-Hodograph (PH) B-Spline curves. They can be seen as a generalization of the well-known class of planar Pythagorean-Hodograph (PH) Bézier curves, presented by R. Farouki and T. Sakkalis in 1990, including the latter ones as special cases. Pythagorean-Hodograph B-Spline curves are non-uniform parametric B-Spline curves whose arc-length is a B-Spline function as well. An important consequence of this special property is that the offsets of Pythagorean-Hodograph B-Spline curves are non-uniform rational B-Spline (NURBS) curves. Thus, although Pythagorean-Hodograph B-Spline curves have fewer degrees of freedom than general B-Spline curves of the same degree, they offer unique advantages for computer-aided design and manufacturing, robotics, motion control, path planning, computer graphics, animation, and related fields. After providing a general definition for this new class of planar parametric curves, we present useful formulae for their construction, discuss their remarkable attractive properties and give some examples of their practical use.

**Keywords:** Plane curve; Non-uniform B-Spline; Pythagorean-Hodograph; Arc-length; Offset;  $G^2/C^1$  Hermite Interpolation

---

## 1. Introduction

The purpose of the present article is to introduce the general concept of Pythagorean-Hodograph (PH) B-Spline curves. On the one hand, B-Spline curves, since their introduction by Schoenberg [21] in 1946 have become the standard for curve representation in all areas where curve design is an issue, see, e.g., [3, 11, 12]. On the other hand, the concept of polynomial PH curves has widely been studied since its introduction by Farouki and Sakkalis in [10]. The essential characteristic of these curves is that the Euclidean norm of their hodograph is also polynomial, thus yielding the useful properties of admitting a closed-form polynomial representation of their arc-length as well as exact rational parameterizations of their offset curves. These polynomial curves are defined over the space of polynomials using its Bernstein basis thus yielding a control point or so-called Bézier representation for them. Rational and spatial counterparts of polynomial PH curves have as well been proposed, and most recently an algebraic-trigonometric counterpart, so-called Algebraic-Trigonometric Pythagorean-Hodograph (ATPH) curves have been introduced in [20].

So far a general theory for B-Spline curves having the PH property is missing. To the best of the authors' knowledge the only partial attempt in this direction has been made in [7], where the problem of determining a B-Spline form of a  $C^2$  PH quintic spline curve interpolating given points is addressed. Prior to this, based on [1, 8] in [19] a relation between a planar  $C^2$  PH quintic spline curve and the control polygon of a related  $C^2$  cubic B-Spline curve is presented.

The present article shows how to construct a general PH B-Spline curve of arbitrary degree, over an arbitrary knot sequence. To this end, we start by defining the complex variable model of a B-Spline curve  $\mathbf{z}(t)$  of degree  $n$ , defined

---

\*Corresponding author.

Email addresses: [gudrun.albrecht@univ-valenciennes.fr](mailto:gudrun.albrecht@univ-valenciennes.fr) (Gudrun Albrecht), [carolina.beccari2@unibo.it](mailto:carolina.beccari2@unibo.it) (Carolina Vittoria Beccari), [jean-charles.canonne@univ-valenciennes.fr](mailto:jean-charles.canonne@univ-valenciennes.fr) (Jean-Charles Canonne), [lucia.romani@unimib.it](mailto:lucia.romani@unimib.it) (Lucia Romani)

over a knot partition  $\mu$ . We then square  $\mathbf{z}(t)$  by using results for the product of normalized B-Spline basis functions from [2, 18]. Here, the determination of the required coefficients involves the solution of linear systems of equations. Finally, the result is integrated in order to obtain the general expression of the PH B-Spline curve, i.e., its B-Spline control points and its knot partition  $\rho$ . General formulae are derived also for the parametric speed, the arc length and the offsets of the resulting curves. The interesting subclasses of *clamped* and *closed* PH B-Spline curves are discussed in great detail. When the degree is 3 and 5, explicit expressions of their control points are given together with the B-Spline representation of the associated arc-length and the rational B-Spline representation of their offsets. Finally, clamped quintic PH B-Spline curves are used to solve a second order Hermite interpolation problem.

The remainder of the paper is organized as follows. In section 2 we recall the basic definition of B-Spline curves as well as the Pythagorean Hodograph (PH) concept, thus defining the notion of a PH B-Spline curve. In section 3, the general construction of PH B-Spline curves is developed (section 3.1), and then adapted to the important particular cases of clamped and closed PH B-Spline curves (section 3.2). In section 4, general formulae for their parametric speed, arc length and offsets are given. Section 5 is devoted to presenting the explicit expressions regarding clamped and closed PH B-Spline curves of degree 3 and 5. Finally, in section 6 we solve a second order Hermite interpolation problem by clamped PH B-Spline curves of degree 5. Conclusions are drawn in section 7.

## 2. Preliminary notions and notation

While a Bézier curve is univocally identified by its degree, a B-Spline curve involves more information, namely an arbitrary number of control points, a knot vector and a degree, which are related by the formula *number of knots - number of control points = degree + 1*. For readers not familiar with B-Spline curves, we first recall the definition of normalized B-Spline basis functions and successively the one of planar B-Spline curve (see, e.g., [12]).

**Definition 1.** Let  $\mu = \{t_i \in \mathbb{R} \mid t_i \leq t_{i+1}\}_{i \in \mathbb{Z}}$  be a sequence of non-decreasing real numbers called knots, and let  $n \in \mathbb{N}$ . The  $i$ -th normalized B-spline basis function of degree  $n$  defined over the knot partition  $\mu$  is the function  $N_{i,\mu}^n(t)$  having support  $[t_i, t_{i+n+1}]$  and defined recursively as

$$N_{i,\mu}^n(t) = \frac{t - t_i}{t_{i+n} - t_i} N_{i,\mu}^{n-1}(t) + \frac{t_{i+n+1} - t}{t_{i+n+1} - t_{i+1}} N_{i+1,\mu}^{n-1}(t),$$

where

$$N_{i,\mu}^0(t) = \begin{cases} 1, & \text{if } t \in [t_i, t_{i+1}) \\ 0, & \text{otherwise} \end{cases}$$

and " $\frac{0}{0} = 0$ ".

**Definition 2.** Let  $m, n \in \mathbb{N}$  with  $m \geq n$ ,  $\mu = \{t_i\}_{i=0, \dots, m+n+1}$  be a finite knot partition, and  $\mathbf{s}_0, \dots, \mathbf{s}_m \in \mathbb{R}^2$ . Then, the planar parametric curve

$$\mathbf{s}(t) = \sum_{i=0}^m \mathbf{s}_i N_{i,\mu}^n(t), \quad t \in [t_n, t_{m+1}],$$

is called a planar B-Spline curve (of degree  $n$  associated with the knot partition  $\mu$ ) with de Boor points or control points  $\mathbf{s}_0, \dots, \mathbf{s}_m$ .

**Remark 1.** If  $M_i$  denotes the multiplicity of the knot  $t_i$ , then  $\mathbf{s}(t)$  is of continuity class  $C^{n-\max_i(M_i)}(t_n, t_{m+1})$ .

If the knot vector  $\mu$  does not have any particular structure, the B-Spline curve  $\mathbf{s}(t)$  will not pass through the first and last control points neither will be tangent to the first and last legs of the control polygon. In this case  $\mathbf{s}(t)$  is simply called *open* B-spline curve. In order to clamp  $\mathbf{s}(t)$  so that it is tangent to the first and the last legs at the first and last control points, respectively (as a Bézier curve does), the multiplicity of the first and the last knot must be adapted. For later use, the precise conditions we use for identifying a clamped B-Spline curve are the following.

**Remark 2.** If  $t_0 = t_1 = \dots = t_n$  and  $t_{m+1} = \dots = t_{m+n+1}$ , then the B-Spline curve  $\mathbf{s}(t)$  given in Definition 2 verifies

$$\mathbf{s}(t_n) = \mathbf{s}_0, \quad \mathbf{s}(t_{m+1}) = \mathbf{s}_m$$

as well as

$$\mathbf{s}'(t_n) = \frac{n}{t_{n+1} - t_1} (\mathbf{s}_1 - \mathbf{s}_0), \quad \mathbf{s}'(t_{m+1}) = \frac{n}{t_{m+n} - t_m} (\mathbf{s}_m - \mathbf{s}_{m-1}),$$

i.e.,  $\mathbf{s}(t)$  is a clamped B-Spline curve. Moreover, if all the knots  $t_{n+1}, \dots, t_m$  are simple, then  $\mathbf{s}(t) \in C^{n-1}(t_n, t_{m+1})$ .

On the other hand, to make the B-Spline curve  $\mathbf{s}(t)$  closed, some knot intervals and control points must be repeated such that the start and the end of the generated curve join together forming a closed loop. The precise conditions to be satisfied by knot intervals and control points in order to get a closed B-Spline curve are recalled in the following.

**Remark 3.** If, in Definition 2 we replace  $m$  by  $m+n$ , consider the knot partition  $\boldsymbol{\mu} = \{t_i\}_{i=0, \dots, m+2n+1}$  with  $t_{m+1+k} - t_{m+k} = t_k - t_{k-1}$  for  $k = 2, \dots, 2n-1$ , assume  $\mathbf{s}_0, \dots, \mathbf{s}_m \in \mathbb{R}^2$  to be distinct control points and  $\mathbf{s}_{m+1} = \mathbf{s}_0, \dots, \mathbf{s}_{m+n} = \mathbf{s}_{n-1}$ , then the B-Spline curve

$$\mathbf{s}(t) = \sum_{i=0}^{m+n} \mathbf{s}_i N_{i, \boldsymbol{\mu}}^n(t), \quad t \in [t_n, t_{m+n+1}],$$

has the additional property

$$\mathbf{s}(t_n) = \mathbf{s}(t_{m+n+1}),$$

i.e.,  $\mathbf{s}(t)$  is a closed B-Spline curve. Moreover, if all the knots  $t_n, \dots, t_{m+n+1}$  are simple, then  $\mathbf{s}(t) \in C^{n-1}[t_n, t_{m+n+1}]$ .

At this point, we have all the required preliminary notions to generalize the definition of Pythagorean-Hodograph Bézier curves (see [10]) to *Pythagorean-Hodograph B-Spline curves*.

**Definition 3.** For  $p, n \in \mathbb{N}$ ,  $p \geq n$ , let  $u(t)$ ,  $v(t)$  and  $w(t)$  be non-zero degree- $n$  spline functions over the knot partition  $\boldsymbol{\mu} = \{t_i\}_{i=0, \dots, p+n+1}$ , i.e., let

$$u(t) = \sum_{i=0}^p u_i N_{i, \boldsymbol{\mu}}^n(t), \quad v(t) = \sum_{i=0}^p v_i N_{i, \boldsymbol{\mu}}^n(t), \quad w(t) = \sum_{i=0}^p w_i N_{i, \boldsymbol{\mu}}^n(t), \quad t \in [t_n, t_{p+1}],$$

with  $u_i, v_i, w_i \in \mathbb{R}$  for all  $i = 0, \dots, p$ , such that  $u(t)$  and  $v(t)$  are non-constant and do not have a non-constant spline function over the partition  $\boldsymbol{\mu}$  as common factor. Then, the planar parametric curve  $(x(t), y(t))$  whose coordinate components have first derivatives of the form

$$x'(t) = w(t)(u^2(t) - v^2(t)) \quad \text{and} \quad y'(t) = 2w(t)u(t)v(t), \quad (1)$$

is called a planar Pythagorean-Hodograph B-Spline curve or a planar PH B-Spline curve of degree  $2n+1$ .

Indeed, as in the case of PH polynomial Bézier curves [9, 10], the parametric speed of the plane curve  $(x(t), y(t))$  is given by

$$\sigma(t) := \sqrt{(x'(t))^2 + (y'(t))^2} = w(t)(u^2(t) + v^2(t)), \quad (2)$$

and its unit tangent, unit normal and (signed) curvature are given respectively by

$$\mathbf{t} = \frac{(u^2 - v^2, 2uv)}{u^2 + v^2}, \quad \mathbf{n} = \frac{(2uv, v^2 - u^2)}{u^2 + v^2}, \quad \kappa = \frac{2(uv' - u'v)}{w(u^2 + v^2)^2}, \quad (3)$$

where, for conciseness, in (3) the parameter  $t$  is omitted.

In the following we will restrict our attention to the so-called *primitive* case  $w(t) = 1$ . Since in this case equation (2) simplifies as  $\sigma(t) = u^2(t) + v^2(t)$ , the primitive case coincides with the *regular* case. In this case, the representation (1) may be obtained by squaring the complex function  $\mathbf{z}(t) = u(t) + iv(t)$  yielding  $\mathbf{z}^2(t) = u^2(t) - v^2(t) + i2u(t)v(t)$ . The coordinate components  $x'(t), y'(t)$  of the hodograph  $\mathbf{r}'(t)$  of the parametric curve  $\mathbf{r}(t) = (x(t), y(t))$  are thus given by the real and imaginary part of  $\mathbf{z}^2(t)$ , respectively. In the remainder of the paper we will exclusively use this complex notation, and we will thus write

$$\mathbf{r}'(t) = x'(t) + iy'(t) = u^2(t) - v^2(t) + i2u(t)v(t) = \mathbf{z}^2(t), \quad (4)$$

as also previously done for planar PH quintics [9, 10]. Since, by construction,  $\mathbf{r}'(t)$  is a degree- $2n$  B-spline curve, then the PH B-Spline curve  $\mathbf{r}(t) = \int \mathbf{r}'(t)dt$  has degree  $2n+1$ . In the next section we will construct the corresponding knot vector and thus know the continuity class of the resulting PH B-Spline curve  $\mathbf{r}(t)$ .

### 3. Construction of Pythagorean–Hodograph B–Spline curves

#### 3.1. The general approach

We start with a knot partition of the form

$$\boldsymbol{\mu} = \{t_i\}_{i=0,\dots,p+n+1} \quad (5)$$

over which a degree- $n$  B-Spline curve

$$\mathbf{z}(t) = u(t) + iv(t)$$

is defined for  $t \in [t_n, t_{p+1}]$ . Thus, according to Definition 2, the planar parametric curve  $\mathbf{z}(t)$  can be written as

$$\mathbf{z}(t) = \sum_{i=0}^p \mathbf{z}_i N_{i,\boldsymbol{\mu}}^n(t), \quad t \in [t_n, t_{p+1}], \quad (6)$$

where  $\mathbf{z}_i = u_i + iv_i$ ,  $i = 0, \dots, p$ . To express the product  $\mathbf{z}^2(t)$  as a B-Spline curve, according to [2, 18], we have to augment the multiplicity of each single knot  $t_i$  to  $n + 1$ . We thus obtain the knot partition

$$\boldsymbol{\nu} = \{s_i\}_{i=0,\dots,(p+n+2)(n+1)-1} = \{< t_i >^{n+1}\}_{i=0,\dots,p+n+1}, \quad (7)$$

where  $< t_i >^k$  denotes a knot  $t_i$  of multiplicity  $k$ . The product  $\mathbf{z}^2(t)$  is thus a degree- $2n$  B-Spline curve over the knot partition  $\boldsymbol{\nu}$ , which can be written in the form

$$\mathbf{p}(t) = \mathbf{z}^2(t) = \sum_{i=0}^p \sum_{j=0}^p \mathbf{z}_i \mathbf{z}_j N_{i,\boldsymbol{\mu}}^n(t) N_{j,\boldsymbol{\mu}}^n(t) = \sum_{k=0}^q \mathbf{p}_k N_{k,\boldsymbol{\nu}}^{2n}(t), \quad (8)$$

with  $q = (n + 1)(p + n)$ , according to Definition 2. Our goal is thus to obtain the explicit expressions of the coefficients  $\mathbf{p}_k$ , for  $k = 0, \dots, q$ . To this end we set  $f_{i,j}(t) := N_{i,\boldsymbol{\mu}}^n(t) N_{j,\boldsymbol{\mu}}^n(t)$  and look for the unknown coefficients  $\boldsymbol{\chi}^{i,j} := (\chi_0^{i,j}, \chi_1^{i,j}, \dots, \chi_q^{i,j})^T$ ,  $i, j = 0, \dots, p$  such that

$$f_{i,j}(t) = \sum_{k=0}^q \chi_k^{i,j} N_{k,\boldsymbol{\nu}}^{2n}(t). \quad (9)$$

For accomplishing this we apply the method from [2] as follows. Let  $\langle \cdot, \cdot \rangle$  be an inner product of the linear space of B-splines of degree  $2n$  with knot vector  $\boldsymbol{\nu}$ . According to [2], for any pair of functions  $a(t)$ ,  $b(t)$  defined over the interval  $[t_0, t_{p+n+1}]$ , we use  $\langle a(t), b(t) \rangle = \int_{t_0}^{t_{p+n+1}} a(t)b(t) dt$  to construct the  $(q + 1) \times (q + 1)$  linear equation system

$$\mathbf{A} \boldsymbol{\chi}^{i,j} = \mathbf{b}^{i,j}, \quad (10)$$

with

$$\mathbf{A} = (a_{k,l})_{k,l=0,\dots,q}, \quad a_{k,l} := \langle N_{k,\boldsymbol{\nu}}^{2n}, N_{l,\boldsymbol{\nu}}^{2n} \rangle = \int_{t_0}^{t_{p+n+1}} N_{k,\boldsymbol{\nu}}^{2n}(t) N_{l,\boldsymbol{\nu}}^{2n}(t) dt$$

and

$$\mathbf{b}^{i,j} = (b_l^{i,j})_{l=0,\dots,q}, \quad b_l^{i,j} := \langle f_{i,j}, N_{l,\boldsymbol{\nu}}^{2n} \rangle = \int_{t_0}^{t_{p+n+1}} f_{i,j}(t) N_{l,\boldsymbol{\nu}}^{2n}(t) dt.$$

Since  $\{N_{k,\boldsymbol{\nu}}^{2n}(t)\}_{k=0,\dots,q}$  are linearly independent, the matrix  $\mathbf{A}$  is a Gramian and therefore nonsingular. This allows us to work out the unknown coefficients  $\{\chi_k^{i,j}\}_{k=0,\dots,q}$  by solving the linear system in (10).

**Remark 4.** Since  $\mathbf{b}^{i,j} = \mathbf{b}^{j,i}$  for all  $i, j = 0, \dots, p$ , then  $\chi^{i,j} = \chi^{j,i}$  for all  $i, j = 0, \dots, p$ . Therefore, the unknown vectors to be obtained from (10) are indeed  $\chi^{i,j}$ ,  $i = 0, \dots, p$ ,  $j = 0, \dots, i$ . Being  $\mathbf{A}$  a non-singular Gramian matrix, all the corresponding linear systems always have a unique solution. Moreover, since  $a_{h,k} = 0$  if  $|h - k| > 2n$ ,  $\mathbf{A}$  is not only symmetric and positive definite, but also of band form. Thus, by applying the Cholesky decomposition algorithm one

can compute the factorization  $\mathbf{A} = \mathbf{L}\mathbf{L}^T$ , where  $\mathbf{L}$  is a lower triangular matrix of the same band form of  $\mathbf{A}$  (i.e. such that  $l_{h,k} = 0$  if  $h - k > 2n$ ). The non-zero elements of  $\mathbf{L}$  may be determined row by row by the formulas

$$\begin{aligned} l_{h,k} &= \left( a_{h,k} - \sum_{s=h-2n}^{h-1} l_{h,s} l_{k,s} \right) / l_{k,k}, \quad k = h - 2n, \dots, h - 1 \\ l_{h,h} &= \left( a_{h,h} - \sum_{s=h-2n}^{h-1} l_{h,s}^2 \right)^{\frac{1}{2}}, \end{aligned}$$

with the convention that  $l_{r,c} = 0$  if  $c \leq 0$  or  $c > r$ . Hence, the solution of each linear system in (10) can be easily obtained by solving the two triangular linear systems  $\mathbf{L}\mathbf{y}^{i,j} = \mathbf{b}^{i,j}$  and  $\mathbf{L}^T\boldsymbol{\chi}^{i,j} = \mathbf{y}^{i,j}$  via the formulas

$$\begin{aligned} y_h^{i,j} &= \left( b_h - \sum_{k=h-2n}^{h-1} l_{h,k} y_k^{i,j} \right) / l_{h,h}, \quad h = 0, \dots, q \\ \chi_h^{i,j} &= \left( y_h^{i,j} - \sum_{k=h+1}^{h+2n} l_{k,h} \chi_k^{i,j} \right) / l_{h,h}, \quad h = 0, \dots, q \end{aligned}$$

where a similar convention as above is adopted with respect to suffices outside the permitted ranges (see [17]).

From the computed expressions of  $\chi_k^{i,j}$ ,  $k = 0, \dots, q$ ,  $0 \leq i, j \leq p$ , we thus get

$$\mathbf{p}(t) = \mathbf{z}^2(t) = \sum_{k=0}^q \sum_{i=0}^p \sum_{j=0}^p \chi_k^{i,j} \mathbf{z}_i \mathbf{z}_j N_{k,\mathbf{v}}^{2n}(t) \quad \text{and} \quad \mathbf{p}_k = \sum_{i=0}^p \sum_{j=0}^p \chi_k^{i,j} \mathbf{z}_i \mathbf{z}_j, \quad k = 0, \dots, q. \quad (11)$$

The resulting PH B-Spline curve  $\mathbf{r}(t)$  is now obtained by integrating  $\mathbf{p}(t)$  as:

$$\mathbf{r}(t) = \int \mathbf{p}(t) dt = \sum_{i=0}^{q+1} \mathbf{r}_i N_{i,\boldsymbol{\rho}}^{2n+1}(t), \quad t \in [t_n, t_{p+1}], \quad (12)$$

where  $\boldsymbol{\rho} = \{s'_i\}_{i=0, \dots, (p+n+2)(n+1)+1}$  with  $s'_i = s_{i-1}$  for  $i = 1, \dots, (p+n+2)(n+1)$ ,  $t_{-1} = s'_0 \leq s'_1$  and  $s'_{(p+n+2)(n+1)+1} = t_{p+n+2}$ , i.e.,

$$\boldsymbol{\rho} = \{t_{-1}, \{< t_k >^{n+1}\}_{k=0, \dots, p+n+1}, t_{p+n+2}\} \quad (13)$$

with the additional knots  $t_{-1}, t_{p+n+2}$ , as well as

$$\mathbf{r}_{i+1} = \mathbf{r}_i + \frac{s'_{i+2n+2} - s'_{i+1}}{2n+1} \mathbf{p}_i = \mathbf{r}_i + \frac{s_{i+2n+1} - s_i}{2n+1} \mathbf{p}_i, \quad (14)$$

for  $i = 0, \dots, q$  and arbitrary  $\mathbf{r}_0$ .

**Remark 5.** Note that, by construction,  $s_{2n} = s'_{2n+1} = t_n$  as well as  $s_{q+1} = s'_{q+2} = t_{p+1}$ , namely the B-spline curves  $\mathbf{z}(t)$ ,  $\mathbf{p}(t)$  and  $\mathbf{r}(t)$  are defined on the same domain. If the knot partition  $\boldsymbol{\mu}$  contains simple inner knots  $t_{n+1}, \dots, t_p$ , then the degree- $n$  spline  $\mathbf{z}(t) \in C^{n-1}(t_n, t_{p+1})$ . As a consequence, the degree- $2n$  spline  $\mathbf{r}'(t) \in C^{n-1}(t_n, t_{p+1})$  and the degree- $(2n+1)$  spline  $\mathbf{r}(t) \in C^n(t_n, t_{p+1})$ .

### 3.2. Construction of clamped and closed PH B-Spline curves

We now consider the conditions for obtaining a clamped, respectively closed, PH B-Spline curve  $\mathbf{r}(t)$ .

**Proposition 1.** Let  $\mathbf{r}(t)$  be the PH B-Spline curve in (12) defined over the knot partition  $\boldsymbol{\rho}$  in (13), where for a clamped, respectively, closed PH B-Spline curve  $\mathbf{r}(t)$  we assume  $p = m$ , respectively,  $p = m + n$ .

a) For  $\mathbf{r}(t)$  to be clamped, i.e., satisfying

$$\begin{aligned} \mathbf{r}(t_n) &= \mathbf{r}_0, \quad \mathbf{r}(t_{m+1}) = \mathbf{r}_{q+1}, \\ \mathbf{r}'(t_n) &= \frac{2n+1}{s'_{2n+2} - s'_1} (\mathbf{r}_1 - \mathbf{r}_0), \quad \mathbf{r}'(t_{m+1}) = \frac{2n+1}{s'_{q+2n+2} - s'_{q+1}} (\mathbf{r}_{q+1} - \mathbf{r}_q), \end{aligned} \quad (15)$$

the following conditions have to be fulfilled

$$\sum_{k=0}^n \mathbf{r}_{(n-1)(n+1)+k+1} B_k^n(\alpha) = \mathbf{r}_0 \quad \text{and} \quad \sum_{k=0}^{n-1} \mathbf{p}_{(n-1)(n+1)+k+1} B_k^{n-1}(\alpha) = \mathbf{p}_0 \quad \text{with} \quad \alpha = \frac{t_n - t_{n-1}}{t_{n+1} - t_{n-1}}, \quad (16)$$

$$\sum_{k=0}^n \mathbf{r}_{m(n+1)+k+1} B_k^n(\beta) = \mathbf{r}_{q+1} \quad \text{and} \quad \sum_{k=0}^{n-1} \mathbf{p}_{m(n+1)+k+1} B_k^{n-1}(\beta) = \mathbf{p}_q \quad \text{with} \quad \beta = \frac{t_{m+1} - t_m}{t_{m+2} - t_m}, \quad (17)$$

where  $B_k^n(t) = \binom{n}{k} t^k (1-t)^{n-k}$ ,  $k = 0, \dots, n$  denote the Bernstein polynomials of degree  $n$ .

b) For  $\mathbf{r}(t)$  to be closed and of continuity class  $C^n$  at the junction point  $\mathbf{r}(t_n) = \mathbf{r}(t_{m+n+1})$ , we require the fulfillment of the conditions

$$\sum_{j=n(n+1)-k}^{(m+n+1)(n+1)-k-1} (s_{j+2n+1} - s_j) \mathbf{p}_j = \mathbf{0}, \quad \text{for} \quad k = 0, \dots, n, \quad (18)$$

and

$$t_{m+1+k} - t_{m+k} = t_k - t_{k-1}, \quad \text{for} \quad k = n, n+1. \quad (19)$$

*Proof.* According to [11] for every degree- $n$  B-Spline curve  $\mathbf{x}(u) = \sum_{i=0}^q \mathbf{x}_i N_{i,\boldsymbol{\mu}}^n(u) \in \mathbb{R}^d$  over the knot partition  $\boldsymbol{\mu} = \{t_i\}_{i=0, \dots, n+q+1}$  there exists a unique multi-affine, symmetric application or blossom  $X : \mathbb{R}^n \rightarrow \mathbb{R}^d$ ,  $(u_1, \dots, u_n) \mapsto X(u_1, \dots, u_n)$  such that  $\mathbf{x}(u) = X(u, \dots, u) = X(\langle u \rangle^n)$ . Its control points are  $\mathbf{x}_i = X(t_{i+1}, \dots, t_{n+i})$ ,  $i = 0, \dots, q$ . Thus, denoting  $P(u_1, \dots, u_{2n})$  the blossom of the curve  $\mathbf{p}(u)$  from (8) over the knot partition  $\boldsymbol{\nu}$  from (7), the control points  $\mathbf{p}_i$  may be written as:

$$\begin{aligned} \mathbf{p}_{k-1} &= P(\langle t_0 \rangle^{n+1-k}, \langle t_1 \rangle^{\min\{n-1+k, n+1\}}, \langle t_2 \rangle^{\max\{k-2, 0\}}), & \text{for } k = 1, \dots, n, \\ \mathbf{p}_{j(n+1)+k-1} &= P(\langle t_j \rangle^{n+1-k}, \langle t_{j+1} \rangle^{\min\{n-1+k, n+1\}}, \langle t_{j+2} \rangle^{\max\{k-2, 0\}}), & \text{for } j = 1, \dots, p+n-1 \text{ and } k = 0, \dots, n, \\ \mathbf{p}_{(p+n)(n+1)+k-1} &= P(\langle t_{p+n} \rangle^{n+1-k}, \langle t_{p+n+1} \rangle^{\min\{n-1+k, n+1\}}), & \text{for } k = 0, 1. \end{aligned}$$

Analogously, denoting  $R(u_1, \dots, u_{2n+1})$  the blossom of the curve  $\mathbf{r}(u)$  from (12) over the knot partition  $\boldsymbol{\rho}$  from (13), the control points  $\mathbf{r}_i$  may be written as

$$\begin{aligned} \mathbf{r}_{j(n+1)+k} &= R(\langle t_j \rangle^{n+1-k}, \langle t_{j+1} \rangle^{\min\{n+k, n+1\}}, \langle t_{j+2} \rangle^{\max\{k-1, 0\}}), & \text{for } j = 0, \dots, p+n-1 \text{ and } k = 0, \dots, n, \\ \mathbf{r}_{(p+n)(n+1)+k} &= R(\langle t_{p+n} \rangle^{n+1-k}, \langle t_{p+n+1} \rangle^{\min\{n+k, n+1\}}), & \text{for } k = 0, 1. \end{aligned}$$

Recalling de Boor's algorithm and the properties of blossoms, the control points involved for calculating a point  $\mathbf{r}(t_j) = R(\langle t_j \rangle^{2n+1})$  are the following:

$$R(\langle t_{j-1} \rangle^n, \langle t_j \rangle^{n+1}) = \mathbf{r}_{j(n+1)-n}, \dots, R(\langle t_j \rangle^{n+1}, \langle t_{j+1} \rangle^n) = \mathbf{r}_{j(n+1)} \quad (20)$$

a) We wish to obtain a clamped curve satisfying conditions (15). In order to satisfy the positional constraints we thus apply de Boor's algorithm for calculating  $\mathbf{r}(t_n)$ , respectively,  $\mathbf{r}(t_{m+1})$  to the control points (20) for  $j = n$ , respectively,  $j = m+1$ . For  $j = n$  we obtain

$$\begin{aligned} R(\langle t_{n-1} \rangle^{n-l}, \langle t_n \rangle^{n+1+k}, \langle t_{n+1} \rangle^{l-k}) &= (1-\alpha) R(\langle t_{n-1} \rangle^{n+1-l}, \langle t_n \rangle^{n+k}, \langle t_{n+1} \rangle^{l-k}) \\ + \alpha R(\langle t_{n-1} \rangle^{n-l}, \langle t_n \rangle^{n+k}, \langle t_{n+1} \rangle^{l+1-k}) & \text{for } k, l = 1, \dots, n. \end{aligned} \quad (21)$$

This yields the following condition for  $\alpha$ , which results thus to be independent of the indices  $k, l$ :

$$(1-\alpha)t_{n-1} + \alpha t_{n+1} = t_n.$$

De Boor's algorithm thus degenerates to de Casteljau's algorithm yielding the first equation of condition (16). The first equation of condition (17) is obtained analogously.

In order to satisfy the tangential constraints of (15), we first note that they are equivalent to the following positional constraints for  $\mathbf{p}(t)$ :  $\mathbf{p}(t_n) = \mathbf{p}_0$ ,  $\mathbf{p}(t_{m+1}) = \mathbf{p}_q$ . We thus apply the same reasoning as above to  $\mathbf{p}(t)$ , and obtain the second equations in (16) and (17).

b) We wish to obtain a closed curve  $\mathbf{r}(t)$  with

$$\mathbf{r}(t_n) = \mathbf{r}(t_{m+n+1}). \quad (22)$$

Recalling de Boor's algorithm and the properties of blossoms the control points involved for calculating a point  $\mathbf{r}(t_j) = R(\langle t_j \rangle^{2n+1})$  are the following:

$$R(\langle t_{j-1} \rangle^n, \langle t_j \rangle^{n+1}) = \mathbf{r}_{j(n+1)-n}, \dots, R(\langle t_j \rangle^{n+1}, \langle t_{j+1} \rangle^n) = \mathbf{r}_{j(n+1)}$$

In order for condition (22) to hold the following points and their corresponding knot intervals thus have to coincide:

$$\mathbf{r}_{n(n+1)-k} = \mathbf{r}_{(m+n+1)(n+1)-k}, \quad \text{for } k = 0, \dots, n, \quad (23)$$

as well as

$$t_{m+1+k} - t_{m+k} = t_k - t_{k-1}, \quad \text{for } k = n, n+1. \quad (24)$$

Setting  $f_j = \frac{s_{j+2n+1} - s_j}{2n+1}$  for  $j = 0, \dots, q$  and considering condition (14), condition (23) is equivalent to

$$\sum_{j=0}^{n(n+1)-k-1} f_j \mathbf{p}_j = \sum_{j=0}^{(m+n+1)(n+1)-k-1} f_j \mathbf{p}_j, \quad \text{for } k = 0, \dots, n,$$

or equivalently

$$\sum_{j=n(n+1)-k}^{(m+n+1)(n+1)-k-1} f_j \mathbf{p}_j = \mathbf{0}, \quad \text{for } k = 0, \dots, n.$$

These conditions also guarantee the maximum possible continuity class at the junction point.  $\square$

In the clamped case of the above proposition we notice that if  $t_{n-1} = t_n$  then  $\alpha = 0$  which yields  $\mathbf{r}(t_n) = \mathbf{r}_{n(n+1)-n}$  and  $\mathbf{p}(t_n) = \mathbf{p}_{n(n+1)-n}$ , and if  $t_{m+1} = t_{m+2}$  then  $\beta = 1$  which yields  $\mathbf{r}(t_{m+1}) = \mathbf{r}_{(m+1)(n+1)}$  and  $\mathbf{p}(t_{m+1}) = \mathbf{p}_{(m+1)(n+1)-1}$ . If in the knot partition  $\boldsymbol{\mu}$  from (5) we have  $t_0 = \dots = t_n$  and  $t_{m+1} = \dots = t_{m+n+1}$ , i.e., if  $\mathbf{z}(t)$  from (6) is a clamped curve itself, the first respectively last  $(n-1)(n+1)+2$  control points of  $\mathbf{r}(t)$  and  $\mathbf{p}(t)$  coincide, i.e.,

$$\mathbf{r}_0 = \dots = \mathbf{r}_{n(n+1)-n} \quad \text{and} \quad \mathbf{r}_{(m+1)(n+1)} = \dots = \mathbf{r}_{(m+n)(n+1)+1}, \quad (25)$$

as well as

$$\mathbf{p}_0 = \dots = \mathbf{p}_{n(n+1)-n} \quad \text{and} \quad \mathbf{p}_{(m+1)(n+1)-1} = \dots = \mathbf{p}_{(m+n)(n+1)}. \quad (26)$$

In this case condition (15) from Proposition 1 a) is automatically satisfied yielding a more intuitive way of obtaining a clamped PH B-Spline curve. In order to simplify the notation we remove redundant knots in the knot partition  $\boldsymbol{\nu}$  from (7) together with the control point multiplicities from (25) and summarize the result in the following Corollary.

**Corollary 1.** Let  $\mathbf{z}(t) = \sum_{i=0}^m \mathbf{z}_i N_{i,\boldsymbol{\mu}}^n(t)$ ,  $t \in [t_n, t_{m+1}]$  be a clamped B-Spline curve over the knot partition

$$\boldsymbol{\mu} = \{ \langle t_n \rangle^{n+1}, \{t_i\}_{i=n+1, \dots, m}, \langle t_{m+1} \rangle^{n+1} \} \quad (27)$$

as in Remark 2. Then,

$$\mathbf{p}(t) = \mathbf{z}^2(t) = \sum_{k=0}^q \mathbf{p}_k N_{k,\boldsymbol{\nu}}^{2n}(t), \quad (28)$$

where  $q = 2n + (n+1)(m-n)$  and

$$\boldsymbol{\nu} = \{s_i\}_{i=0, \dots, 4n+3+(n+1)(m-n)} = \{ \langle t_n \rangle^{2n+1}, \{t_i\}_{i=n+1, \dots, m}, \langle t_{m+1} \rangle^{2n+1} \},$$

as well as

$$\mathbf{r}(t) = \int \mathbf{p}(t) dt = \sum_{i=0}^{q+1} \mathbf{r}_i N_{i,\boldsymbol{\rho}}^{2n+1}(t), \quad t \in [t_n, t_{m+1}]$$

where  $\boldsymbol{\rho} = \{s'_i\}_{i=0, \dots, 4n+3+(n+1)(m-n)}$  with  $s'_i = s_{i-1}$  for  $i = 1, \dots, 4n+2 + (n+1)(m-n)$ ,  $s'_0 = s'_1$  and  $s'_{4n+3+(n+1)(m-n)} = s'_{4n+2+(n+1)(m-n)}$ , i.e.,

$$\boldsymbol{\rho} = \{ \langle t_n \rangle^{2n+2}, \{t_i\}_{i=n+1, \dots, m}, \langle t_{m+1} \rangle^{2n+2} \}, \quad (29)$$

and the control points  $\mathbf{r}_i$  satisfy (14).



*Proof.* The result is obtained by removing  $(n-1)(n+1)+1$  of the multiple control points from (25) together with  $n^2$  of the multiple knots of  $\nu$  from (7) at the beginning and at the end. The same result is obtained by proceeding with the general construction of the PH B-Spline curve starting with a clamped B-Spline curve over the knot partition  $\mu$  from (27).  $\square$

In this way, in both cases (the clamped and the closed one), the resulting PH B-Spline curve is of degree  $2n+1$  and of continuity class  $C^n$ . For example, for  $n=1$  we obtain PH B-Spline curves of degree 3 and continuity class  $C^1$ , while for  $n=2$  we have PH B-Spline curves of degree 5 and continuity class  $C^2$ .

#### 4. Parametric speed, arc length and offsets

According to (2), the parametric speed of the regular PH curve  $\mathbf{r}(t) = x(t) + iy(t)$  is given by

$$\sigma(t) = |\mathbf{r}'(t)| = |\mathbf{z}'(t)| = \mathbf{z}(t) \bar{\mathbf{z}}(t).$$

Exploiting (6) we thus obtain

$$\sigma(t) = \sum_{i=0}^p \sum_{j=0}^p \mathbf{z}_i \bar{\mathbf{z}}_j N_{i,\mu}^n(t) N_{j,\mu}^n(t) = \sum_{k=0}^q \sigma_k N_{k,\nu}^{2n}(t), \quad (30)$$

where

$$\sigma_k = \sum_{i=0}^p \sum_{j=0}^p \chi_k^{i,j} \mathbf{z}_i \bar{\mathbf{z}}_j \quad (31)$$

in analogy to (11).

##### 4.1. Arc-length

The arc length of the PH B-Spline curve is thus obtained as

$$\int \sigma(t) dt = \sum_{i=0}^{q+1} l_i N_{i,\rho}^{2n+1}(t), \quad t \in [t_n, t_{p+1}], \quad (32)$$

where

$$l_{i+1} = l_i + \frac{s'_{i+2n+2} - s'_{i+1}}{2n+1} \sigma_i = l_i + \frac{s_{i+2n+1} - s_i}{2n+1} \sigma_i, \quad (33)$$

with  $l_0 = 0$ . The cumulative arc length is given by

$$\ell(\xi) = \int_{t_n}^{\xi} \sigma(t) dt = \sum_{i=0}^{q+1} l_i (N_{i,\rho}^{2n+1}(\xi) - N_{i,\rho}^{2n+1}(t_n))$$

and the curve's total arc length thus is

$$L = \ell(t_{p+1}) = \int_{t_n}^{t_{p+1}} \sigma(t) dt = \sum_{i=0}^{q+1} l_i (N_{i,\rho}^{2n+1}(t_{p+1}) - N_{i,\rho}^{2n+1}(t_n)). \quad (34)$$

This general formula simplifies in the clamped and closed cases as follows. In the clamped case for the knot partition  $\rho$  from (29) we notice that

$$N_{i,\rho}^{2n+1}(t_n) = \begin{cases} 1, & \text{if } i = 0 \\ 0, & \text{else} \end{cases}$$

and

$$N_{i,\rho}^{2n+1}(t_{m+1}) = \begin{cases} 1, & \text{if } i = 2n+1 + (n+1)(m-n) \\ 0, & \text{else.} \end{cases}$$



Considering  $l_0 = 0$  and recalling Corollary 1, in the clamped case the total arc length  $L$  in (34) thus becomes

$$L = l_{2n+1+(n+1)(m-n)}. \quad (35)$$

Due to the structure of the knot partition  $\boldsymbol{\rho}$  in (13), we notice that

$$N_{i,\boldsymbol{\rho}}^{2n+1}(t_n) \begin{cases} \neq 0, & \text{if } (n-1)(n+1) < i < n(n+1) + 1 \\ = 0, & \text{else} \end{cases}$$

and

$$N_{i,\boldsymbol{\rho}}^{2n+1}(t_{p+1}) \begin{cases} \neq 0, & \text{if } p(n+1) < i < (p+1)(n+1) + 1 \\ = 0, & \text{else.} \end{cases}$$

In this case the total arc length  $L$  from (34) thus becomes

$$\begin{aligned} L &= \sum_{i=p(n+1)+1}^{(p+1)(n+1)} l_i N_{i,\boldsymbol{\rho}}^{2n+1}(t_{p+1}) - \sum_{i=(n-1)(n+1)+1}^{n(n+1)} l_i N_{i,\boldsymbol{\rho}}^{2n+1}(t_n) \\ &= \sum_{k=0}^n \left( l_{p(n+1)+1+k} N_{p(n+1)+1+k,\boldsymbol{\rho}}^{2n+1}(t_{p+1}) - l_{(n-1)(n+1)+1+k} N_{(n-1)(n+1)+1+k,\boldsymbol{\rho}}^{2n+1}(t_n) \right). \end{aligned} \quad (36)$$

In the case of a closed curve from Proposition 1 b) we have  $p = m + n$  and conditions (19). On the knot partition  $\boldsymbol{\rho}$  from (13) the normalized B-Spline basis functions having as support  $[t_{n-1}, t_{n+1}]$  are  $N_{i,\boldsymbol{\rho}}^{2n+1}(t)$  for  $i = (n-1)(n+1) + 1, \dots, n(n+1)$ , and those having as support  $[t_{m+n}, t_{m+n+2}]$  are  $N_{i,\boldsymbol{\rho}}^{2n+1}(t)$  for  $i = (m+n)(n+1) + 1, \dots, (m+n+1)(n+1)$ . With conditions (19) this means

$$N_{(n-1)(n+1)+1+k,\boldsymbol{\rho}}^{2n+1}(t_n) = N_{(m+n)(n+1)+1+k,\boldsymbol{\rho}}^{2n+1}(t_{m+n+1}), \quad \text{for } k = 0, \dots, n.$$

In the case of a closed curve its total arc length  $L$  from (36) thus reads

$$L = \sum_{k=0}^n \left( l_{p(n+1)+1+k} - l_{(n-1)(n+1)+1+k} \right) N_{(n-1)(n+1)+1+k,\boldsymbol{\rho}}^{2n+1}(t_n), \quad (37)$$

which, by taking into account (33), becomes

$$L = \sum_{k=0}^n \left( \sum_{j=(n-1)(n+1)+k+1}^{(m+n)(n+1)+k} \frac{s_{j+2n+1} - s_j}{2n+1} \sigma_j \right) N_{(n-1)(n+1)+1+k,\boldsymbol{\rho}}^{2n+1}(t_n). \quad (38)$$

#### 4.2. Offsets

The offset curve  $\mathbf{r}_h(t)$  at (signed) distance  $h$  of a PH B-Spline curve  $\mathbf{r}(t)$  is the locus defined by

$$\mathbf{r}_h(t) = \mathbf{r}(t) + h \mathbf{n}(t)$$

where

$$\mathbf{n}(t) = \frac{(y'(t), -x'(t))}{\sqrt{(x'(t))^2 + (y'(t))^2}} = \frac{-i\mathbf{r}'(t)}{\sigma(t)} = \frac{-i\mathbf{z}^2(t)}{\sigma(t)}.$$

(Note that, since we are dealing with the regular case,  $\sigma(t) \neq 0$  and the offset curve is always well defined.) Thus

$$\mathbf{r}_h(t) = \frac{\sigma(t)\mathbf{r}(t) - i h \mathbf{z}^2(t)}{\sigma(t)}.$$

Herein the product  $\sigma(t)\mathbf{r}(t)$  reads as

$$\sigma(t)\mathbf{r}(t) = \sum_{i=0}^{q+1} \sum_{j=0}^q \sigma_j \mathbf{r}_i N_{i,\boldsymbol{\rho}}^{2n+1}(t) N_{j,\boldsymbol{\nu}}^{2n}(t).$$

Again, according to [2, 18], we can write

$$N_{i,\boldsymbol{\rho}}^{2n+1}(t)N_{j,\boldsymbol{\nu}}^{2n}(t) = \sum_{k=0}^w \zeta_k^{i,j} N_{k,\boldsymbol{\tau}}^{4n+1}(t) \quad (39)$$

with the knot partition

$$\boldsymbol{\tau} = \{ \langle t_{-1} \rangle^{2n+1}, \{ \langle t_k \rangle^{3n+2} \}_{k=0,\dots,p+n+1}, \langle t_{p+n+2} \rangle^{2n+1} \} \quad (40)$$

and

$$w = (3n+2)(p+n+2) - 1. \quad (41)$$

**Remark 6.** In the clamped case, from Corollary 1 we obtain

$$\boldsymbol{\tau} = \{ \langle t_n \rangle^{4n+2}, \{ \langle t_k \rangle^{3n+2} \}_{k=n+1,\dots,m}, \langle t_{m+1} \rangle^{4n+2} \} \quad (42)$$

and

$$w = 4n+1 + (m-n)(3n+2). \quad (43)$$

Differently, in the closed case, we have

$$\boldsymbol{\tau} = \{ \langle t_{-1} \rangle^{2n+1}, \{ \langle t_k \rangle^{3n+2} \}_{k=0,\dots,m+2n+1}, \langle t_{m+2n+2} \rangle^{2n+1} \} \quad (44)$$

and

$$w = (3n+2)(m+2n+2) - 1. \quad (45)$$

To work out the unknown coefficients  $\boldsymbol{\zeta}^{i,j} := (\zeta_0^{i,j}, \zeta_1^{i,j}, \dots, \zeta_w^{i,j})^T$  in (39) we solve the linear system

$$\mathbf{C}\boldsymbol{\zeta}^{i,j} = \mathbf{e}^{i,j}, \quad (46)$$

with

$$\mathbf{C} = (c_{k,h})_{k,h=0,\dots,w}, \quad c_{k,h} := \langle N_{k,\boldsymbol{\tau}}^{4n+1}, N_{h,\boldsymbol{\tau}}^{4n+1} \rangle = \int_{t_0}^{t_{p+n+1}} N_{k,\boldsymbol{\tau}}^{4n+1}(t) N_{h,\boldsymbol{\tau}}^{4n+1}(t) dt$$

and

$$\mathbf{e}^{i,j} = (e_h^{i,j})_{h=0,\dots,w}, \quad e_h^{i,j} := \langle g_{i,j}, N_{h,\boldsymbol{\tau}}^{4n+1} \rangle = \int_{t_0}^{t_{p+n+1}} g_{i,j}(t) N_{h,\boldsymbol{\tau}}^{4n+1}(t) dt \quad \text{where} \quad g_{i,j}(t) := N_{i,\boldsymbol{\rho}}^{2n+1}(t) N_{j,\boldsymbol{\nu}}^{2n}(t).$$

Like in the previous case,  $\mathbf{C}$  is a banded Gramian, and thus nonsingular. This guarantees that each of the linear systems in (46) has a unique solution that can be efficiently computed by means of the Cholesky decomposition algorithm for symmetric positive definite band matrices.

The computed expressions of  $\zeta_k^{i,j}$ ,  $k = 0, \dots, w$ ,  $i = 0, \dots, q+1$ ,  $j = 0, \dots, q$  thus yield

$$\sigma(t)\mathbf{r}(t) = \sum_{k=0}^w \sum_{i=0}^{q+1} \sum_{j=0}^q \zeta_k^{i,j} \sigma_j \mathbf{r}_i N_{k,\boldsymbol{\tau}}^{4n+1}(t).$$

By writing

$$\mathbf{p}(t) = \mathbf{p}(t) \cdot \mathbf{1} = \left( \sum_{j=0}^q \mathbf{p}_j N_{j,\boldsymbol{\nu}}^{2n}(t) \right) \left( \sum_{i=0}^{q+1} N_{i,\boldsymbol{\rho}}^{2n+1}(t) \right)$$

and

$$\sigma(t) = \sigma(t) \cdot \mathbf{1} = \left( \sum_{j=0}^q \sigma_j N_{j,\boldsymbol{\nu}}^{2n}(t) \right) \left( \sum_{i=0}^{q+1} N_{i,\boldsymbol{\rho}}^{2n+1}(t) \right),$$

we thus obtain

$$\mathbf{p}(t) = \sum_{k=0}^w \sum_{i=0}^{q+1} \sum_{j=0}^q \zeta_k^{i,j} \mathbf{p}_j N_{k,\boldsymbol{\tau}}^{4n+1}(t)$$

$$\sigma(t) = \sum_{k=0}^w \sum_{i=0}^{q+1} \sum_{j=0}^q \zeta_k^{i,j} \sigma_j N_{k,\tau}^{4n+1}(t).$$

The offset curve  $\mathbf{r}_h(t)$  finally has the form

$$\mathbf{r}_h(t) = \frac{\sum_{k=0}^w \mathbf{q}_k N_{k,\tau}^{4n+1}(t)}{\sum_{k=0}^w \gamma_k N_{k,\tau}^{4n+1}(t)}, \quad (47)$$

where, for  $k = 0, \dots, w$ ,

$$\mathbf{q}_k = \sum_{i=0}^{q+1} \sum_{j=0}^q (\sigma_j \mathbf{r}_i - i h \mathbf{p}_j) \zeta_k^{i,j} \quad (48)$$

and

$$\gamma_k = \sum_{i=0}^{q+1} \sum_{j=0}^q \sigma_j \zeta_k^{i,j}. \quad (49)$$

## 5. General explicit formulas for the cubic and quintic case

### 5.1. Clamped cubic PH B-Splines ( $n = 1$ )

Let  $m \in \mathbb{N}$ ,  $m \geq 1$ . For a general knot vector  $\boldsymbol{\mu} = \{\langle 0 \rangle^2 < t_2 < \dots < t_m < \langle t_{m+1} \rangle^2\}$  satisfying the constraints  $t_0 = t_1 = 0$  and  $t_{m+1} = t_{m+2}$  (see Figure 1 first row), by applying the above method we construct the knot partitions

$$\begin{aligned} \mathbf{v} &= \{\langle 0 \rangle^3 < \langle t_2 \rangle^2 < \dots < \langle t_m \rangle^2 < \langle t_{m+1} \rangle^3\}, \\ \boldsymbol{\rho} &= \{\langle 0 \rangle^4 < \langle t_2 \rangle^2 < \dots < \langle t_m \rangle^2 < \langle t_{m+1} \rangle^4\}, \\ \boldsymbol{\tau} &= \{\langle 0 \rangle^6 < \langle t_2 \rangle^5 < \dots < \langle t_m \rangle^5 < \langle t_{m+1} \rangle^6\}, \end{aligned}$$

illustrated in Figure 1. Then, by solving the linear systems (10) we calculate the coefficients  $\chi_k^{i,j}$ ,  $0 \leq i, j \leq m$ ,  $0 \leq k \leq 2m$ . All of them turn out to be zero with the exception of

$$\begin{aligned} \chi_{2k}^{k,k} &= 1, \quad k = 0, \dots, m, \\ \chi_{2k+1}^{k,k+1} &= \chi_{2k+1}^{k+1,k} = \frac{1}{2}, \quad k = 0, \dots, m-1. \end{aligned} \quad (50)$$

In addition, we compute the coefficients  $\zeta_k^{i,j}$ ,  $0 \leq i \leq 2m+1$ ,  $0 \leq j \leq 2m$ ,  $0 \leq k \leq 5m$  as the solutions to the linear systems (46). All of them turn out to be zero with the exception of

$$\begin{aligned} \zeta_{5k}^{2k,2k} &= \frac{d_{k+1}}{D_k}, \quad \zeta_{5k}^{2k+1,2k} = \frac{d_k}{D_k}, \quad k = 0, \dots, m, \\ \zeta_{5k+1}^{2k,2k+1} &= \frac{2d_{k+1}}{5D_k}, \quad \zeta_{5k+1}^{2k+1,2k} = \frac{3}{5}, \quad \zeta_{5k+1}^{2k+1,2k+1} = \frac{2d_k}{5D_k}, \quad k = 0, \dots, m-1, \\ \zeta_{5k+2}^{2k,2k+2} &= \frac{d_{k+1}}{10D_k}, \quad \zeta_{5k+2}^{2k+1,2k+1} = \frac{3}{5}, \quad \zeta_{5k+2}^{2k+1,2k+2} = \frac{d_k}{10D_k}, \quad \zeta_{5k+2}^{2k+2,2k} = \frac{3}{10}, \quad k = 0, \dots, m-1, \\ \zeta_{5k+3}^{2k+1,2k+2} &= \frac{3}{10}, \quad \zeta_{5k+3}^{2k+2,2k} = \frac{d_{k+2}}{10D_{k+1}}, \quad \zeta_{5k+3}^{2k+2,2k+1} = \frac{3}{5}, \quad \zeta_{5k+3}^{2k+3,2k} = \frac{d_{k+1}}{10D_{k+1}}, \quad k = 0, \dots, m-1, \\ \zeta_{5k+4}^{2k+2,2k+1} &= \frac{2d_{k+2}}{5D_{k+1}}, \quad \zeta_{5k+4}^{2k+2,2k+2} = \frac{3}{5}, \quad \zeta_{5k+4}^{2k+3,2k+1} = \frac{2d_{k+1}}{5D_{k+1}}, \quad k = 0, \dots, m-1, \end{aligned} \quad (51)$$

where  $D_k := d_k + d_{k+1}$ ,  $k = 0, \dots, m$  and  $d_0 = d_{m+1} := 0$ .

By means of the computed coefficients  $\{\chi_k^{i,j}\}_{0 \leq i, j \leq m}$  we can thus shortly write the control points of  $\mathbf{r}'(t)$  as

$$\begin{aligned} \mathbf{p}_{2k} &= \mathbf{z}_k^2, \quad k = 0, \dots, m, \\ \mathbf{p}_{2k+1} &= \mathbf{z}_k \mathbf{z}_{k+1}, \quad k = 0, \dots, m-1, \end{aligned}$$

and the coefficients of the parametric speed  $\sigma(t)$  as

$$\begin{aligned} \sigma_{2k} &= \mathbf{z}_k \bar{\mathbf{z}}_k, \quad k = 0, \dots, m, \\ \sigma_{2k+1} &= \frac{1}{2} (\mathbf{z}_k \bar{\mathbf{z}}_{k+1} + \mathbf{z}_{k+1} \bar{\mathbf{z}}_k), \quad k = 0, \dots, m-1. \end{aligned}$$

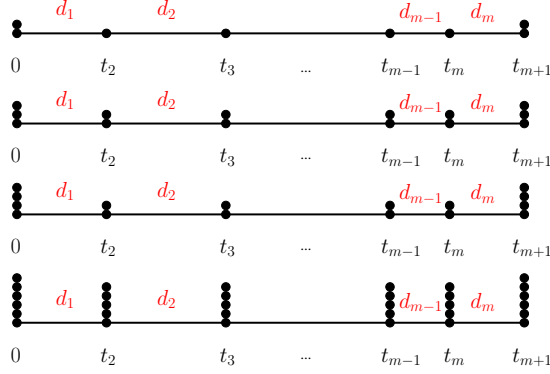


Figure 1: Knot partitions for the clamped case  $n = 1$ . From top to bottom:  $\mu, \nu, \rho, \tau$ .

Thus, according to (12), the clamped cubic PH B-Spline curve defined over the knot partition  $\rho$  is given by

$$\mathbf{r}(t) = \sum_{i=0}^{2m+1} \mathbf{r}_i N_{i,\rho}^3(t), \quad t \in [t_1, t_{m+1}] \quad (t_1 = 0),$$

with control points

$$\begin{aligned} \mathbf{r}_1 &= \mathbf{r}_0 + \frac{d_1}{3} \mathbf{z}_0^2, \\ \mathbf{r}_{2i+2} &= \mathbf{r}_{2i+1} + \frac{d_{i+1}}{3} \mathbf{z}_i \mathbf{z}_{i+1}, \quad i = 0, \dots, m-1, \\ \mathbf{r}_{2i+3} &= \mathbf{r}_{2i+2} + \frac{d_{i+1} + d_{i+2}}{3} \mathbf{z}_{i+1}^2, \quad i = 0, \dots, m-2, \\ \mathbf{r}_{2m+1} &= \mathbf{r}_{2m} + \frac{d_m}{3} \mathbf{z}_m^2, \end{aligned}$$

and arbitrary  $\mathbf{r}_0$ .

**Remark 7.** Note that, when  $m = 1$  and  $t_2 = t_3 = 1$ , the expressions of the control points coincide with those of Farouki's PH Bézier cubic from [4, 10].

According to (35) the total arc length of the clamped PH B-Spline curve of degree 3 is given by  $L = l_{2m+1}$ , where

$$\begin{aligned} l_0 &= 0, \\ l_1 &= l_0 + \frac{d_1}{3} \mathbf{z}_0 \bar{\mathbf{z}}_0, \\ l_{2i+2} &= l_{2i+1} + \frac{d_{i+1}}{6} (\mathbf{z}_i \bar{\mathbf{z}}_{i+1} + \mathbf{z}_{i+1} \bar{\mathbf{z}}_i), \quad i = 0, \dots, m-1, \\ l_{2i+3} &= l_{2i+2} + \frac{d_{i+1} + d_{i+2}}{3} \mathbf{z}_{i+1} \bar{\mathbf{z}}_{i+1}, \quad i = 0, \dots, m-2, \\ l_{2m+1} &= l_{2m} + \frac{d_m}{3} \mathbf{z}_m \bar{\mathbf{z}}_m. \end{aligned}$$

Over the knot partition  $\tau$ , the offset curve  $\mathbf{r}_h(t)$  has the rational B-Spline form

$$\mathbf{r}_h(t) = \frac{\sum_{k=0}^{5m} \mathbf{q}_k N_{k,\tau}^5(t)}{\sum_{k=0}^{5m} \gamma_k N_{k,\tau}^5(t)}, \quad t \in [t_1, t_{m+1}], \quad (52)$$

where, by exploiting the explicit expressions of the coefficients  $\{\zeta_k^{i,j}\}_{0 \leq i \leq 2m+1, 0 \leq j \leq 2m, 0 \leq k \leq 5m}$  from (51), weights and control points can easily be obtained; they are reported in the Appendix.

Some examples of clamped cubic PH B-Spline curves are shown in Figure 2, and their offsets are displayed in Figure 3.

### 5.2. Clamped quintic PH B-Splines ( $n = 2$ )

Let  $m \in \mathbb{N}$ ,  $m \geq 2$ . For a general knot vector  $\mu = \{\langle 0 \rangle^3 < t_3 < \dots < t_m < \langle t_{m+1} \rangle^3\}$  satisfying the constraints  $t_0 = t_1 = t_2 = 0$  and  $t_{m+1} = t_{m+2} = t_{m+3}$  (see Figure 4 first row), by applying the above method we construct the knot

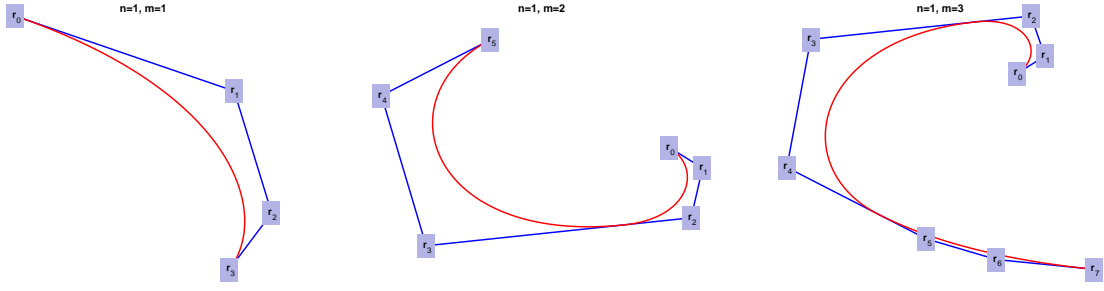


Figure 2: Clamped cubic PH B-Spline curves with:  $m = 1$  (left),  $m = 2$  (center) and  $m = 3$  (right).

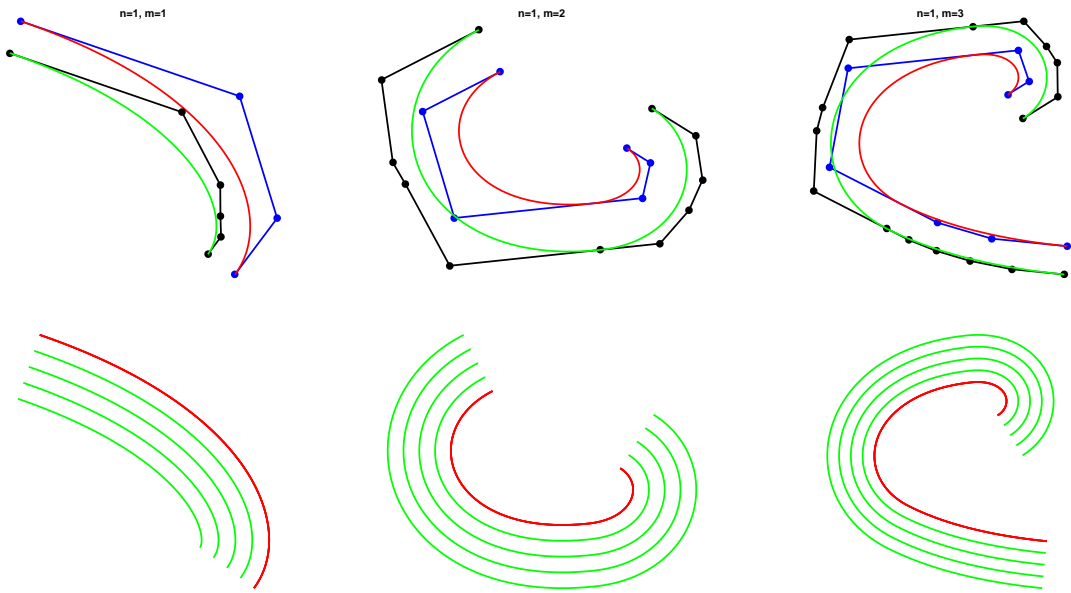


Figure 3: Offsets of clamped cubic PH B-Spline curves from Figure 2 with (1. row) and without (2. row) control polygon where:  $m = 1$  (left column),  $m = 2$  (center column) and  $m = 3$  (right column).

partitions

$$\begin{aligned}
 \nu &= \{\langle 0 \rangle^5 < \langle t_3 \rangle^3 < \dots < \langle t_m \rangle^3 < \langle t_{m+1} \rangle^5\}, \\
 \rho &= \{\langle 0 \rangle^6 < \langle t_3 \rangle^3 < \dots < \langle t_m \rangle^3 < \langle t_{m+1} \rangle^6\}, \\
 \tau &= \{\langle 0 \rangle^{10} < \langle t_3 \rangle^8 < \dots < \langle t_m \rangle^8 < \langle t_{m+1} \rangle^{10}\},
 \end{aligned} \tag{53}$$

illustrated in Figure 4. Then, by solving the linear systems (10) we calculate the coefficients  $\chi_k^{i,j}$ ,  $0 \leq i, j \leq m$ ,  $0 \leq k \leq 3m - 2$ . All of them turn out to be zero with the exception of

$$\begin{aligned}
\chi_0^{0,0} &= 1, \\
\chi_1^{0,1} &= \chi_1^{1,0} = \frac{1}{2}, \\
\chi_{3k-1}^{k-1,k} &= \chi_{3k-1}^{k,k-1} = \frac{1}{6} \frac{d_k d_{k+1}}{(d_{k-1}+d_k)(d_k+d_{k+1})}, \quad k = 1, \dots, m-1, \\
\chi_{3k-1}^{k-1,k+1} &= \chi_{3k-1}^{k+1,k-1} = \frac{1}{6} \frac{(d_k)^2}{(d_{k-1}+d_k)(d_k+d_{k+1})}, \quad k = 1, \dots, m-1, \\
\chi_{3k-1}^{k,k} &= \frac{2}{3} + \frac{1}{3} \frac{d_{k-1} d_{k+1}}{(d_{k-1}+d_k)(d_k+d_{k+1})}, \quad k = 1, \dots, m-1, \\
\chi_{3k-1}^{k,k+1} &= \chi_{3k-1}^{k+1,k} = \frac{1}{6} \frac{d_{k-1} d_k}{(d_{k-1}+d_k)(d_k+d_{k+1})}, \quad k = 1, \dots, m-1, \\
\chi_{3k}^{k,k} &= \frac{d_{k+1}}{d_k+d_{k+1}}, \quad k = 1, \dots, m-2, \\
\chi_{3k}^{k,k+1} &= \chi_{3k}^{k+1,k} = \frac{1}{2} \frac{d_k}{d_k+d_{k+1}}, \quad k = 1, \dots, m-2, \\
\chi_{3k+1}^{k,k+1} &= \chi_{3k+1}^{k+1,k} = \frac{1}{2} \frac{d_{k+1}}{d_k+d_{k+1}}, \quad k = 1, \dots, m-2, \\
\chi_{3k+1}^{k+1,k+1} &= \frac{d_k}{d_k+d_{k+1}}, \quad k = 1, \dots, m-2, \\
\chi_{3m-3}^{m-1,m} &= \chi_{3m-3}^{m,m-1} = \frac{1}{2}, \\
\chi_{3m-2}^{m,m} &= 1,
\end{aligned}$$

where  $d_k = t_{k+2} - t_{k+1}$ ,  $k = 1, \dots, m-1$  and  $d_0 = d_m = 0$ .

In addition, we compute the coefficients  $\zeta_k^{i,j}$ ,  $0 \leq i \leq 3m-1$ ,  $0 \leq j \leq 3m-2$ ,  $0 \leq k \leq 8m-7$  as the solutions to the linear systems (46). All of them turn out to be zero with the exception of

$$\begin{aligned}
\zeta_{8k}^{3k,3k} &= \frac{d_{k+1}^2}{D_k^2}, \quad \zeta_{8k}^{3k+1,3k} = \frac{13d_k d_{k+1}}{9D_k^2}, \quad \zeta_{8k}^{3k+2,3k} = \frac{4d_k^2}{9D_k^2}, \quad \zeta_{8k}^{3k,3k+1} = \frac{5d_k d_{k+1}}{9D_k^2}, \quad \zeta_{8k}^{3k+1,3k+1} = \frac{5d_k^2}{9D_k^2}, \quad k = 0, \dots, m-1, \\
\zeta_{8k+1}^{3k+1,3k} &= \frac{5d_{k+1}^2}{9D_k^2}, \quad \zeta_{8k+1}^{3k+2,3k} = \frac{5d_k d_{k+1}}{9D_k^2}, \quad \zeta_{8k+1}^{3k+1,3k+1} = \frac{13d_k d_{k+1}}{9D_k^2}, \quad \zeta_{8k+1}^{3k+2,3k+1} = \frac{d_k^2}{D_k^2}, \quad \zeta_{8k+1}^{3k,3k+1} = \frac{4d_{k+1}^2}{9D_k^2}, \quad k = 0, \dots, m-1, \\
\zeta_{8k+2}^{3k,3k+2} &= \frac{d_{k+1}^2}{6D_k^2}, \quad \zeta_{8k+2}^{3k+1,3k+2} = \frac{d_k d_{k+1}}{3D_k^2}, \quad \zeta_{8k+2}^{3k+2,3k+2} = \frac{d_k^2}{6D_k^2}, \quad \zeta_{8k+2}^{3k+1,3k+1} = \frac{5d_{k+1}}{9D_k}, \\
\zeta_{8k+2}^{3k+2,3k+1} &= \frac{15d_k}{18D_k}, \quad \zeta_{8k+2}^{3k+2,3k} = \frac{5d_{k+1}}{18D_k}, \quad k = 0, \dots, m-2, \\
\zeta_{8k+3}^{3k,3k+3} &= \frac{d_{k+1}^2}{21D_k^2}, \quad \zeta_{8k+3}^{3k+1,3k+3} = \frac{2d_k d_{k+1}}{21D_k^2}, \quad \zeta_{8k+3}^{3k+2,3k+3} = \frac{d_k^2}{21D_k^2}, \quad \zeta_{8k+3}^{3k+1,3k+2} = \frac{5d_{k+1}}{14D_k}, \quad \zeta_{8k+3}^{3k+2,3k+2} = \frac{5d_k}{14D_k}, \\
\zeta_{8k+3}^{3k+2,3k+1} &= \frac{10}{21}, \quad \zeta_{8k+3}^{3k+3,3k+1} = \frac{5d_k}{42D_k}, \quad \zeta_{8k+3}^{3k+3,3k} = \frac{5d_{k+1}}{42D_k}, \quad k = 0, \dots, m-2, \\
\zeta_{8k+4}^{3k,3k+4} &= \frac{d_{k+1}^3}{126D_k^2 D_{k+1}}, \quad \zeta_{8k+4}^{3k+1,3k+4} = \frac{d_k d_{k+1}^2}{63D_k^2 D_{k+1}}, \quad \zeta_{8k+4}^{3k+2,3k+4} = \frac{d_k^2 d_{k+1}}{126D_k^2 D_{k+1}}, \quad \zeta_{8k+4}^{3k,3k+3} = \frac{d_{k+1}^2 d_{k+2}}{126D_k^2 D_{k+1}}, \\
\zeta_{8k+4}^{3k+1,3k+3} &= \frac{d_k d_{k+1} d_{k+2}}{63D_k^2 D_{k+1}} + \frac{10d_{k+1}}{63D_k}, \quad \zeta_{8k+4}^{3k+2,3k+3} = \frac{d_k^2 d_{k+2}}{126D_k^2 D_{k+1}} + \frac{10d_k}{63D_k}, \quad \zeta_{8k+4}^{3k+2,3k+2} = \frac{10}{21}, \quad \zeta_{8k+4}^{3k+3,3k+1} = \frac{5d_k d_{k+2}}{126D_k D_{k+1}} + \frac{20}{63}, \\
\zeta_{8k+4}^{3k+4,3k+1} &= \frac{5d_k d_{k+1}}{126D_k D_{k+1}}, \quad \zeta_{8k+4}^{3k+3,3k} = \frac{5d_{k+1} d_{k+2}}{126D_k D_{k+1}}, \quad \zeta_{8k+4}^{3k+4,3k} = \frac{5d_{k+1}^2}{126D_k D_{k+1}}, \quad k = 0, \dots, m-2, \\
\zeta_{8k+5}^{3k+1,3k+4} &= \frac{5d_{k+1}^2}{126D_k D_{k+1}}, \quad \zeta_{8k+5}^{3k+2,3k+4} = \frac{5d_k d_{k+1}}{126D_k D_{k+1}}, \quad \zeta_{8k+5}^{3k+1,3k+3} = \frac{5d_{k+1} d_{k+2}}{126D_k D_{k+1}}, \quad \zeta_{8k+5}^{3k+2,3k+3} = \frac{5d_k d_{k+2}}{126D_k D_{k+1}} + \frac{20}{63}, \\
\zeta_{8k+5}^{3k+3,3k+2} &= \frac{10}{21}, \quad \zeta_{8k+5}^{3k+3,3k+1} = \frac{d_k d_{k+2}^2}{126D_k D_{k+1}^2} + \frac{10d_{k+2}}{63D_{k+1}}, \quad \zeta_{8k+5}^{3k+4,3k+1} = \frac{d_k d_{k+1} d_{k+2}}{63D_k D_{k+1}^2} + \frac{10d_{k+1}}{63D_{k+1}}, \\
\zeta_{8k+5}^{3k+5,3k+1} &= \frac{d_k d_{k+1}^2}{126D_k D_{k+1}^2}, \quad \zeta_{8k+5}^{3k+3,3k} = \frac{d_{k+1} d_{k+2}^2}{126D_k D_{k+1}^2}, \quad \zeta_{8k+5}^{3k+4,3k} = \frac{d_{k+1}^2 d_{k+2}}{63D_k D_{k+1}^2}, \quad \zeta_{8k+5}^{3k+5,3k} = \frac{d_{k+1}^3}{126D_k D_{k+1}^2}, \quad k = 0, \dots, m-2, \\
\zeta_{8k+6}^{3k+2,3k+4} &= \frac{5d_{k+1}}{42D_{k+1}}, \quad \zeta_{8k+6}^{3k+2,3k+3} = \frac{5d_{k+2}}{42D_{k+1}}, \quad \zeta_{8k+6}^{3k+3,3k+3} = \frac{10}{21}, \quad \zeta_{8k+6}^{3k+4,3k+2} = \frac{5d_{k+1}}{14D_{k+1}}, \quad \zeta_{8k+6}^{3k+3,3k+2} = \frac{5d_{k+2}}{14D_{k+1}}, \\
\zeta_{8k+6}^{3k+3,3k+1} &= \frac{d_{k+2}^2}{21D_{k+1}^2}, \quad \zeta_{8k+6}^{3k+4,3k+1} = \frac{2d_{k+1} d_{k+2}}{21D_{k+1}^2}, \quad \zeta_{8k+6}^{3k+5,3k+1} = \frac{d_{k+1}^2}{21D_{k+1}^2}, \quad k = 0, \dots, m-2, \\
\zeta_{8k+7}^{3k+3,3k+4} &= \frac{5d_{k+1}}{18D_{k+1}}, \quad \zeta_{8k+7}^{3k+3,3k+3} = \frac{15d_{k+2}}{18D_{k+1}}, \quad \zeta_{8k+7}^{3k+4,3k+3} = \frac{5d_{k+1}}{9D_{k+1}}, \quad \zeta_{8k+7}^{3k+3,3k+2} = \frac{d_{k+2}^2}{6D_{k+1}^2}, \\
\zeta_{8k+7}^{3k+4,3k+2} &= \frac{d_{k+1} d_{k+2}}{3D_{k+1}^2}, \quad \zeta_{8k+7}^{3k+5,3k+2} = \frac{d_{k+1}^2}{6D_{k+1}^2}, \quad k = 0, \dots, m-2,
\end{aligned} \tag{54}$$

where  $D_k := d_k + d_{k+1}$ ,  $k = 0, \dots, m-1$  with  $d_0 = d_m := 0$ .

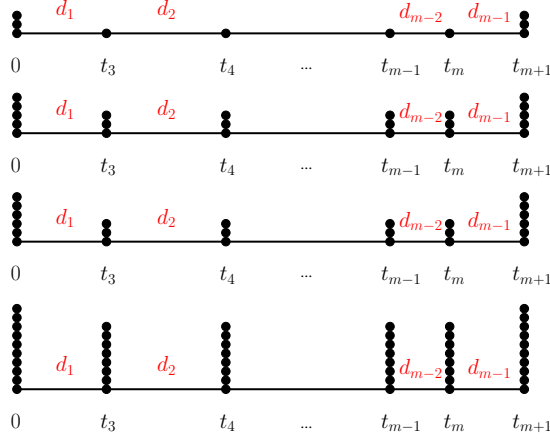


Figure 4: Knot partitions for the clamped case  $n = 2$ . From top to bottom:  $\mu, \nu, \rho, \tau$ .

By means of the computed coefficients  $\{\chi_k^{i,j}\}_{0 \leq i, j \leq m}$  we can thus shortly write the control points of  $\mathbf{r}'(t)$  as

$$\begin{aligned}
\mathbf{p}_0 &= \mathbf{z}_0^2, \\
\mathbf{p}_1 &= \mathbf{z}_0 \mathbf{z}_1, \\
\mathbf{p}_{3k-1} &= \frac{2}{3} \mathbf{z}_k^2 + \frac{1}{3} \left( \frac{d_k \mathbf{z}_{k-1} + d_{k-1} \mathbf{z}_k}{d_{k-1} + d_k} \right) \left( \frac{d_{k+1} \mathbf{z}_k + d_k \mathbf{z}_{k+1}}{d_k + d_{k+1}} \right), \quad k = 1, \dots, m-1, \\
\mathbf{p}_{3k} &= \mathbf{z}_k \frac{d_{k+1} \mathbf{z}_k + d_k \mathbf{z}_{k+1}}{d_k + d_{k+1}}, \quad k = 1, \dots, m-2, \\
\mathbf{p}_{3k+1} &= \mathbf{z}_{k+1} \frac{d_{k+1} \mathbf{z}_k + d_k \mathbf{z}_{k+1}}{d_k + d_{k+1}}, \quad k = 1, \dots, m-2, \\
\mathbf{p}_{3m-3} &= \mathbf{z}_{m-1} \mathbf{z}_m, \\
\mathbf{p}_{3m-2} &= \mathbf{z}_m^2,
\end{aligned}$$

and the coefficients of the parametric speed  $\sigma(t)$  as

$$\begin{aligned}
\sigma_0 &= \mathbf{z}_0 \bar{\mathbf{z}}_0, \\
\sigma_1 &= \frac{1}{2} (\mathbf{z}_0 \bar{\mathbf{z}}_1 + \mathbf{z}_1 \bar{\mathbf{z}}_0), \\
\sigma_{3k-1} &= \frac{1}{6} \frac{d_k d_{k+1}}{(d_{k-1} + d_k)(d_k + d_{k+1})} (\mathbf{z}_{k-1} \bar{\mathbf{z}}_k + \mathbf{z}_k \bar{\mathbf{z}}_{k-1}) + \frac{1}{6} \frac{(d_k)^2}{(d_{k-1} + d_k)(d_k + d_{k+1})} (\mathbf{z}_{k-1} \bar{\mathbf{z}}_{k+1} + \mathbf{z}_{k+1} \bar{\mathbf{z}}_{k-1}) \\
&\quad + \left( \frac{2}{3} + \frac{1}{3} \frac{d_{k-1} d_{k+1}}{(d_{k-1} + d_k)(d_k + d_{k+1})} \right) \mathbf{z}_k \bar{\mathbf{z}}_k + \frac{1}{6} \frac{d_{k-1} d_k}{(d_{k-1} + d_k)(d_k + d_{k+1})} (\mathbf{z}_k \bar{\mathbf{z}}_{k+1} + \mathbf{z}_{k+1} \bar{\mathbf{z}}_k), \quad k = 1, \dots, m-1, \\
\sigma_{3k} &= \frac{d_{k+1}}{d_k + d_{k+1}} \mathbf{z}_k \bar{\mathbf{z}}_k + \frac{1}{2} \frac{d_k}{d_k + d_{k+1}} (\mathbf{z}_k \bar{\mathbf{z}}_{k+1} + \mathbf{z}_{k+1} \bar{\mathbf{z}}_k), \quad k = 1, \dots, m-2, \\
\sigma_{3k+1} &= \frac{1}{2} \frac{d_{k+1}}{d_k + d_{k+1}} (\mathbf{z}_k \bar{\mathbf{z}}_{k+1} + \mathbf{z}_{k+1} \bar{\mathbf{z}}_k) + \frac{d_k}{d_k + d_{k+1}} \mathbf{z}_{k+1} \bar{\mathbf{z}}_{k+1}, \quad k = 1, \dots, m-2, \\
\sigma_{3m-3} &= \frac{1}{2} (\mathbf{z}_{m-1} \bar{\mathbf{z}}_m + \mathbf{z}_m \bar{\mathbf{z}}_{m-1}), \\
\sigma_{3m-2} &= \mathbf{z}_m \bar{\mathbf{z}}_m,
\end{aligned}$$

with  $d_0 := 0$  and  $d_m := 0$ . Thus, according to (12), the clamped quintic PH B-Spline curve defined over the knot partition  $\rho$  is given by

$$\mathbf{r}(t) = \sum_{i=0}^{3m-1} \mathbf{r}_i N_i^5 \rho(t), \quad t \in [t_2, t_{m+1}] \quad (t_2 = 0),$$



with control points

$$\begin{aligned}
\mathbf{r}_1 &= \mathbf{r}_0 + \frac{d_1}{5} \mathbf{z}_0^2, \\
\mathbf{r}_2 &= \mathbf{r}_1 + \frac{d_1}{5} \mathbf{z}_0 \mathbf{z}_1, \\
\mathbf{r}_{3i} &= \mathbf{r}_{3i-1} + \frac{d_i}{5} \left( \frac{2}{3} \mathbf{z}_i^2 + \frac{1}{3} \left( \frac{d_i \mathbf{z}_{i-1} + d_{i-1} \mathbf{z}_i}{d_{i-1} + d_i} \right) \left( \frac{d_{i+1} \mathbf{z}_i + d_i \mathbf{z}_{i+1}}{d_i + d_{i+1}} \right) \right), \quad i = 1, \dots, m-1, \\
\mathbf{r}_{3i+1} &= \mathbf{r}_{3i} + \frac{z_i}{5} (d_{i+1} \mathbf{z}_i + d_i \mathbf{z}_{i+1}), \quad i = 1, \dots, m-2, \\
\mathbf{r}_{3i+2} &= \mathbf{r}_{3i+1} + \frac{z_{i+1}}{5} (d_{i+1} \mathbf{z}_i + d_i \mathbf{z}_{i+1}), \quad i = 1, \dots, m-2, \\
\mathbf{r}_{3m-2} &= \mathbf{r}_{3m-3} + \frac{d_{m-1}}{5} \mathbf{z}_{m-1} \mathbf{z}_m, \\
\mathbf{r}_{3m-1} &= \mathbf{r}_{3m-2} + \frac{d_{m-1}}{5} \mathbf{z}_m^2,
\end{aligned} \tag{55}$$

and arbitrary  $\mathbf{r}_0$ .

**Remark 8.** Note that, when  $m = 2$  and  $t_3 = t_4 = t_5 = 1$ , the expressions of the control points coincide with those of Farouki's PH Bézier quintic from [4, 10].

According to (35) the total arc length of the clamped PH B-Spline curve of degree 5 is given by  $L = l_{3m-1}$ , where

$$\begin{aligned}
l_0 &= 0, \\
l_1 &= l_0 + \frac{d_1}{5} \mathbf{z}_0 \bar{\mathbf{z}}_0, \\
l_2 &= l_1 + \frac{d_1}{10} (\mathbf{z}_0 \bar{\mathbf{z}}_1 + \mathbf{z}_1 \bar{\mathbf{z}}_0), \\
l_{3i} &= l_{3i-1} + \frac{2d_i}{15} \mathbf{z}_i \bar{\mathbf{z}}_i + \frac{d_i}{15(d_{i-1} + d_i)(d_i + d_{i+1})} \left( d_{i-1} d_{i+1} \mathbf{z}_i \bar{\mathbf{z}}_i + \frac{d_i^2}{2} (\mathbf{z}_{i-1} \bar{\mathbf{z}}_{i+1} + \mathbf{z}_{i+1} \bar{\mathbf{z}}_{i-1}) \right. \\
&\quad \left. + \frac{d_i d_{i+1}}{2} (\mathbf{z}_{i-1} \bar{\mathbf{z}}_i + \mathbf{z}_i \bar{\mathbf{z}}_{i-1}) + \frac{d_{i-1} d_i}{2} (\mathbf{z}_i \bar{\mathbf{z}}_{i+1} + \mathbf{z}_{i+1} \bar{\mathbf{z}}_i) \right), \quad i = 1, \dots, m-1, \\
l_{3i+1} &= l_{3i} + \frac{1}{5} \left( d_{i+1} \mathbf{z}_i \bar{\mathbf{z}}_i + \frac{d_i}{2} (\mathbf{z}_i \bar{\mathbf{z}}_{i+1} + \mathbf{z}_{i+1} \bar{\mathbf{z}}_i) \right), \quad i = 1, \dots, m-2, \\
l_{3i+2} &= l_{3i+1} + \frac{1}{5} \left( d_i \mathbf{z}_{i+1} \bar{\mathbf{z}}_{i+1} + \frac{d_{i+1}}{2} (\mathbf{z}_i \bar{\mathbf{z}}_{i+1} + \mathbf{z}_{i+1} \bar{\mathbf{z}}_i) \right), \quad i = 1, \dots, m-2, \\
l_{3m-2} &= l_{3m-3} + \frac{d_{m-1}}{10} (\mathbf{z}_{m-1} \bar{\mathbf{z}}_m + \mathbf{z}_m \bar{\mathbf{z}}_{m-1}), \\
l_{3m-1} &= l_{3m-2} + \frac{d_{m-1}}{5} \mathbf{z}_m \bar{\mathbf{z}}_m.
\end{aligned}$$

Over the knot partition  $\tau$ , the offset curve  $\mathbf{r}_h(t)$  has the rational B-Spline form

$$\mathbf{r}_h(t) = \frac{\sum_{k=0}^{8m-7} \mathbf{q}_k N_{k,\tau}^9(t)}{\sum_{k=0}^{8m-7} \gamma_k N_{k,\tau}^9(t)}, \quad t \in [t_2, t_{m+1}], \tag{56}$$

where, by exploiting the explicit expressions of the coefficients  $\{\zeta_k^{i,j}\}_{0 \leq i \leq 3m-1, 0 \leq j \leq 3m-2}$  from (54), weights and control points are easily obtained; the explicit formulae are reported in the Appendix.

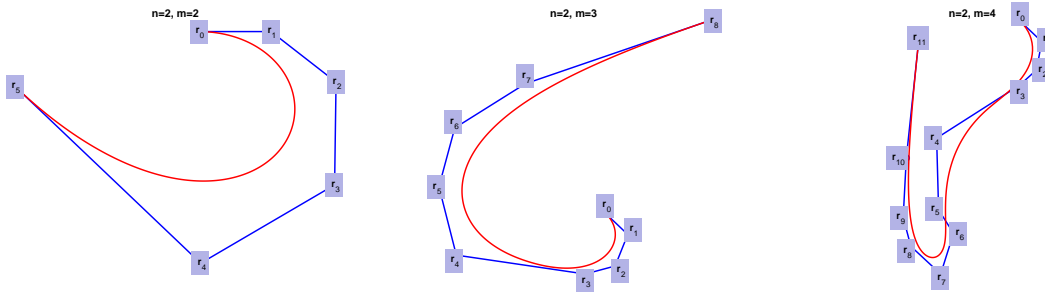


Figure 5: Clamped quintic PH B-Spline curves with:  $m = 2$  (left),  $m = 3$  (center) and  $m = 4$  (right).

Some examples of clamped quintic PH B-Spline curves are shown in Figure 5, and their offsets are displayed in Figure 6.

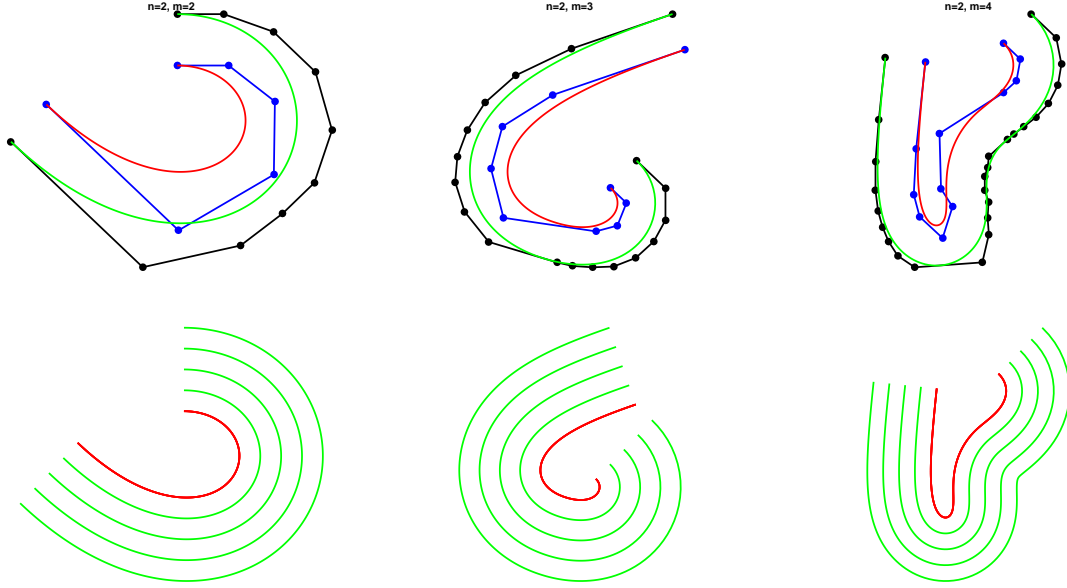


Figure 6: Offsets of clamped quintic PH B-Spline curves from Figure 5 with (1. row) and without (2. row) control polygon where:  $m = 2$  (left column),  $m = 3$  (center column) and  $m = 4$  (right column).

### 5.3. Closed cubic PH B-Splines ( $n = 1$ )

Let  $m \in \mathbb{N}$ ,  $m \geq 1$ . For a general knot vector  $\mu = \{0 = t_0 < t_1 < \dots < t_{m+3}\}$  (see Figure 7 first row), by applying the above method we construct the knot partitions

$$\begin{aligned} \nu &= \{\langle 0 \rangle^2 < \langle t_1 \rangle^2 < \dots < \langle t_{m+3} \rangle^2\}, \\ \rho &= \{t_{-1} < \langle 0 \rangle^2 < \langle t_1 \rangle^2 < \dots < \langle t_{m+3} \rangle^2 < t_{m+4}\}, \\ \tau &= \{\langle t_{-1} \rangle^3 < \langle 0 \rangle^5 < \langle t_1 \rangle^5 < \dots < \langle t_{m+3} \rangle^5 < \langle t_{m+4} \rangle^3\}, \end{aligned}$$

illustrated in Figure 7. Then, by solving the linear systems (10) we calculate the coefficients  $\chi_k^{i,j}$ ,  $0 \leq i, j \leq m+1$ ,  $0 \leq k \leq 2m+4$ . All of them turn out to be zero with the exception of

$$\begin{aligned} \chi_{2k+1}^{k,k} &= 1, \quad k = 0, \dots, m+1, \\ \chi_{2k+2}^{k,k+1} &= \chi_{2k+2}^{k+1,k} = \frac{1}{2}, \quad k = 0, \dots, m. \end{aligned}$$

In addition, we compute the coefficients  $\zeta_k^{i,j}$ ,  $0 \leq i \leq 2m+5$ ,  $0 \leq j \leq 2m+4$ ,  $0 \leq k \leq 5m+19$  as the solutions to the linear systems (46). All of them turn out to be zero with the exception of

$$\begin{aligned} \zeta_3^{0,0} &= \frac{2d_0}{5D_0}, \quad \zeta_4^{0,0} = \frac{3}{5}, \quad \zeta_4^{0,1} = \frac{d_0}{10D_0}, \\ \zeta_5^{0,1} &= \frac{3}{10}, \quad \zeta_5^{1,0} = \frac{3}{5}, \quad \zeta_6^{1,0} = \frac{2d_1}{5D_1}, \quad \zeta_6^{1,1} = \frac{3}{5}, \quad \zeta_6^{2,0} = \frac{2d_1}{5D_1}, \\ \zeta_{5k+7}^{2k+1,2k+1} &= \frac{d_{k+2}}{D_{k+1}}, \quad \zeta_{5k+7}^{2k+2,2k+1} = \frac{d_{k+1}}{D_{k+1}}, \quad k = 0, \dots, m+1, \\ \zeta_{5k+8}^{2k+1,2k+2} &= \frac{2d_{k+2}}{5D_{k+1}}, \quad \zeta_{5k+8}^{2k+2,2k+1} = \frac{3}{5}, \quad \zeta_{5k+8}^{2k+2,2k+2} = \frac{2d_{k+1}}{5D_{k+1}}, \quad k = 0, \dots, m, \\ \zeta_{5k+9}^{2k+1,2k+3} &= \frac{d_{k+2}}{10D_{k+1}}, \quad \zeta_{5k+9}^{2k+2,2k+2} = \frac{3}{5}, \quad \zeta_{5k+9}^{2k+2,2k+3} = \frac{d_{k+1}}{10D_{k+1}}, \quad \zeta_{5k+9}^{2k+3,2k+1} = \frac{3}{10}, \quad k = 0, \dots, m, \\ \zeta_{5k+10}^{2k+2,2k+3} &= \frac{3}{10}, \quad \zeta_{5k+10}^{2k+3,2k+1} = \frac{d_{k+3}}{10D_{k+2}}, \quad \zeta_{5k+10}^{2k+3,2k+2} = \frac{3}{5}, \quad \zeta_{5k+10}^{2k+4,2k+1} = \frac{d_{k+2}}{10D_{k+2}}, \quad k = 0, \dots, m, \\ \zeta_{5k+11}^{2k+3,2k+2} &= \frac{2d_{k+3}}{5D_{k+2}}, \quad \zeta_{5k+11}^{2k+3,2k+3} = \frac{3}{5}, \quad \zeta_{5k+11}^{2k+4,2k+2} = \frac{2d_{k+2}}{5D_{k+2}}, \quad k = 0, \dots, m, \\ \zeta_{5m+13}^{2m+3,2m+4} &= \frac{2d_{m+3}}{5D_{m+2}}, \quad \zeta_{5m+13}^{2m+4,2m+3} = \frac{3}{5}, \quad \zeta_{5m+13}^{2m+4,2m+4} = \frac{2d_{m+2}}{5D_{m+2}}, \quad \zeta_{5m+14}^{2m+4,2m+4} = \frac{3}{5}, \quad \zeta_{5m+14}^{2m+5,2m+3} = \frac{3}{10}, \\ \zeta_{5m+15}^{2m+5,2m+3} &= \frac{d_{m+4}}{10D_{m+3}}, \quad \zeta_{5m+15}^{2m+5,2m+4} = \frac{3}{5}, \quad \zeta_{5m+15}^{2m+5,2m+4} = \frac{2d_{m+4}}{5D_{m+3}}, \end{aligned} \tag{57}$$

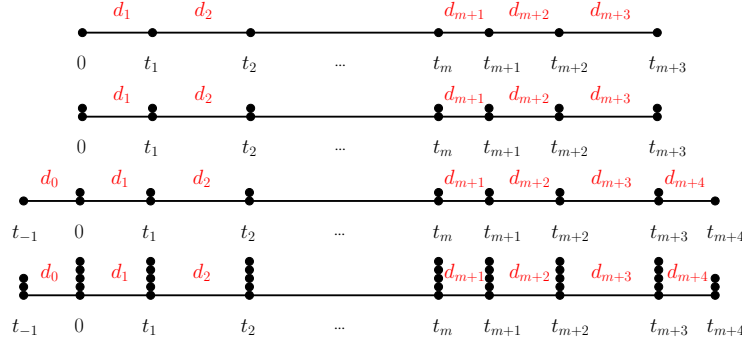


Figure 7: Knot partitions for the closed case  $n = 1$ . From top to bottom:  $\mu, \nu, \rho, \tau$ .

where  $D_k := d_k + d_{k+1}$ ,  $k = 0, \dots, m + 3$ .

By means of the computed coefficients  $\{\chi_k^{i,j}\}_{0 \leq i, j \leq m+1}^{0 \leq k \leq 2m+4}$  we can thus shortly write the control points of  $\mathbf{r}'(t)$  as

$$\begin{aligned} \mathbf{p}_0 &= \mathbf{0}, \\ \mathbf{p}_{2k+1} &= \mathbf{z}_k^2, \quad k = 0, \dots, m + 1, \\ \mathbf{p}_{2k+2} &= \mathbf{z}_k \mathbf{z}_{k+1}, \quad k = 0, \dots, m, \\ \mathbf{p}_{2m+4} &= \mathbf{0}, \end{aligned}$$

and the coefficients of the parametric speed  $\sigma(t)$  as

$$\begin{aligned} \sigma_0 &= 0, \\ \sigma_{2k+1} &= \mathbf{z}_k \bar{\mathbf{z}}_k, \quad k = 0, \dots, m + 1, \\ \sigma_{2k+2} &= \frac{1}{2}(\mathbf{z}_k \bar{\mathbf{z}}_{k+1} + \mathbf{z}_{k+1} \bar{\mathbf{z}}_k), \quad k = 0, \dots, m, \\ \sigma_{2m+4} &= 0. \end{aligned}$$

Thus, according to (12), the closed cubic PH B-Spline curve defined over the knot partition  $\rho$  is given by

$$\mathbf{r}(t) = \sum_{i=0}^{2m+5} \mathbf{r}_i N_{i,\rho}^3(t), \quad t \in [t_1, t_{m+2}] \quad (t_0 = 0),$$

with control points

$$\begin{aligned} \mathbf{r}_1 &= \mathbf{r}_0, \\ \mathbf{r}_{2i+2} &= \mathbf{r}_{2i+1} + \frac{d_{i+1} + d_{i+2}}{3} \mathbf{z}_i^2, \quad i = 0, \dots, m + 1, \\ \mathbf{r}_{2i+3} &= \mathbf{r}_{2i+2} + \frac{d_{i+2}}{3} \mathbf{z}_i \mathbf{z}_{i+1}, \quad i = 0, \dots, m, \\ \mathbf{r}_{2m+5} &= \mathbf{r}_{2m+4}, \end{aligned}$$

and arbitrary  $\mathbf{r}_0$ . Note that, due to condition (19),  $d_{m+2} = d_1$ ,  $d_{m+3} = d_2$ . Moreover,  $\mathbf{z}_m$  and  $\mathbf{z}_{m+1}$  must be suitably fixed in order to satisfy condition (18). According to (37) and using the partition of unity  $N_{1,\rho}^3(t_1) + N_{2,\rho}^3(t_1) = 1$ , the total arc length of the closed PH B-Spline curve of degree 3 is given by

$$L = l_{2m+3} + (l_{2m+4} - l_{2m+3} - l_2) N_{2,\rho}^3(t_1),$$

where

$$\begin{aligned} l_1 &= l_0 = 0, \\ l_{2i+2} &= l_{2i+1} + \frac{d_{i+1} + d_{i+2}}{3} \mathbf{z}_i \bar{\mathbf{z}}_i, \quad i = 0, \dots, m + 1, \\ l_{2i+3} &= l_{2i+2} + \frac{d_{i+2}}{6} (\mathbf{z}_i \bar{\mathbf{z}}_{i+1} + \mathbf{z}_{i+1} \bar{\mathbf{z}}_i), \quad i = 0, \dots, m, \\ l_{2m+5} &= l_{2m+4}. \end{aligned}$$

Over the knot partition  $\tau$  the offset curve  $\mathbf{r}_h(t)$  has the rational B-Spline form

$$\mathbf{r}_h(t) = \frac{\sum_{k=0}^{5m+19} \mathbf{q}_k N_{k,\tau}^5(t)}{\sum_{k=0}^{5m+19} \gamma_k N_{k,\tau}^5(t)}, \quad t \in [t_1, t_{m+2}], \quad (58)$$

$m$	$\mathbf{z}(t)$ open/closed	Conditions on $\mathbf{z}(t)$ in order to satisfy (18)	Illustration
1	closed	$\mathbf{z}_1 = \frac{-1-\sqrt{3}i}{2} \mathbf{z}_0, \quad \mathbf{z}_2 = \mathbf{z}_0$	Figure 8, first column
2	closed	$\mathbf{z}_2 = -\frac{d_1 \mathbf{z}_0 + d_3 \mathbf{z}_1 + \sqrt{r_-}}{2(d_1 + d_3)}, \quad \mathbf{z}_3 = \mathbf{z}_0,$	Figure 8, second column
3	closed	$\mathbf{z}_3 = -\frac{d_1 \mathbf{z}_0 + d_4 \mathbf{z}_2 + \sqrt{R_+}}{2(d_1 + d_4)}, \quad \mathbf{z}_4 = \mathbf{z}_0$	Figure 8, third column
1	open	$\mathbf{z}_1 = \frac{d_1 - d_2 + \sqrt{(d_1 + 3d_2)(3d_1 + d_2)i}}{2(d_1 + d_2)} \mathbf{z}_0, \quad \mathbf{z}_2 = -\mathbf{z}_0$	Figure 9, first column
2	open	$\mathbf{z}_2 = \frac{d_1 \mathbf{z}_0 - d_3 \mathbf{z}_1 + \sqrt{r_+}}{2(d_1 + d_3)}, \quad \mathbf{z}_3 = -\mathbf{z}_0,$	Figure 9, second column
3	open	$\mathbf{z}_3 = \frac{d_1 \mathbf{z}_0 - d_4 \mathbf{z}_2 + \sqrt{R_-}}{2(d_1 + d_4)}, \quad \mathbf{z}_4 = -\mathbf{z}_0$	Figure 9, third column

Table 1: Data for the examples in the closed case for  $n = 1$ .

where, by exploiting the explicit expressions of the coefficients  $\{\zeta_k^{i,j}\}_{0 \leq i \leq 2m+5, 0 \leq j \leq 2m+4, 0 \leq k \leq 5m+19}$  from (57), weights and control points can easily be obtained; their explicit formulae are reported in the Appendix.

We now illustrate some closed degree 3 PH B-Spline curves. To this end we define

$$r_{\pm} = -(4d_1d_2 + 4d_1d_3 + 4d_2d_3 + 3d_1^2)\mathbf{z}_0^2 - (4d_1d_2 \pm 2d_1d_3 + 4d_2d_3)\mathbf{z}_0\mathbf{z}_1 - (4d_1d_2 + 4d_1d_3 + 4d_2d_3 + 3d_3^2)\mathbf{z}_1^2,$$

$$R_{\pm} = -(4d_1d_2 + 4d_1d_4 + 4d_2d_4 + 3d_1^2)\mathbf{z}_0^2 - (4d_1d_2 + 4d_2d_4)\mathbf{z}_0\mathbf{z}_1 \pm 2d_1d_4\mathbf{z}_0\mathbf{z}_2 - (4d_1d_2 + 4d_1d_3 + 4d_2d_4 + 4d_3d_4)\mathbf{z}_1^2 - (4d_1d_3 + 4d_3d_4)\mathbf{z}_1\mathbf{z}_2 - (4d_1d_3 + 4d_1d_4 + 4d_3d_4 + 3d_4^2)\mathbf{z}_2^2.$$

Figures 8 and 9 contain examples of cubic PH B-Spline curves obtained for the data in Table 1. Figure 10 shows the offsets of the PH B-Spline curves of Figure 9.

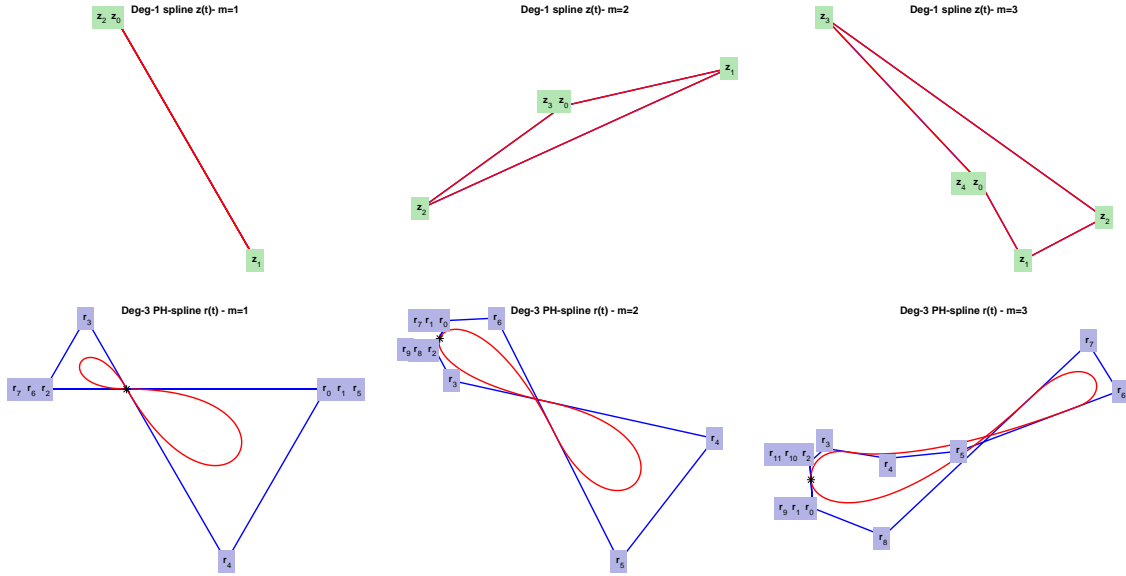


Figure 8: Closed cubic PH B-Spline curves with  $m = 1$  (left),  $m = 2$  (center),  $m = 3$  (right) originated from closed degree-1 splines  $\mathbf{z}(t)$ .

#### 5.4. Closed quintic PH B-Splines ( $n = 2$ )

Let  $m \in \mathbb{N}$ ,  $m \geq 2$ . For a general knot vector  $\boldsymbol{\mu} = \{0 = t_0 < t_1 < \dots < t_{m+5}\}$  (see Figure 11 first row), by applying the above method we construct the knot partitions

$$\boldsymbol{\nu} = \{\langle 0 \rangle^3 < \langle t_1 \rangle^3 < \dots < \langle t_{m+5} \rangle^3\},$$

$$\boldsymbol{\rho} = \{t_{-1} < \langle 0 \rangle^3 < \langle t_1 \rangle^3 < \dots < \langle t_{m+5} \rangle^3 < t_{m+6}\},$$

$$\boldsymbol{\tau} = \{\langle t_{-1} \rangle^5 < \langle 0 \rangle^8 < \langle t_1 \rangle^8 < \dots < \langle t_{m+5} \rangle^8 < \langle t_{m+6} \rangle^5\},$$

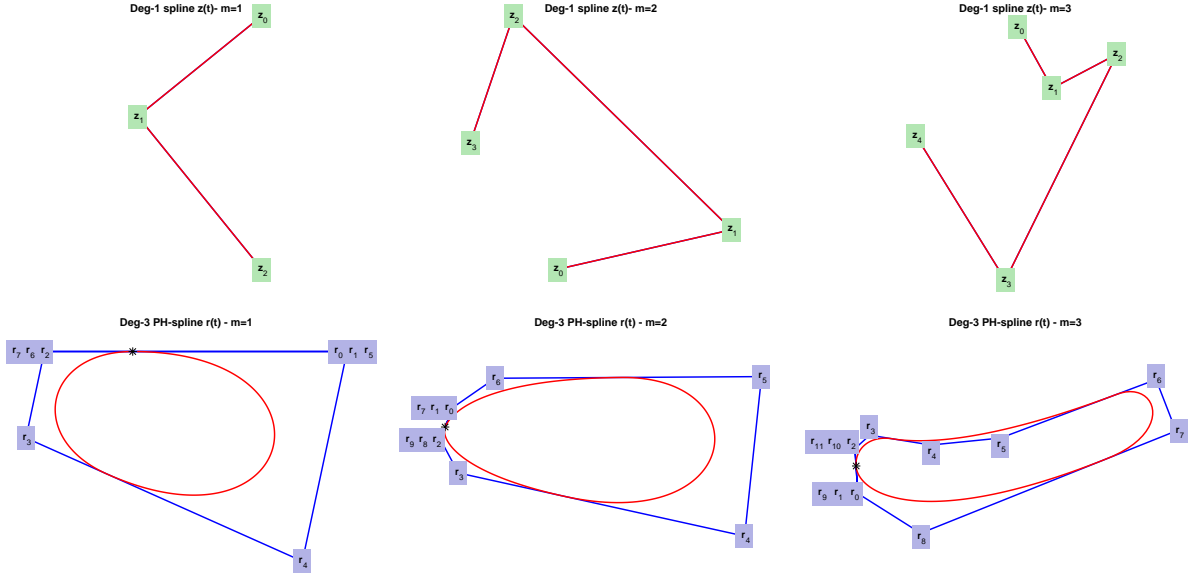


Figure 9: Closed cubic PH B-Spline curves with  $m = 1$  (left),  $m = 2$  (center),  $m = 3$  (right) originated from open degree-1 splines  $z(t)$ .

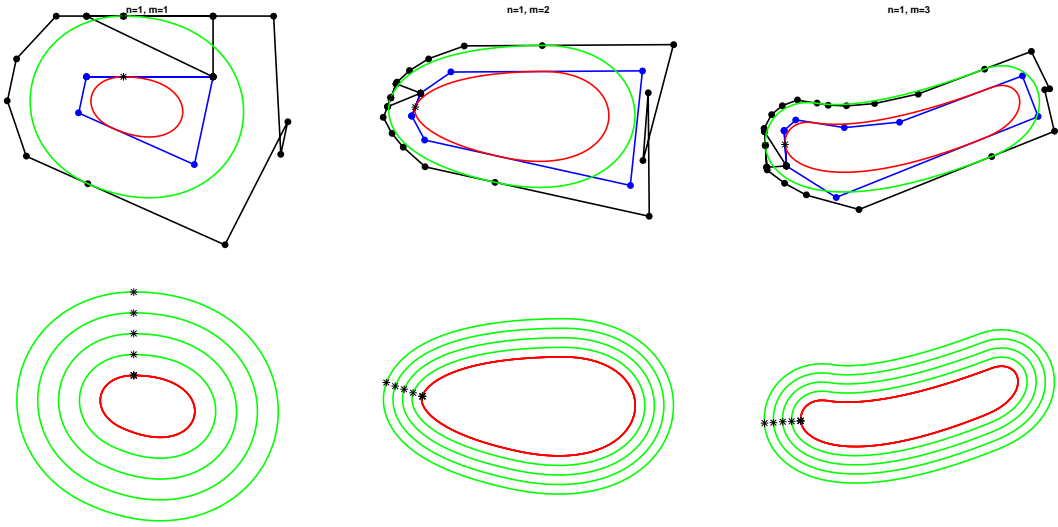


Figure 10: Offsets of closed cubic PH B-Spline curves with:  $m = 1$  (left),  $m = 2$  (center),  $m = 3$  (right).

illustrated in Figure 11. Then, by solving the linear systems (10) we calculate the coefficients  $\chi_k^{i,j}$ ,  $0 \leq i, j \leq m + 2$ ,  $0 \leq k \leq 3m + 12$ . All of them turn out to be zero with the exception of

$$\begin{aligned} \chi_2^{0,0} &= \frac{d_1}{d_1 + d_2}, \\ \chi_{3k}^{k-2, k-1} &= \chi_{3k}^{k-1, k-2} = \frac{1}{6} \frac{d_{k+1} d_{k+2}}{(d_k + d_{k+1})(d_{k+1} + d_{k+2})}, \quad k = 1, \dots, m + 3, \\ \chi_{3k}^{k-2, k} &= \chi_{3k}^{k, k-2} = \frac{1}{6} \frac{(d_{k+1})^2}{(d_k + d_{k+1})(d_{k+1} + d_{k+2})}, \quad k = 1, \dots, m + 3, \\ \chi_{3k}^{k-1, k-1} &= \frac{2}{3} + \frac{1}{3} \frac{d_k d_{k+2}}{(d_k + d_{k+1})(d_{k+1} + d_{k+2})}, \quad k = 1, \dots, m + 3, \\ \chi_{3k}^{k-1, k} &= \chi_{3k}^{k, k-1} = \frac{1}{6} \frac{d_k d_{k+1}}{(d_k + d_{k+1})(d_{k+1} + d_{k+2})}, \quad k = 1, \dots, m + 3, \end{aligned}$$

$$\begin{aligned}
\chi_{3k+1}^{k-1,k-1} &= \frac{d_{k+2}}{d_{k+1}+d_{k+2}}, \quad k = 1, \dots, m+2, \\
\chi_{3k+1}^{k-1,k} &= \chi_{3k+1}^{k,k-1} = \frac{1}{2} \frac{d_{k+1}}{d_{k+1}+d_{k+2}}, \quad k = 1, \dots, m+2, \\
\chi_{3k+2}^{k-1,k} &= \chi_{3k+2}^{k,k-1} = \frac{1}{2} \frac{d_{k+2}}{d_{k+1}+d_{k+2}}, \quad k = 1, \dots, m+2, \\
\chi_{3k+2}^{k,k} &= \frac{d_{k+1}}{d_{k+1}+d_{k+2}}, \quad k = 1, \dots, m+2, \\
\chi_{3m+10}^{m+2,m+2} &= \frac{d_{m+5}}{d_{m+4}+d_{m+5}},
\end{aligned}$$

where  $d_k = t_k - t_{k-1}$ ,  $k = 1, \dots, m+5$ .

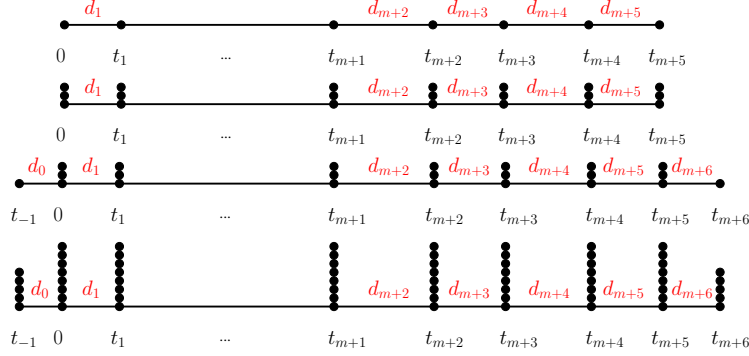


Figure 11: Knot partitions for the closed case  $n = 2$ . From top to bottom:  $\mu, \nu, \rho, \tau$ .

In addition, we compute the coefficients  $\zeta_k^{i,j}$ ,  $0 \leq i \leq 3m+13$ ,  $0 \leq j \leq 3m+12$ ,  $0 \leq k \leq 8m+47$  as the solutions to the linear systems (46). All of them turn out to be zero with the exception of

$$\begin{aligned}
\zeta_5^{0,0} &= \frac{d_0^2}{6D_0^2}, \quad \zeta_6^{0,0} = \frac{5d_0}{14D_0}, \quad \zeta_6^{0,1} = \frac{d_0^2}{21D_0^2}, \\
\zeta_7^{0,0} &= \frac{10}{21}, \quad \zeta_7^{0,1} = \frac{d_0^2 d_2}{126D_0^2 D_1} + \frac{10d_0}{63D_0}, \quad \zeta_7^{0,2} = \frac{d_0^2 d_1}{126D_0^2 D_1}, \\
\zeta_8^{0,1} &= \frac{5d_0 d_2}{126D_0 D_1} + \frac{20}{63}, \quad \zeta_8^{0,2} = \frac{5d_0 d_1}{126D_0 D_1}, \quad \zeta_8^{1,0} = \frac{10}{21}, \\
\zeta_9^{0,1} &= \frac{5d_2}{42D_1}, \quad \zeta_9^{0,2} = \frac{5d_1}{42D_1}, \quad \zeta_9^{1,0} = \frac{5d_2}{14D_1}, \quad \zeta_9^{1,1} = \frac{10}{21}, \quad \zeta_9^{2,0} = \frac{5d_1}{14D_1}, \\
\zeta_{10}^{1,0} &= \frac{d_2^2}{6D_1^2}, \quad \zeta_{10}^{1,1} = \frac{15d_2}{18D_1}, \quad \zeta_{10}^{1,2} = \frac{5d_1}{18D_1}, \\
\zeta_{10}^{2,0} &= \frac{d_1 d_2}{3D_1^2}, \quad \zeta_{10}^{2,1} = \frac{5d_1}{9D_1}, \quad \zeta_{10}^{3,0} = \frac{d_1^2}{6D_1^2}, \\
\zeta_{8k+11}^{3k+1,3k+1} &= \frac{d_{k+2}^2}{D_{k+1}^2}, \quad \zeta_{8k+11}^{3k+1,3k+2} = \frac{5d_{k+1} d_{k+2}}{9D_{k+1}^2}, \quad \zeta_{8k+11}^{3k+2,3k+1} = \frac{13d_{k+1} d_{k+2}}{9D_{k+1}^2}, \quad \zeta_{8k+11}^{3k+2,3k+2} = \frac{5d_{k+1}^2}{9D_{k+1}^2}, \quad \zeta_{8k+11}^{3k+3,3k+1} = \frac{4d_{k+1}^2}{9D_{k+1}^2}, \quad k = 0, \dots, m+3, \\
\zeta_{8k+12}^{3k+1,3k+2} &= \frac{4d_{k+2}^2}{9D_{k+1}^2}, \quad \zeta_{8k+12}^{3k+2,3k+1} = \frac{5d_{k+2}^2}{9D_{k+1}^2}, \quad \zeta_{8k+12}^{3k+2,3k+2} = \frac{13d_{k+1} d_{k+2}}{9D_{k+1}^2}, \quad \zeta_{8k+12}^{3k+3,3k+1} = \frac{5d_{k+1} d_{k+2}}{9D_{k+1}^2}, \quad \zeta_{8k+12}^{3k+3,3k+2} = \frac{d_{k+1}^2}{D_{k+1}^2}, \quad k = 0, \dots, m+3, \\
\zeta_{8k+13}^{3k+1,3k+3} &= \frac{d_{k+2}^2}{6D_{k+1}^2}, \quad \zeta_{8k+13}^{3k+2,3k+2} = \frac{5d_{k+2}}{9D_{k+1}}, \quad \zeta_{8k+13}^{3k+2,3k+3} = \frac{d_{k+1} d_{k+2}}{3D_{k+1}^2}, \quad \zeta_{8k+13}^{3k+3,3k+1} = \frac{5d_{k+2}}{18D_{k+1}}, \\
\zeta_{8k+13}^{3k+3,3k+2} &= \frac{15d_{k+1}}{18D_{k+1}}, \quad \zeta_{8k+13}^{3k+3,3k+3} = \frac{d_{k+1}^2}{6D_{k+1}^2}, \quad k = 0, \dots, m+2, \\
\zeta_{8k+14}^{3k+1,3k+4} &= \frac{d_{k+2}^2}{21D_{k+1}^2}, \quad \zeta_{8k+14}^{3k+2,3k+3} = \frac{5d_{k+2}}{14D_{k+1}}, \quad \zeta_{8k+14}^{3k+2,3k+4} = \frac{2d_{k+1} d_{k+2}}{21D_{k+1}^2}, \quad \zeta_{8k+14}^{3k+3,3k+2} = \frac{10}{21}, \quad \zeta_{8k+14}^{3k+3,3k+3} = \frac{5d_{k+1}}{14D_{k+1}}, \\
\zeta_{8k+14}^{3k+3,3k+4} &= \frac{d_{k+1}^2}{21D_{k+1}^2}, \quad \zeta_{8k+14}^{3k+4,3k+1} = \frac{5d_{k+2}}{42D_{k+1}}, \quad \zeta_{8k+14}^{3k+4,3k+2} = \frac{5d_{k+1}}{42D_{k+1}}, \quad k = 0, \dots, m+2, \\
\zeta_{8k+15}^{3k+1,3k+4} &= \frac{d_{k+2}^2 d_{k+3}}{126D_{k+1}^2 D_{k+2}}, \quad \zeta_{8k+15}^{3k+1,3k+5} = \frac{d_{k+2}^3}{126D_{k+1}^2 D_{k+2}}, \quad \zeta_{8k+15}^{3k+2,3k+4} = \frac{d_{k+1} d_{k+2} d_{k+3}}{63D_{k+1}^2 D_{k+2}} + \frac{10d_{k+2}}{63D_{k+1}}, \quad \zeta_{8k+15}^{3k+2,3k+5} = \frac{d_{k+1} d_{k+2}^2}{63D_{k+1}^2 D_{k+2}}, \\
\zeta_{8k+15}^{3k+3,3k+3} &= \frac{10}{21}, \quad \zeta_{8k+15}^{3k+3,3k+4} = \frac{d_{k+1}^2 d_{k+3}}{126D_{k+1}^2 D_{k+2}} + \frac{10d_{k+1}}{63D_{k+1}}, \quad \zeta_{8k+15}^{3k+3,3k+5} = \frac{d_{k+1}^2 d_{k+2}}{126D_{k+1}^2 D_{k+2}}, \quad \zeta_{8k+15}^{3k+4,3k+1} = \frac{5d_{k+2} d_{k+3}}{126D_{k+1} D_{k+2}}, \\
\zeta_{8k+15}^{3k+4,3k+2} &= \frac{5d_{k+1} d_{k+3}}{126D_{k+1} D_{k+2}} + \frac{20}{63}, \quad \zeta_{8k+15}^{3k+5,3k+1} = \frac{5d_{k+2}^2}{126D_{k+1} D_{k+2}}, \quad \zeta_{8k+15}^{3k+5,3k+2} = \frac{5d_{k+1} d_{k+2}}{126D_{k+1} D_{k+2}}, \quad k = 0, \dots, m+2,
\end{aligned}$$

(59)

$$\begin{aligned}
\zeta_{8k+16}^{3k+2,3k+4} &= \frac{5d_{k+2}d_{k+3}}{126D_{k+1}D_{k+2}}, \quad \zeta_{8k+16}^{3k+2,3k+5} = \frac{5d_{k+2}^2}{126D_{k+1}D_{k+2}}, \quad \zeta_{8k+16}^{3k+3,3k+4} = \frac{5d_{k+1}d_{k+3}}{126D_{k+1}D_{k+2}} + \frac{20}{63}, \quad \zeta_{8k+16}^{3k+3,3k+5} = \frac{5d_{k+1}d_{k+2}}{126D_{k+1}D_{k+2}}, \\
\zeta_{8k+16}^{3k+4,3k+1} &= \frac{d_{k+2}d_{k+3}^2}{126D_{k+1}D_{k+2}^2}, \quad \zeta_{8k+16}^{3k+4,3k+2} = \frac{d_{k+1}d_{k+3}^2}{126D_{k+1}D_{k+2}^2} + \frac{10d_{k+3}}{63D_{k+2}}, \quad \zeta_{8k+16}^{3k+4,3k+3} = \frac{10}{21}, \\
\zeta_{8k+16}^{3k+5,3k+1} &= \frac{d_{k+2}^2d_{k+3}}{63D_{k+1}D_{k+2}^2}, \quad \zeta_{8k+16}^{3k+5,3k+2} = \frac{d_{k+1}d_{k+2}d_{k+3}}{63D_{k+1}D_{k+2}^2} + \frac{10d_{k+2}}{63D_{k+2}}, \quad \zeta_{8k+16}^{3k+6,3k+1} = \frac{d_{k+2}^3}{126D_{k+1}D_{k+2}^2}, \quad \zeta_{8k+16}^{3k+6,3k+2} = \frac{d_{k+1}d_{k+2}^2}{126D_{k+1}D_{k+2}^2}, \quad k = 0, \dots, m+2, \\
\zeta_{8k+17}^{3k+3,3k+4} &= \frac{5d_{k+3}}{42D_{k+2}}, \quad \zeta_{8k+17}^{3k+3,3k+5} = \frac{5d_{k+2}}{42D_{k+2}}, \quad \zeta_{8k+17}^{3k+4,3k+2} = \frac{d_{k+3}^2}{21D_{k+2}^2}, \quad \zeta_{8k+17}^{3k+4,3k+3} = \frac{5d_{k+3}}{14D_{k+2}}, \quad \zeta_{8k+17}^{3k+4,3k+4} = \frac{10}{21}, \\
\zeta_{8k+17}^{3k+5,3k+2} &= \frac{2d_{k+2}d_{k+3}}{21D_{k+2}^2}, \quad \zeta_{8k+17}^{3k+5,3k+3} = \frac{5d_{k+2}}{14D_{k+2}}, \quad \zeta_{8k+17}^{3k+6,3k+2} = \frac{d_{k+2}^2}{21D_{k+2}^2}, \quad k = 0, \dots, m+2, \\
\zeta_{8k+18}^{3k+4,3k+3} &= \frac{d_{k+3}^2}{6D_{k+2}^2}, \quad \zeta_{8k+18}^{3k+4,3k+4} = \frac{15d_{k+3}}{18D_{k+2}}, \quad \zeta_{8k+18}^{3k+4,3k+5} = \frac{5d_{k+2}}{18D_{k+2}}, \quad \zeta_{8k+18}^{3k+5,3k+3} = \frac{d_{k+2}d_{k+3}}{3D_{k+2}^2}, \\
\zeta_{8k+18}^{3k+5,3k+4} &= \frac{5d_{k+2}}{9D_{k+2}}, \quad \zeta_{8k+18}^{3k+6,3k+3} = \frac{d_{k+2}^2}{6D_{k+2}^2}, \quad k = 0, \dots, m+2, \\
\zeta_{8m+37}^{3m+10,3m+12} &= \frac{d_{m+5}^2}{6D_{m+4}^2}, \quad \zeta_{8m+37}^{3m+11,3m+11} = \frac{5d_{m+5}}{9D_{m+4}}, \quad \zeta_{8m+37}^{3m+11,3m+12} = \frac{d_{m+4}d_{m+5}}{3D_{m+4}^2}, \\
\zeta_{8m+37}^{3m+12,3m+10} &= \frac{5d_{m+5}}{18D_{m+4}}, \quad \zeta_{8m+37}^{3m+12,3m+11} = \frac{15d_{m+4}}{18D_{m+4}}, \quad \zeta_{8m+37}^{3m+12,3m+12} = \frac{d_{m+4}^2}{6D_{m+4}^2}, \\
\zeta_{8m+38}^{3m+11,3m+12} &= \frac{5d_{m+5}}{14D_{m+4}}, \quad \zeta_{8m+38}^{3m+12,3m+11} = \frac{10}{21}, \quad \zeta_{8m+38}^{3m+12,3m+12} = \frac{5d_{m+4}}{14D_{m+4}}, \quad \zeta_{8m+38}^{3m+13,3m+10} = \frac{5d_{m+5}}{42D_{m+4}}, \quad \zeta_{8m+38}^{3m+13,3m+11} = \frac{5d_{m+4}}{42D_{m+4}}, \\
\zeta_{8m+39}^{3m+12,3m+12} &= \frac{10}{21}, \quad \zeta_{8m+39}^{3m+13,3m+10} = \frac{5d_{m+5}d_{m+6}}{126D_{m+4}D_{m+5}}, \quad \zeta_{8m+39}^{3m+13,3m+11} = \frac{5d_{m+4}d_{m+6}}{126D_{m+4}D_{m+5}} + \frac{20}{63}, \\
\zeta_{8m+40}^{3m+13,3m+10} &= \frac{d_{m+5}d_{m+6}^2}{126D_{m+4}D_{m+5}^2}, \quad \zeta_{8m+40}^{3m+13,3m+11} = \frac{d_{m+4}d_{m+6}^2}{126D_{m+4}D_{m+5}^2} + \frac{10d_{m+6}}{63D_{m+5}}, \quad \zeta_{8m+40}^{3m+13,3m+12} = \frac{10}{21}, \\
\zeta_{8m+41}^{3m+13,3m+11} &= \frac{d_{m+6}^2}{21D_{m+5}^2}, \quad \zeta_{8m+41}^{3m+13,3m+12} = \frac{5d_{m+6}}{14D_{m+5}}, \quad \zeta_{8m+42}^{3m+13,3m+12} = \frac{d_{m+6}^2}{6D_{m+5}^2},
\end{aligned}$$

where  $D_k := d_k + d_{k+1}$ ,  $k = 0, \dots, m+5$ .

By means of the computed coefficients  $\{\chi_k^{i,j}\}_{0 \leq i,j \leq m+2, 0 \leq k \leq 3m+12}$  we can thus shortly write the control points of  $\mathbf{r}'(t)$  as

$$\begin{aligned}
\mathbf{p}_0 &= \mathbf{p}_1 = 0, \\
\mathbf{p}_2 &= \frac{d_1}{d_1+d_2} \mathbf{z}_0^2, \\
\mathbf{p}_{3k} &= \frac{2}{3} \mathbf{z}_{k-1}^2 + \frac{1}{3} \left( \frac{d_{k+1} \mathbf{z}_{k-2} + d_k \mathbf{z}_{k-1}}{d_k + d_{k+1}} \right) \left( \frac{d_{k+2} \mathbf{z}_{k-1} + d_{k+1} \mathbf{z}_k}{d_{k+1} + d_{k+2}} \right), \quad k = 1, \dots, m+3, \\
\mathbf{p}_{3k+1} &= \mathbf{z}_{k-1} \frac{d_{k+2} \mathbf{z}_{k-1} + d_{k+1} \mathbf{z}_k}{d_{k+1} + d_{k+2}}, \quad k = 1, \dots, m+2, \\
\mathbf{p}_{3k+2} &= \mathbf{z}_k \frac{d_{k+2} \mathbf{z}_{k-1} + d_{k+1} \mathbf{z}_k}{d_{k+1} + d_{k+2}}, \quad k = 1, \dots, m+2, \\
\mathbf{p}_{3m+10} &= \frac{d_{m+5}}{d_{m+4} + d_{m+5}} \mathbf{z}_{m+2}^2, \\
\mathbf{p}_{3m+11} &= \mathbf{p}_{3m+12} = 0,
\end{aligned}$$

and the coefficients of the parametric speed  $\sigma(t)$  as

$$\begin{aligned}
\sigma_0 &= \sigma_1 = 0, \\
\sigma_2 &= \frac{d_1}{d_1+d_2} \mathbf{z}_0 \bar{\mathbf{z}}_0, \\
\sigma_{3k} &= \frac{1}{6} \frac{d_{k+1} d_{k+2}}{(d_k + d_{k+1})(d_{k+1} + d_{k+2})} (\mathbf{z}_{k-2} \bar{\mathbf{z}}_{k-1} + \mathbf{z}_{k-1} \bar{\mathbf{z}}_{k-2}) + \frac{1}{6} \frac{(d_{k+1})^2}{(d_k + d_{k+1})(d_{k+1} + d_{k+2})} (\mathbf{z}_{k-2} \bar{\mathbf{z}}_k + \mathbf{z}_k \bar{\mathbf{z}}_{k-2}) \\
&\quad + \left( \frac{2}{3} + \frac{1}{3} \frac{d_k d_{k+2}}{(d_k + d_{k+1})(d_{k+1} + d_{k+2})} \right) \mathbf{z}_{k-1} \bar{\mathbf{z}}_{k-1} + \frac{1}{6} \frac{d_k d_{k+1}}{(d_k + d_{k+1})(d_{k+1} + d_{k+2})} (\mathbf{z}_{k-1} \bar{\mathbf{z}}_k + \mathbf{z}_k \bar{\mathbf{z}}_{k-1}), \quad k = 1, \dots, m+3, \\
\sigma_{3k+1} &= \frac{d_{k+2}}{d_{k+1} + d_{k+2}} \mathbf{z}_{k-1} \bar{\mathbf{z}}_{k-1} + \frac{1}{2} \frac{d_{k+1}}{d_{k+1} + d_{k+2}} (\mathbf{z}_{k-1} \bar{\mathbf{z}}_k + \mathbf{z}_k \bar{\mathbf{z}}_{k-1}), \quad k = 1, \dots, m+2, \\
\sigma_{3k+2} &= \frac{1}{2} \frac{d_{k+2}}{d_{k+1} + d_{k+2}} (\mathbf{z}_{k-1} \bar{\mathbf{z}}_k + \mathbf{z}_k \bar{\mathbf{z}}_{k-1}) + \frac{d_{k+1}}{d_{k+1} + d_{k+2}} \mathbf{z}_k \bar{\mathbf{z}}_k, \quad k = 1, \dots, m+2, \\
\sigma_{3m+10} &= \frac{d_{m+5}}{d_{m+4} + d_{m+5}} \mathbf{z}_{m+2} \bar{\mathbf{z}}_{m+2}, \\
\sigma_{3m+11} &= \sigma_{3m+12} = 0.
\end{aligned}$$



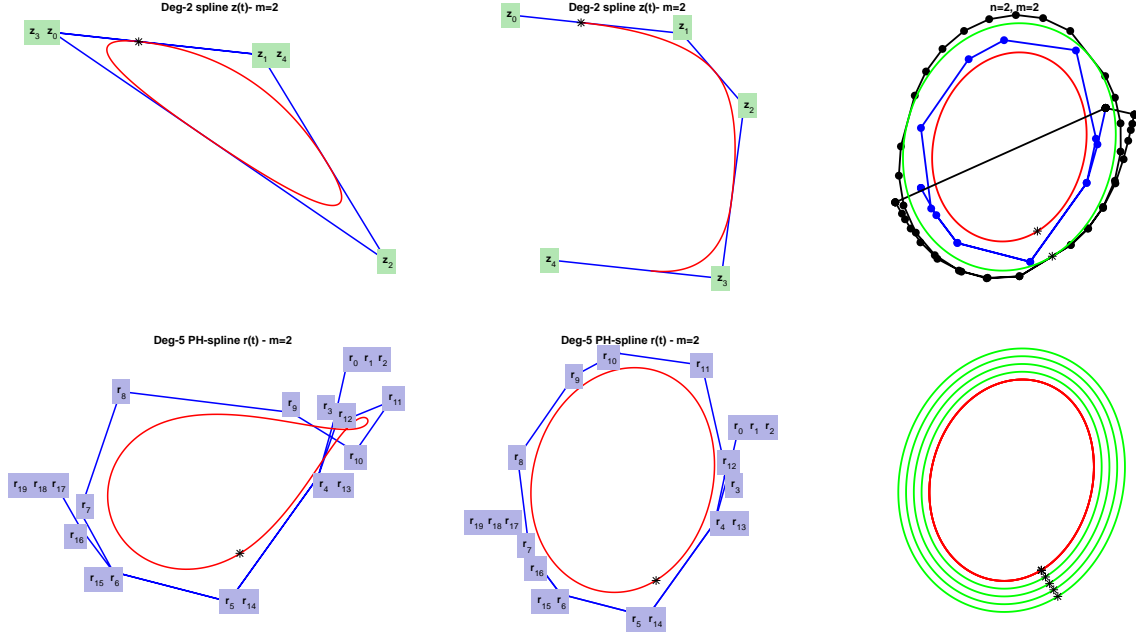


Figure 12: Closed quintic PH B-Spline curve with  $m = 2$  originated from a closed/open degree-2 spline  $\mathbf{z}(t)$  (first/second column) and offsets of the non self-intersecting curve with and without control polygon (third column).

Thus, according to (12), the closed quintic PH B-Spline curve defined over the knot partition  $\rho$  is given by

$$\mathbf{r}(t) = \sum_{i=0}^{3m+13} \mathbf{r}_i N_{i,\rho}^5(t), \quad t \in [t_2, t_{m+3}] \quad (t_0 = 0)$$

with control points

$$\begin{aligned} \mathbf{r}_2 &= \mathbf{r}_1 = \mathbf{r}_0, \\ \mathbf{r}_3 &= \mathbf{r}_2 + \frac{d_1}{5} \mathbf{z}_0^2, \\ \mathbf{r}_{3i+1} &= \mathbf{r}_{3i} + \frac{d_{i+1}}{5} \left( \frac{2}{3} \mathbf{z}_{i-1}^2 + \frac{1}{3} \left( \frac{d_{i+1} \mathbf{z}_{i-2} + d_i \mathbf{z}_{i-1}}{d_i + d_{i+1}} \right) \left( \frac{d_{i+2} \mathbf{z}_{i-1} + d_{i+1} \mathbf{z}_i}{d_{i+1} + d_{i+2}} \right) \right), \quad i = 1, \dots, m+3, \\ \mathbf{r}_{3i+2} &= \mathbf{r}_{3i+1} + \frac{d_{i+1}}{5} (d_{i+2} \mathbf{z}_{i-1} + d_{i+1} \mathbf{z}_i), \quad i = 1, \dots, m+2, \\ \mathbf{r}_{3i+3} &= \mathbf{r}_{3i+2} + \frac{d_i}{5} (d_{i+2} \mathbf{z}_{i-1} + d_{i+1} \mathbf{z}_i), \quad i = 1, \dots, m+2, \\ \mathbf{r}_{3m+11} &= \mathbf{r}_{3m+10} + \frac{d_{m+5}}{5} \mathbf{z}_{m+2}^2, \\ \mathbf{r}_{3m+13} &= \mathbf{r}_{3m+12} = \mathbf{r}_{3m+11}, \end{aligned}$$

and arbitrary  $\mathbf{r}_0$ . Note that, due to condition (19),  $d_{m+3} = d_2$ ,  $d_{m+4} = d_3$ . Moreover,  $\mathbf{z}_m, \mathbf{z}_{m+1}, \mathbf{z}_{m+2}$  must be suitably fixed in order to satisfy condition (18). According to (37) the total arc length of the closed PH B-Spline curve of degree 5 is given by

$$L = (l_{3m+7} - l_4) N_{4,\rho}^5(t_2) + (l_{3m+8} - l_5) N_{5,\rho}^5(t_2) + (l_{3m+9} - l_6) N_{6,\rho}^5(t_2),$$

where  $N_{4,\rho}^5(t_2) + N_{5,\rho}^5(t_2) + N_{6,\rho}^5(t_2) = 1$  and

$$\begin{aligned}
l_2 &= l_1 = l_0 = 0, \\
l_3 &= l_2 + \frac{d_1}{5} \mathbf{z}_0 \bar{\mathbf{z}}_0, \\
l_{3i+1} &= l_{3i} + \frac{2d_{i+1}}{15} \mathbf{z}_{i-1} \bar{\mathbf{z}}_{i-1} + \frac{d_{i+1}}{15(d_i+d_{i+1})(d_{i+1}+d_{i+2})} \left( d_i d_{i+2} \mathbf{z}_{i-1} \bar{\mathbf{z}}_{i-1} + \frac{d_{i+1}^2}{2} (\mathbf{z}_{i-2} \bar{\mathbf{z}}_i + \mathbf{z}_i \bar{\mathbf{z}}_{i-2}) \right. \\
&\quad \left. + \frac{d_{i+1} d_{i+2}}{2} (\mathbf{z}_{i-2} \bar{\mathbf{z}}_{i-1} + \mathbf{z}_{i-1} \bar{\mathbf{z}}_{i-2}) + \frac{d_{i+1}^2}{2} (\mathbf{z}_{i-1} \bar{\mathbf{z}}_i + \mathbf{z}_i \bar{\mathbf{z}}_{i-1}) \right), \quad i = 1, \dots, m+3, \\
l_{3i+2} &= l_{3i+1} + \frac{1}{5} \left( d_{i+2} \mathbf{z}_{i-1} \bar{\mathbf{z}}_{i-1} + \frac{d_{i+1}}{2} (\mathbf{z}_{i-1} \bar{\mathbf{z}}_i + \mathbf{z}_i \bar{\mathbf{z}}_{i-1}) \right), \quad i = 1, \dots, m+2, \\
l_{3i+3} &= l_{3i+2} + \frac{1}{5} \left( d_{i+1} \mathbf{z}_i \bar{\mathbf{z}}_i + \frac{d_{i+2}}{2} (\mathbf{z}_{i-1} \bar{\mathbf{z}}_i + \mathbf{z}_i \bar{\mathbf{z}}_{i-1}) \right), \quad i = 1, \dots, m+2, \\
l_{3m+11} &= l_{3m+10} + \frac{d_{m+5}}{5} \mathbf{z}_{m+2} \bar{\mathbf{z}}_{m+2}, \\
l_{3m+13} &= l_{3m+12} = l_{3m+11}.
\end{aligned}$$

Over the knot partition  $\tau$  the offset curve  $\mathbf{r}_h(t)$  has the rational B-Spline form

$$\mathbf{r}_h(t) = \frac{\sum_{k=0}^{8m+47} \mathbf{q}_k N_{k,\tau}^9(t)}{\sum_{k=0}^{8m+47} \gamma_k N_{k,\tau}^9(t)}, \quad t \in [t_2, t_{m+3}] \quad (60)$$

where, by exploiting the explicit expressions of the coefficients  $\{\rho_k^{i,j}\}_{0 \leq i \leq 3m+13, 0 \leq j \leq 3m+12, 0 \leq k \leq 8m+47}$  from (59), weights and control points can easily be obtained; their explicit formulae are reported in the Appendix.

Some examples of closed PH B-Spline curves of degree 5 are shown together with offsets in Figure 12.

## 6. A practical interpolation problem

We are concerned with  $C^2$  continuous quintic PH B-Spline curves defined by setting  $n = 2$  and  $m = 3$ . According to Corollary 1, starting from  $\mathbf{z}(t) = \sum_{i=0}^3 \mathbf{z}_i N_{i,\mu}^2(t)$  over the partition  $\mu = \{0, 0, 0, a, 1, 1, 1\}$ , we obtain the PH B-Spline curve

$$\mathbf{r}(t) = \sum_{i=0}^8 \mathbf{r}_i N_{i,\rho}^5(t), \quad t \in [0, 1], \quad (61)$$

over the knot vector  $\rho = \{0, 0, 0, 0, 0, 0, a, a, a, 1, 1, 1, 1, 1\}$  from (53).

We will now use these curves in order to solve the following practical interpolation problem, several variants of which have been of interest to the PH community up to date, see, e.g., [13–16, 20, 22].

**Problem 1.** *Given arbitrary points  $\mathbf{p}_0^*$ ,  $\mathbf{p}_1^*$ , tangents  $\mathbf{d}_0$ ,  $\mathbf{d}_1$  and curvature values  $\kappa_0$ ,  $\kappa_1$  to be interpolated by a PH quintic B-Spline curve from (61) such that*

$$\mathbf{r}(0) = \mathbf{p}_0^*, \quad \mathbf{r}(1) = \mathbf{p}_1^*, \quad \mathbf{r}'(0) = \mathbf{d}_0, \quad \mathbf{r}'(1) = \mathbf{d}_1, \quad \kappa(0) = \kappa_0, \quad \kappa(1) = \kappa_1,$$

we look for the control points  $\mathbf{r}_0, \mathbf{r}_1, \dots, \mathbf{r}_8$  of the curve (61).

According to (55) this means that we have to determine  $\mathbf{z}_0, \dots, \mathbf{z}_3$ . The positional interpolation constraints clearly imply  $\mathbf{r}_0 = \mathbf{p}_0^*$  and  $\mathbf{r}_8 = \mathbf{p}_1^*$ . According to (4), (8), (11) the tangential interpolation constraints yield the following conditions.

$$\mathbf{r}'(0) = \mathbf{z}^2(0) = \mathbf{p}_0 = \mathbf{z}_0^2 = \mathbf{d}_0, \quad \mathbf{r}'(1) = \mathbf{z}^2(1) = \mathbf{p}_7 = \mathbf{z}_3^2 = \mathbf{d}_1. \quad (62)$$

By applying de Moivre's theorem to the two equations in (62) we obtain the following solutions for  $\mathbf{z}_0$  and  $\mathbf{z}_3$ :

$$\begin{aligned}
\mathbf{z}_0 &= \pm |\mathbf{d}_0|^{\frac{1}{2}} \exp\left(i \frac{\omega_0}{2}\right) = \pm |\mathbf{d}_0|^{\frac{1}{2}} \left( \cos\left(\frac{\omega_0}{2}\right) + i \sin\left(\frac{\omega_0}{2}\right) \right), \\
\mathbf{z}_3 &= \pm |\mathbf{d}_1|^{\frac{1}{2}} \exp\left(i \frac{\omega_1}{2}\right) = \pm |\mathbf{d}_1|^{\frac{1}{2}} \left( \cos\left(\frac{\omega_1}{2}\right) + i \sin\left(\frac{\omega_1}{2}\right) \right),
\end{aligned} \quad (63)$$

where  $\omega_k = \arg(\mathbf{d}_k)$  for  $k = 0, 1$ .

Note that we can limit ourselves to considering the combinations of  $\mathbf{z}_0, \mathbf{z}_3$  with signs  $+, +$  and  $+, -$ , since the others will give rise to the same solutions. Next, recalling the general formula for the curvature of a PH curve (see, e.g., [20])

$$\kappa(t) = 2 \frac{\text{Im}(\bar{\mathbf{z}}(t) \mathbf{z}'(t))}{|\mathbf{z}(t)|^4}, \quad (64)$$

we can express the curvature constraints at  $t = 0$  and  $t = 1$  as

$$\kappa(0) = \frac{4}{a} \cdot \frac{\Im(\bar{\mathbf{z}}_0 \mathbf{z}_1)}{|\mathbf{z}_0|^4} = \frac{4}{a} \cdot \frac{u_0 v_1 - u_1 v_0}{(u_0^2 + v_0^2)^2} = \kappa_0, \quad \kappa(1) = \frac{4}{1-a} \cdot \frac{\Im(\bar{\mathbf{z}}_3 \mathbf{z}_2)}{|\mathbf{z}_3|^4} = \frac{4}{1-a} \cdot \frac{u_2 v_3 - u_3 v_2}{(u_3^2 + v_3^2)^2} = \kappa_1. \quad (65)$$

If  $u_0 \neq 0$  and  $u_3 \neq 0$ , we can derive  $v_1$  and  $v_2$  from (65), obtaining

$$v_1 = \frac{1}{u_0}(u_1 v_0 + \frac{a}{4} \kappa_0 (u_0^2 + v_0^2)^2), \quad v_2 = \frac{1}{u_3}(u_2 v_3 - \frac{(1-a)}{4} \kappa_1 (u_3^2 + v_3^2)^2). \quad (66)$$

If

$$u_0 = 0, \quad \text{respectively,} \quad u_3 = 0, \quad (67)$$

i.e., if  $\mathbf{d}_0$ , respectively,  $\mathbf{d}_1$  has the form  $(-const., 0)$ , we can not proceed as in (66). In this case, by exploiting the affine invariance of B-Spline curves, we propose to rotate the initial data in order to avoid the case (67). We can thus always assume  $u_0 \neq 0$  and  $u_3 \neq 0$ . To determine the remaining unknowns  $u_1$  and  $u_2$  in (66) we consider the equation

$$\mathbf{r}_7 - \mathbf{r}_1 = \sum_{i=1}^6 \Delta \mathbf{r}_i, \quad \text{with} \quad \Delta \mathbf{r}_i = \mathbf{r}_{i+1} - \mathbf{r}_i. \quad (68)$$

Since

$$\mathbf{r}'(0) = \frac{5}{a}(\mathbf{r}_1 - \mathbf{r}_0) = \mathbf{d}_0, \quad \mathbf{r}'(1) = \frac{5}{1-a}(\mathbf{r}_8 - \mathbf{r}_7) = \mathbf{d}_1 \quad (69)$$

the left hand side of equation (68) is completely determined by the given Hermite data as:

$$\mathbf{r}_7 - \mathbf{r}_1 = \mathbf{r}_8 - \mathbf{r}_0 - \frac{(1-a)}{5} \mathbf{d}_1 - \frac{a}{5} \mathbf{d}_0 = \mathbf{p}_1^* - \mathbf{p}_0^* - \frac{(1-a)}{5} \mathbf{d}_1 - \frac{a}{5} \mathbf{d}_0. \quad (70)$$

By (55) the right hand side of (68) reads

$$\frac{1}{5}(1 - \frac{a}{3})\mathbf{z}_1^2 + \frac{1}{15}(2 + a)\mathbf{z}_2^2 + \frac{1}{5}\mathbf{z}_1\mathbf{z}_2 + \frac{1}{15}(1 - a)^2\mathbf{z}_1\mathbf{z}_3 + \frac{1}{15}a(4 - a)\mathbf{z}_0\mathbf{z}_1 + \frac{1}{15}(3 - 2a - a^2)\mathbf{z}_2\mathbf{z}_3 + \frac{1}{15}a^2\mathbf{z}_0\mathbf{z}_2. \quad (71)$$

By separating the real and imaginary parts of this equation we obtain the following system of two real quadratic equations in the two real unknowns  $u_1$  and  $u_2$

$$(1, u_1, u_2)A \begin{pmatrix} 1 \\ u_1 \\ u_2 \end{pmatrix} = 0, \quad (1, u_1, u_2)B \begin{pmatrix} 1 \\ u_1 \\ u_2 \end{pmatrix} = 0, \quad (72)$$

with  $3 \times 3$  real symmetric matrices  $A = (a_{i,j})_{0 \leq i, j \leq 2}$  and  $B = (b_{i,j})_{0 \leq i, j \leq 2}$ , whose coefficients are reported in the Appendix. The two equations in (72) represent two conic sections in the real Euclidean plane. Finding the solutions  $u_1$  and  $u_2$  of these equations is equivalent to determining the intersection points of the two conic sections. In order to obtain them we consider the pencil of conic sections defined by the given conics as

$$(1, u_1, u_2)(A - \lambda B) \begin{pmatrix} 1 \\ u_1 \\ u_2 \end{pmatrix} = 0, \quad \lambda \in \mathbb{R}. \quad (73)$$

Among the one-parameter set of conics there are three degenerate conics given by the  $\lambda$ -values obtained as solutions of the cubic equation in  $\lambda$ :

$$\det(A - \lambda B) = -\lambda^3 \det(B) + \lambda^2(\det(B_3) + \det(B_2) + \det(B_1)) - \lambda(\det(A_3) + \det(A_2) + \det(A_1)) + \det(A) = 0, \quad (74)$$

where the matrices  $A_k$  for  $k = 1, 2, 3$  are obtained by replacing the  $k$ -th column of  $A$  by the  $k$ -th column of  $B$ , and the matrices  $B_k$  for  $k = 1, 2, 3$  are obtained by replacing the  $k$ -th column of  $B$  by the  $k$ -th column of  $A$ . These degenerate conics are pairs of intersecting lines. The intersection points of the conics of the pencil (73) are then easily obtained in the following way. For a solution of the cubic equation (74), by inserting the corresponding  $\lambda$ -value into the equation (73) a quadratic equation easily decomposable into two linear factors is obtained. These two linear equations in  $u_1$  and  $u_2$  can be solved for, e.g.,  $u_1$  in dependency of  $u_2$ , which are then inserted into another conic of the pencil, for example one of the given conics or another degenerate one, yielding a quadratic equation in  $u_2$ . We thus obtain the coordinates of the intersection points of the pencil conics. The control points of the corresponding PH B-Spline curves are obtained by inserting the obtained  $u_i, v_i, i = 0, \dots, 3$  into the expression for  $\mathbf{r}_i$  in (55). Let  $\delta^{++}$  respectively  $\delta^{+-}$  be the number of real intersection points of the conics from (72) for the sign choice  $++$  respectively  $+-$  in (63). Thus, the total number of solutions of our interpolation problem is  $\delta = \delta^{++} + \delta^{+-}$ . Among all solutions, as it is classical, see, e.g., [5, 9], the "good" curve is represented by the curve with minimum absolute rotation index and bending energy.

The following figures show the cubic curve interpolating the assigned values and derivatives and the different quintic PH B-spline curves determined as the solution of the Hermite interpolation problem, where the endpoint curvatures  $\kappa_0$  and  $\kappa_1$  are sampled from the cubic curve. The corresponding conics with coefficient matrices  $A$  and  $B$  from (72) and a degenerate conic of the pencil corresponding to a pair of lines are also displayed.

### 6.1. Existence of solutions

In the following we discuss the problem of studying the existence of a solution for Problem 1. Assigned a set of values, tangents and curvatures, there are two situations where a solution may not be found. The first corresponds to the case where either  $A$  or  $B$  (or both) in (72) yield imaginary conics. The second is the case where the two conics in (72) are real, but have no intersection. The latter situation has never been encountered in our experiments. Thus we will focus on discussing the former problematic case. In particular we will consider the following problem. Suppose that points  $\mathbf{p}_0^*, \mathbf{p}_1^*$  and tangents  $\mathbf{d}_0, \mathbf{d}_1$  are given, how shall we prescribe the curvatures  $\kappa_0, \kappa_1$  in order to guarantee that  $A$  and  $B$  represent real conics?

Type of conic	$I_3^{[M]}$	$I_2^{[M]}$	$I_1^{[M]}$
Ellipse	$\neq 0$	$> 0$	$I_1^{[M]} I_3^{[M]} < 0$
Hyperbola	$\neq 0$	$< 0$	–
Parabola	$\neq 0$	$= 0$	–
Non-degenerate imaginary conic	$\neq 0$	$> 0$	$I_1^{[M]} I_3^{[M]} > 0$
Pair of intersecting real lines	$= 0$	$< 0$	–
Pair of intersecting imaginary lines	$= 0$	$> 0$	–
Pair of parallel real lines	$= 0, \text{rank}(I_3^{[M]}) = 2$	$= 0$	$< 0$
Pair of parallel imaginary lines	$= 0, \text{rank}(I_3^{[M]}) = 2$	$= 0$	$> 0$
Double line (pair of coinciding real lines)	$= 0, \text{rank}(I_3^{[M]}) = 1$	$= 0$	–

Table 2: Classification of conic sections.

For a generic conic  $C_M : m_{1,1}u_1^2 + 2m_{1,2}u_1u_2 + m_{2,2}u_2^2 + 2m_{0,1}u_1 + 2m_{0,2}u_2 + m_{0,0} = 0$  with symmetric matrix  $M := (m_{i,j})_{0 \leq i,j \leq 2}, m_{i,j} = m_{j,i}$ , we suppose  $m_{0,0} \geq 0$  and we denote by  $\tilde{M} := (m_{i,j})_{1 \leq i,j \leq 2}$  the  $2 \times 2$  matrix of the associated quadratic form. We then consider the following invariants:

$$I_1^{[M]} := \text{trace}(\tilde{M}), \quad I_2^{[M]} := \det(\tilde{M}), \quad I_3^{[M]} := \det(M). \quad (75)$$

Then, according to Table 2  $C_M$  represents an imaginary conic in the following cases:

- P1  $I_3^{[M]} \neq 0, I_2^{[M]} > 0, I_1^{[M]} I_3^{[M]} > 0$  ( $C_M$  is a non-degenerate imaginary conic);
- P2  $I_3^{[M]} = 0, I_2^{[M]} > 0$  ( $C_M$  is a pair of intersecting imaginary lines);
- P3  $I_3^{[M]} = 0, \text{rank}(I_3^{[M]}) = 2, I_2^{[M]} = 0, I_1^{[M]} > 0$ . ( $C_M$  is a pair of parallel imaginary lines).

When choosing  $\kappa_0, \kappa_1$  we shall then avoid that  $C_A$  or  $C_B$  fall into one of the points above. To this aim, it is useful to observe that for  $M \in \{A, B\}$ ,  $I_1^{[M]}$  and  $I_2^{[M]}$  depend on the location of knot  $a$  only, whereas  $I_3^{[M]}$  depends on  $a, \kappa_0, \kappa_1$ , see the formulae of the coefficients of  $A$  and  $B$  in the Appendix. For a fixed value of  $a$ , the sign of  $I_1^{[M]}$  and  $I_2^{[M]}$  is thus determined, whereas  $I_3^{[M]} = 0$  is a quadratic equation in the two unknowns  $\kappa_0, \kappa_1$ . The general idea would thus be to first choose the value of  $a$  and based on the corresponding signs of  $I_1^{[M]}$  and  $I_2^{[M]}$ , fix  $\kappa_0, \kappa_1$  in order to prevent that  $M$  falls into one of the items above. We will illustrate the idea by means of the four test cases contained in Examples 1 to 4. This is not an exhaustive discussion of all the possible forms of the two conics  $C_A$  and  $C_B$ , but it suffices to illustrate the general criterion for choosing suitable values of  $a, \kappa_0$  and  $\kappa_1$ . The general procedure is summarized in Algorithm 1.

---

**Algorithm 1** Algorithm for the solution of an Hermite interpolation problem with given interpolation points  $\mathbf{p}_0^*, \mathbf{p}_1^*$  and tangents at these points  $\mathbf{d}_0, \mathbf{d}_1$ .

---

**Input:** interpolation points  $\mathbf{p}_0^*, \mathbf{p}_1^*$  and tangents at these points  $\mathbf{d}_0, \mathbf{d}_1$ .

From (62) and (63) determine all possible values  $\mathbf{z}_0$  and  $\mathbf{z}_3$ , i.e.  $u_0, v_0, u_3, v_3$ , and for each combination with signs  $+, +$  or  $+, -$  in (63) perform the following steps:

1. compute the matrices  $A$  and  $B$  of the two conics in (72). These matrices will depend on the parameters  $a, \kappa_0$  and  $\kappa_1$ ;
2. choose the value of the knot  $a \in (0, 1)$  and compute  $I_1^{[M]}, I_2^{[M]}$ , for  $M = A, B$ . Since these quantities depend on  $a$  only, their sign is determined;
3. Choose  $\kappa_0$  and  $\kappa_1$  in such a way that both  $C_A$  and  $C_B$  are real. In particular,  $C_A$  or  $C_B$  (or both) may represent an imaginary conic when  $I_2^{[A]} > 0$  or  $I_2^{[B]} > 0$  (or both).  $I_3^{[M]} = 0, M = A, B$  is a quadratic function of  $\kappa_0$  and  $\kappa_1$  and represents a conic in the Euclidean plane. Plotting the graph of  $I_3^{[M]} = 0$ , we can choose  $\kappa_0$  and  $\kappa_1$  in the region where the relative signs of  $I_1^{[M]}, I_2^{[M]}$  and  $I_3^{[M]}$  yield a real conic.
4. Solve the system (72) for  $u_1$  and  $u_2$ .
5. For each solution of the system (72), compute  $v_1$  and  $v_2$  from (66). The obtained values  $u_i, v_i, i = 0, \dots, 3$  completely determine a set of complex coefficients  $\mathbf{z}_i, i = 1, \dots, 3$  and thus identify one PH B-spline curve.

**Output:** PH B-spline curves corresponding to the given initial data.

---

**Example 1.** Let us consider the initial data  $\mathbf{p}_0^* = (1, 0), \mathbf{p}_1^* = (3, 0.5), \mathbf{d}_0 = (1, -1), \mathbf{d}_1 = (0.2, 3)$ . Using these data, from (63) we can compute  $\mathbf{z}_0$  and  $\mathbf{z}_3$  (namely  $u_0, v_0, u_3, v_3$ ). For any combination of  $\mathbf{z}_0$  and  $\mathbf{z}_3$  to be considered, i.e. taking signs  $+, +$  and  $+, -$  in (63), we should proceed to computing the intersection of the two conics in equation (72). Each intersection point of  $C_A$  and  $C_B$  will give rise to a solution for  $u_1, v_1, u_2, v_2$ .

The first couple of values corresponds to signs  $+, +$ . In this case, any choice of  $a$  in  $(0, 1)$  yields  $I_1^{[A]} > 0, I_2^{[A]} < 0, I_1^{[B]} > 0, I_2^{[B]} < 0$ . Hence, both  $C_A$  and  $C_B$  are real conics, independently on the choice of  $a, \kappa_0$  and  $\kappa_1$ . In particular, we will set  $a = 0.5$ , and sample the curvature values from the cubic polynomial interpolating  $\mathbf{p}_0^*, \mathbf{p}_1^*$  and  $\mathbf{d}_0, \mathbf{d}_1$ , which results in  $\kappa_0 = 3.040559$  and  $\kappa_1 = 1.066953$ . The two conics  $C_A$  and  $C_B$  are displayed in the left part of Figure 13, while the center and right figures show the PH B-spline curves corresponding to the two intersection points of the conics.

The second couple of values corresponds to signs  $+, -$ . In this setting  $I_1^{[M]}, I_2^{[M]}, M \in \{A, B\}$ , have the same signs as for the previous case. Choosing the same values for  $a, \kappa_0$  and  $\kappa_1$ ,  $C_A$  and  $C_B$  turn out to be the two hyperbolas plotted in the left part of Figure 14, whereas the PH B-spline curves corresponding to each of their intersection points are shown in the center and right part of the figure.

Based on the absolute rotation index and bending energy, displayed in Figures 13 and 14, the best obtained PH B-spline curve turns out to be the one in the center of Figure 13.

**Example 2.** Let us consider the initial data  $\mathbf{p}_0^* = (-6, -1), \mathbf{p}_1^* = (1, 0), \mathbf{d}_0 = (30, 25), \mathbf{d}_1 = (25, -30)$ . Using these data, from (63) we can compute  $\mathbf{z}_0$  and  $\mathbf{z}_3$  (namely  $u_0, v_0, u_3, v_3$ ). For any combination of  $\mathbf{z}_0$  and  $\mathbf{z}_3$  to be considered,

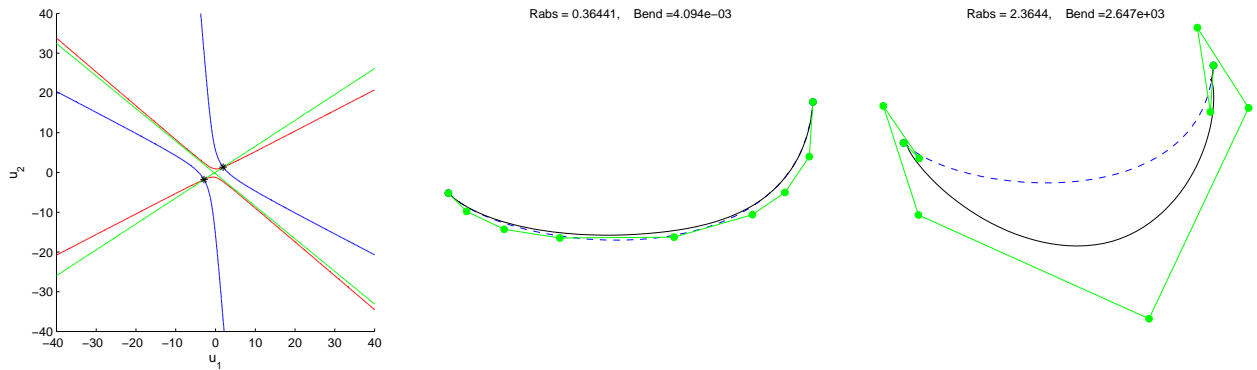


Figure 13: Illustration of Example 1, case ++. Left: The two conics  $C_A$  (blue) and  $C_B$  (red) and a degenerate conic (green). Center and right: The PH B-spline curves (black) corresponding to the two intersection points of the conics marked with an asterisk. The dashed curve is the cubic polynomial interpolating  $\mathbf{p}_0^*$ ,  $\mathbf{p}_1^*$ ,  $\mathbf{d}_0$ ,  $\mathbf{d}_1$ . The values of the absolute rotation index  $Rabs$  and the bending energy  $Bend$  of the PH B-Spline curves are also displayed.

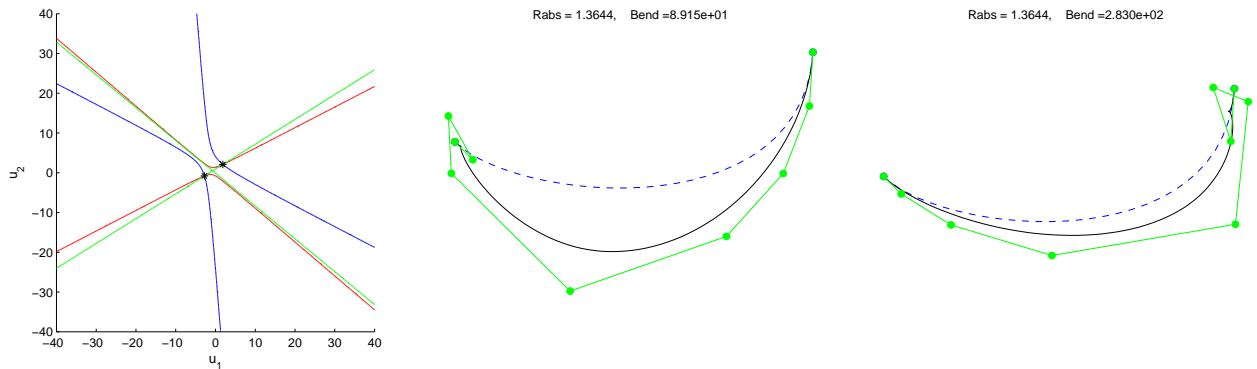


Figure 14: Illustration of Example 1, case +-. Left: The two conics  $C_A$  (blue) and  $C_B$  (red) and a degenerate conic (green). Center and right: The PH B-spline curves (black) corresponding to the two intersection points of the conics marked with an asterisk. The dashed curve is the cubic polynomial interpolating  $\mathbf{p}_0^*$ ,  $\mathbf{p}_1^*$ ,  $\mathbf{d}_0$ ,  $\mathbf{d}_1$ . The values of the absolute rotation index  $Rabs$  and the bending energy  $Bend$  of the PH B-Spline curves are also displayed.

*i.e.* taking signs  $+, +$  and  $+, -$  in (63), we should proceed to computing the intersection of the two conics in equation (72).

The first couple of values corresponds to signs  $+, +$ . In this case, for any  $a \in (0, 1)$ ,  $I_1^{[A]}$  and  $I_2^{[A]}$  are both positive, whereas  $I_1^{[B]}$  and  $I_2^{[B]}$  are both negative. Hence the choice of  $a$  does not influence the signs of these quantities. To proceed we set  $a = 0.5$ . According to the signs of  $I_1^{[B]}$  and  $I_2^{[B]}$ , the conic with matrix  $B$  is an hyperbola, and thus it is a real conic for any choice of  $\kappa_0$  and  $\kappa_1$ .

We shall now investigate whether the conic  $C_A$  may fall into cases P1 or P2 (case P3 is excluded given that  $I_2^{[A]} > 0$ .) To this aim, let us consider the conic  $I_3^{[A]} = 0$ . This is an imaginary conic and in particular  $I_3^{[A]} < 0$  for any  $\kappa_0$  and  $\kappa_1$ . The conic  $C_A$  is thus always a real ellipse.

Since we have no constraint for choosing  $\kappa_0$  and  $\kappa_1$ , we can set them to the curvatures of the cubic polynomial that interpolates  $\mathbf{p}_0^*$ ,  $\mathbf{p}_1^*$ ,  $\mathbf{d}_0$  and  $\mathbf{d}_1$ , which yields  $\kappa_0 = 0.0366$  and  $\kappa_1 = 0.0275$ .

Accordingly, the two conics  $C_A$  and  $C_B$  are represented in Figure 15, left. The green lines correspond to a degenerate conic of the pencil of conic sections (73) and the asterisk markers identify the solutions of system (72). There are thus two solutions which correspond to the PH B-spline curves depicted in Figure 15 (solid line), whereas the dashed line corresponds to the cubic polynomial from which the curvature values were sampled.

Concerning the second couple of values, corresponding to signs  $+, -$  in (63), the signs of  $I_1^{[A]}$ ,  $I_2^{[A]}$  and  $I_1^{[B]}$ ,  $I_2^{[B]}$

are the same as for the previous case and similarly, by setting  $a = 0.5$ ,  $I_2^{[A]}$  is always negative. We can thus choose the same curvature values, obtaining the two conics displayed in Figure 16. This time we have four intersection points, each of which yields one of the curves in the figure.

Among all the solutions shown in Figures 15 and Figures 16, which correspond to the same set of initial data  $\mathbf{p}_0^*$ ,  $\mathbf{p}_1^*$ ,  $\mathbf{d}_0$ ,  $\mathbf{d}_1$ ,  $\kappa_0$ ,  $\kappa_1$ , the best curve can be identified from a study of the absolute rotation index and bending energy and corresponds to the rightmost curve in Figure 16.

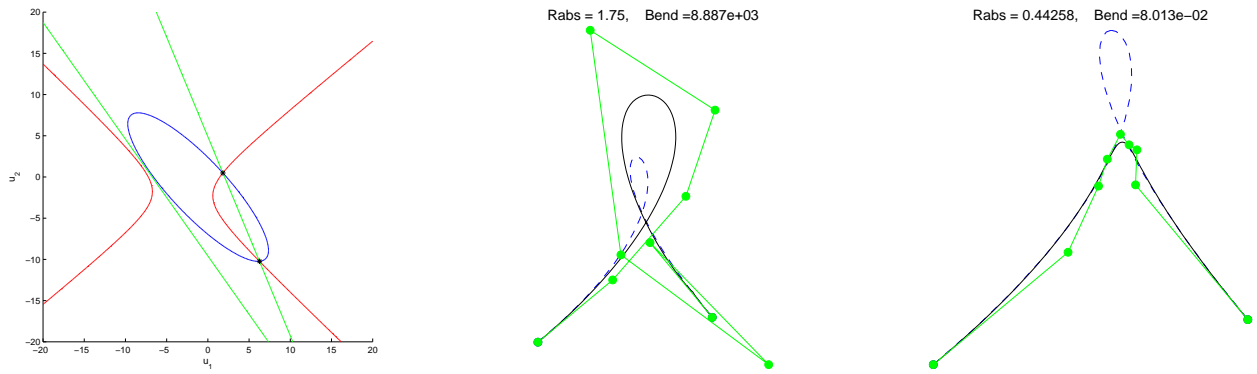


Figure 15: Illustration of Example 2, case ++. Left: The two conics  $C_A$  (blue) and  $C_B$  (red), a degenerate conic of the pencil (green); Center and right: PH B-spline curves (black) corresponding to the two intersection points and cubic polynomial (dashed, blue) interpolating the given endpoints and tangents, together with the values of the absolute rotation index and bending energy of the PH B-Spline curves.

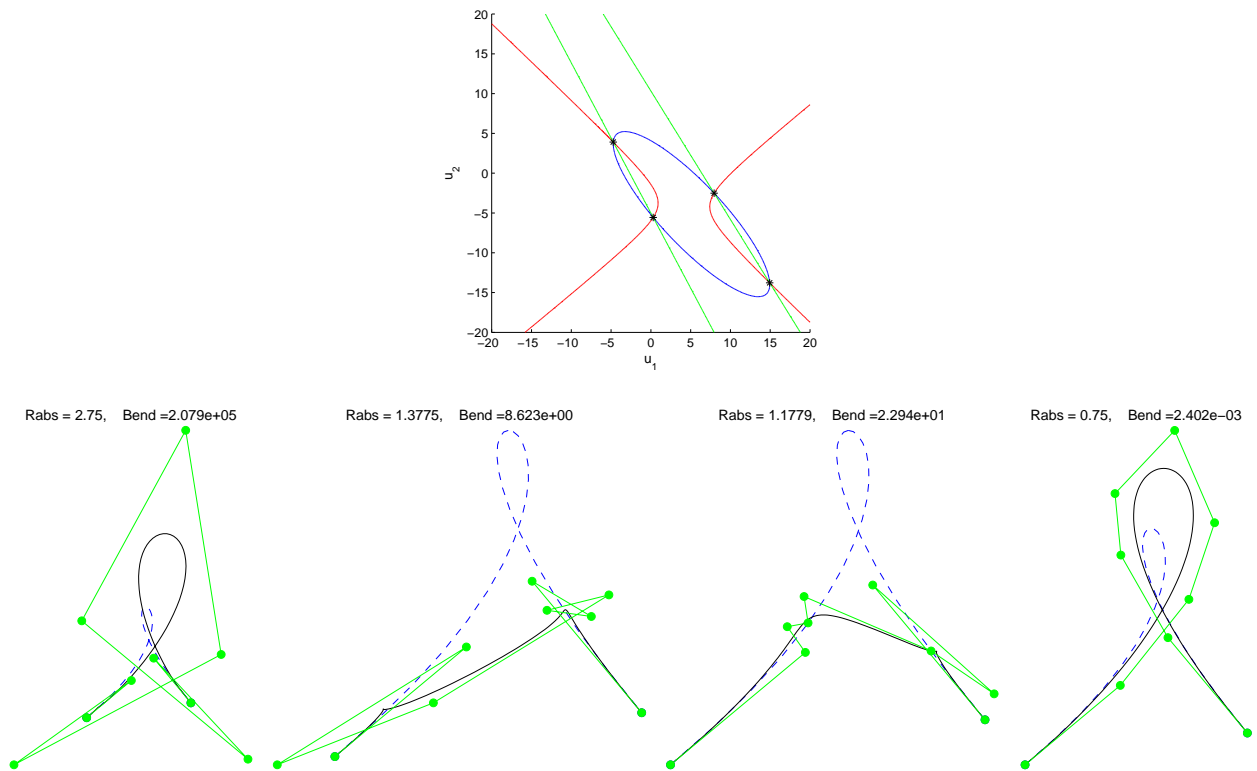


Figure 16: Illustration of Example 2, case +-. Top: The two conics  $C_A$  (blue) and  $C_B$  (red), a degenerate conic of the pencil (green); Bottom: PH B-spline curves (black) corresponding to the four intersection points and cubic polynomial (dashed, blue) interpolating the given endpoints and tangents, together with the values of the absolute rotation index and bending energy of the PH B-Spline curves.



**Example 3.** Let us consider the initial data  $\mathbf{p}_0^* = (0, 0)$ ,  $\mathbf{p}_1^* = (1, 0)$ ,  $\mathbf{d}_0 = (-3, 1)$ ,  $\mathbf{d}_1 = (-3, -1)$ . Using these data, we can compute  $u_0, v_0, u_3, v_3$  and for any combination of these values to be considered, i.e. corresponding to signs  $+, +$  and  $+, -$  in (63), we should proceed to computing the intersections of the two conics in equation (72).

The first couple of values corresponds to signs  $+, +$ . In this case, any choice of  $a \in (0, 1)$  yields  $I_1^{[A]} < 0$ ,  $I_2^{[A]} > 0$  and  $I_2^{[B]} < 0$ . The conic  $C_B$  is thus never imaginary and there remains to determine  $\kappa_0$  and  $\kappa_1$  such that  $I_3^{[A]} > 0$  and thus the conic  $C_A$  is a real ellipse. On account of the symmetry of the initial data it seems logical to set  $a = 0.5$ . Accordingly, the implicit curve  $I_3^{[A]} = 0$  is plotted in Figure 17, from which we can infer that  $I_3^{[A]} > 0$  in the region external to the plot. The curvatures of the cubic polynomial which interpolates the initial data have both the value  $-0.569210$  and do not belong to the feasible region. We will thus choose  $\kappa_0$  and  $\kappa_1$  so as to preserve the symmetry of the data and be as close as possible to the curvatures of the cubic polynomial. For example, setting  $\kappa_0 = \kappa_1 = -2.5$  we get the two conics  $C_A$  and  $C_B$  displayed in Figure 17 (note that  $B$  is precisely a degenerate conic of the pencil.)

The conics have two intersection points each of which corresponds to one of the two curves plotted in the bottom row of the figure.

We perform a similar study for the second couple of values, corresponding to signs  $+, -$  in (63). For  $a = 0.5$ , the situation is similar as above, i.e.  $I_1^{[A]} < 0$ ,  $I_2^{[A]} > 0$  and  $I_2^{[B]} < 0$ . The conic  $C_B$  is never imaginary, thus we can limit ourselves to investigating when  $A$  is an imaginary conic. Taking into exam the plot of  $I_3^{[A]} = 0$  in Figure 18, it can be seen that the previously used values  $\kappa_0 = \kappa_1 = -2.5$  do not belong to the admissible region, which is where  $I_3^{[A]} > 0$ . A set of feasible curvature values, e.g., is  $\kappa_0 = \kappa_1 = -5$ , which result in the conics  $C_A$  and  $C_B$  in Figure 18 ( $C_B$  is a degenerate conic of the pencil). The PH B-spline curves corresponding to the two intersection points are displayed in the same figure. Comparing the obtained curves in Figures 17 and 18, we choose the first one in Figure 17 according to its absolute rotation index and bending energy.

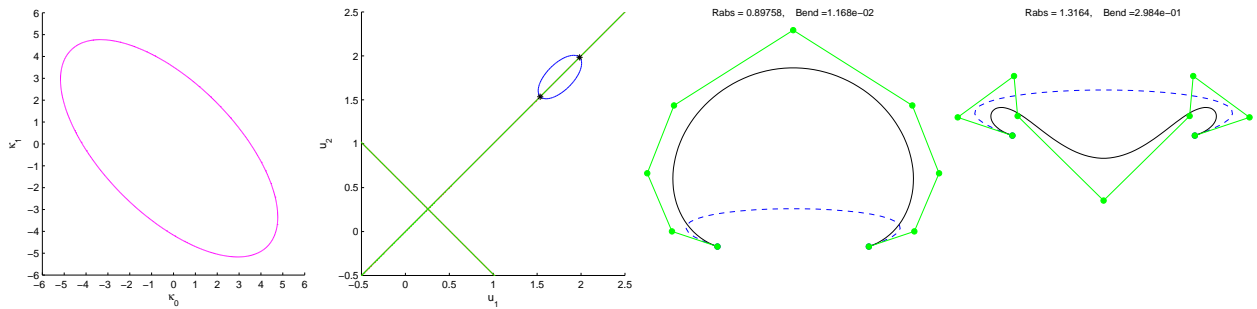


Figure 17: Illustration of Example 3, case  $++$ . From left to right: The conic  $I_3^{[A]} = 0$ ; The two conics  $C_A$  and  $C_B$  (a degenerate conic of the pencil coincides with  $C_B$ ); PH B-spline curves (black) corresponding to the intersection points and cubic polynomial (dashed, blue) interpolating the given endpoints and tangents, together with the values of the absolute rotation index and bending energy of the PH B-Spline curves.

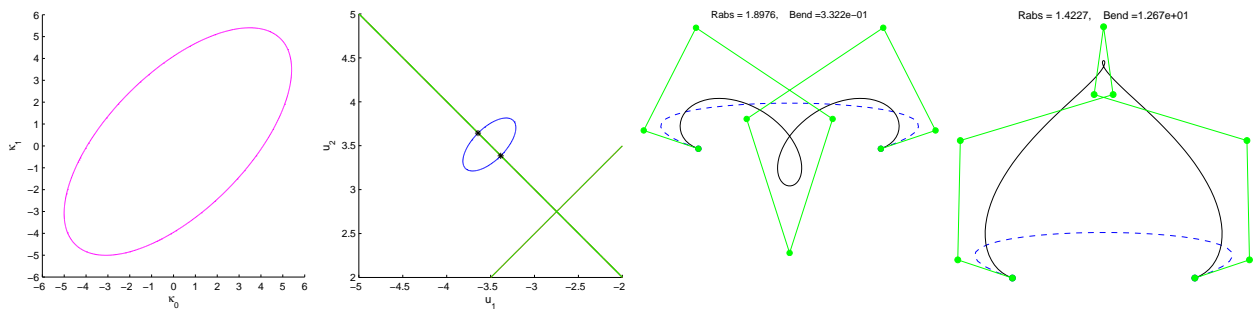


Figure 18: Illustration of Example 3, case  $+-$ . From left to right: The conic  $I_3^{[A]} = 0$ ; The two conics  $C_A$  and  $C_B$  (a degenerate conic of the pencil coincides with  $C_B$ ); PH B-spline curves (black) corresponding to the intersection points and cubic polynomial (dashed, blue) interpolating the given endpoints and tangents, together with the values of the absolute rotation index and bending energy of the PH B-Spline curves.

**Example 4.** Let us consider the initial data  $\mathbf{p}_0^* = (0, 5)$ ,  $\mathbf{p}_1^* = (-3, 4)$ ,  $\mathbf{d}_0 = (25, -15)$ ,  $\mathbf{d}_1 = (25, -15)$ . Using these data, we can compute  $u_0, v_0, u_3, v_3$  and for any combination of these values to be considered, i.e. corresponding to signs  $+, +$  and  $+, -$  in (63), we should proceed to computing the intersection of the two conics in equation (72).

The first couple of values corresponds to signs  $+, +$ . In this case, any choice of  $a$  in  $(0, 1)$  yields  $I_1^{[A]} > 0, I_2^{[A]} > 0, I_1^{[B]} < 0, I_2^{[B]} > 0$ . Hence we set  $a = 0.5$  (this is a natural choice given the symmetry of the data) and accordingly we study the sign of  $I_3^{[A]}$  and  $I_3^{[B]}$ . The equation  $I_3^{[B]} = 0$  describes an imaginary conic and in particular  $I_3^{[B]} > 0$  for any  $\kappa_0$  and  $\kappa_1$ . This condition guarantees that  $B$  is a real ellipse. The implicit curve defined by  $I_3^{[A]} = 0$  is the ellipse plotted in Figure 19, left. Considering that  $I_1^{[A]} > 0$ , we shall then choose  $\kappa_0$  and  $\kappa_1$  in such a way that  $I_3^{[A]} < 0$ , which corresponds to all values external to the ellipse displayed in Figure 19, left.

The curvatures of the cubic polynomial which interpolates the initial data are equal to  $-0.065371$  at  $\mathbf{p}_0^*$  and  $0.065371$  at  $\mathbf{p}_1^*$  and thus they do not belong to the admissible region  $I_3^{[A]} < 0$ . By analogy with the curvatures of the cubic polynomial, which have the same absolute value and opposite sign, we will set  $\kappa_0 = -0.2$  and  $\kappa_1 = 0.2$ . This choice results in the two conics  $C_A$  and  $C_B$  displayed in the Figure 19. The conics have two intersection points each of which corresponds to one of the two curves plotted in the figure.

We perform a similar study for the second couple of values, corresponding to signs  $+, -$  in (63). For any  $a \in (0, 1)$ , the situation is similar as above, i.e.  $I_1^{[A]} > 0, I_2^{[A]} > 0$  and  $I_1^{[B]} < 0, I_2^{[B]} > 0$ . The conic  $C_B$  is never imaginary, thus we can limit ourselves to investigating when  $A$  is an imaginary conic. Setting  $a = 0.5$  and taking into exam the plot of  $I_3^{[A]} = 0$  in Figure 20, left, it can be seen that the previously used values  $\kappa_0 = -0.2$  and  $\kappa_1 = 0.2$  do not belong to the admissible region, which is where  $I_3^{[A]} < 0$ . By similarity with the curvatures of the cubic polynomial, we choose  $\kappa_0$  and  $\kappa_1$  having equal absolute value and opposite sign, e.g.,  $\kappa_0 = -0.4$  and  $\kappa_1 = 0.4$ . This results in the conics  $C_A$  and  $C_B$  in Figure 20. The PH B-spline curves corresponding to the two intersection points are depicted in the same figure. Overall, the four curves obtained in this example have similar absolute rotation number and bending energy.

## 7. Conclusions and future work

We have presented the construction of the very general class of Pythagorean-Hodograph (PH) B-Spline curves. A computational strategy for efficiently calculating their control points as well as their arc-length and offset curves has been proposed. Moreover, for the cases of cubic and quintic clamped and closed PH B-Spline curves, an explicit representation of their control points, their arc-length and their offsets has been provided. Finally, clamped quintic PH B-Spline curves have been exploited to solve a second order Hermite interpolation problem, in order to show an example of practical application of this new class of curves. This new class of curves has a great potential for applications in computer-aided design and manufacturing, robotics, motion control, path planning, computer graphics, animation, and related fields.

The generalization of these planar PH B-Spline curves to 3-space is currently under investigation. In virtue of their high generality and their unique advantages we hope that these curves will be widely used in practice. Among other things, in the future we envisage using these curves for solving different interpolation and approximation problems in the context of reverse engineering applications. It might also be interesting to generalize the idea of the paper [6] to understand if a given B-Spline curve is a PH B-Spline curve and to recover its related complex pre-image spline  $\mathbf{z}(t)$ .

## References

- [1] G. Albrecht and R. T. Farouki. Construction of  $C^2$  Pythagorean-hodograph interpolating splines by the homotopy method. *Advances in Computational Mathematics*, 5:417–442, 1996.
- [2] X. Che, G. Farin, Z. Gao, and D. Hansford. The product of two B-spline functions. *Advanced Materials Research*, 186:445–448, 2011.
- [3] C. de Boor. *A Practical Guide to Splines*. Springer, Applied Mathematical Sciences Vol. 27, New York, Berlin, 2001.
- [4] R.T. Farouki. The conformal map  $z \rightarrow z^2$  of the hodograph plane. *Computer Aided Geometric Design*, 11:363–390, 1994.
- [5] R.T. Farouki. The elastic bending energy of Pythagorean-hodograph curves. *Computer Aided Geometric Design*, 13:227–241, 1996.
- [6] R.T. Farouki, C. Giannelli, and A. Sestini. Identification and “reverse engineering” of Pythagorean-hodograph curves. *Computer Aided Geometric Design*, 34:21–36, 2015.
- [7] R.T. Farouki, C. Giannelli, and A. Sestini. Local modification of pythagorean-hodograph quintic spline curves using the B-spline form. *Adv. Comput. Math.*, 42(1):199–225, 2016.
- [8] R.T. Farouki, B.K. Kuspa, C. Manni, and A. Sestini. Efficient solution of the complex quadratic tridiagonal system for  $C^2$  PH quintic splines. *Numerical Algorithms*, 27:35–60, 2001.

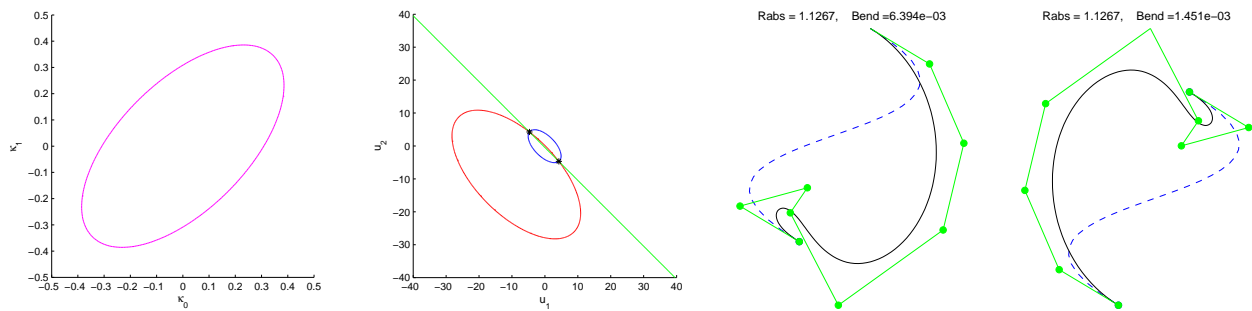


Figure 19: Illustration of Example 4, case ++. From left to right: The conic  $I_3^{[A]} = 0$ ; The two conics  $C_A$  and  $C_B$  (a degenerate conic of the pencil is formed by two coincident lines); PH B-spline curves (black) corresponding to the intersection points and cubic polynomial (dashed, blue) interpolating the given endpoints and tangents, together with the values of the absolute rotation index and bending energy of the PH B-Spline curves.

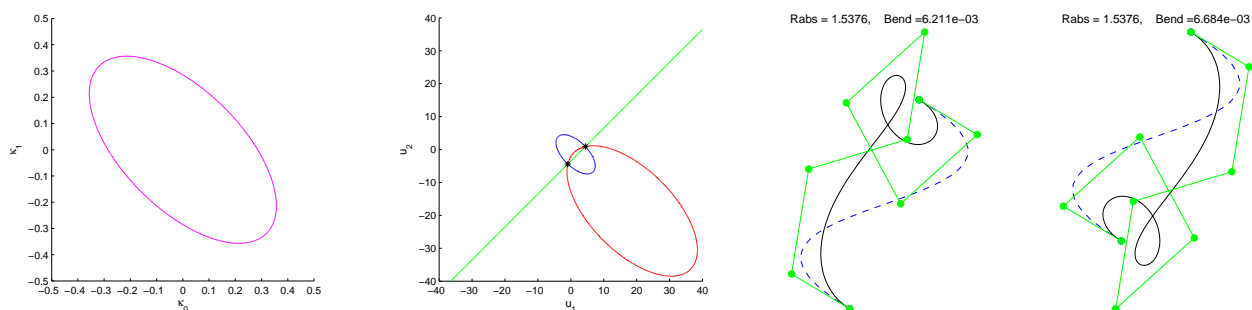


Figure 20: Illustration of Example 4, case +-+. From left to right: The conic  $I_3^{[A]} = 0$ ; The two conics  $C_A$  and  $C_B$  (a degenerate conic of the pencil is formed by two coincident lines); PH B-spline curves (black) corresponding to the intersection points and cubic polynomial (dashed, blue) interpolating the given endpoints and tangents, together with the values of the absolute rotation index and bending energy of the PH B-Spline curves.

- [9] R.T. Farouki and C.A. Neff. Hermite interpolation by pythagorean hodograph quintics. *Math. Comp.*, 64(212):1589–1609, 1995.
- [10] R.T. Farouki and T. Sakkalis. Pythagorean hodographs. *IBM J. Res. Develop.*, 34:736–752, 1990.
- [11] J. Gallier. *Curves and surfaces in geometric modeling*. Morgan Kaufmann Publishers, San Francisco, California, 2000.
- [12] J. Hoschek and D. Lasser. *Fundamentals of Computer Aided Geometric Design*. A K Peters, Wellesley, Massachusetts, 1996.
- [13] G. Jaklic, J. Kozak, M. Krajnc, V. Vitrih, and E. Zagar. On interpolation by planar cubic  $G^2$  Pythagorean-hodograph spline curves. *Mathematics of Computation*, 79(269):305–326, 2010.
- [14] G. Jaklic, J. Kozak, M. Krajnc, V. Vitrih, and E. Zagar. Interpolation by  $G^2$  quintic Pythagorean-hodograph curves. *Numerical Mathematics: Theory, Methods and Applications*, 7(3):374–398, 2014.
- [15] B. Jüttler. Hermite interpolation by pythagorean hodograph curves of degree seven. *Mathematics of Computation*, 70:1089–1111, 2001.
- [16] J.H. Kong, S.P. Jeong, and G.I. Kim. Hermite interpolation using PH curves with undetermined junction points. *Bull. Korean Math. Soc.*, 49:175–195, 2012.
- [17] R.S. Martin and J.H. Wilkinson. Symmetric decomposition of positive definite band matrices. *Numerische Mathematik*, 7:355–361, 1965.
- [18] K. Mörken. Some identities for products and degree raising of splines. *Constructive Approximation*, 7:195–208, 1991.
- [19] F. Pelosi, M.L. Sampoli, R.T. Farouki, and C. Manni. A control polygon scheme for design of planar  $C^2$  PH quintic spline curves. *Computer Aided Geometric Design*, 24:28–52, 2007.
- [20] L. Romani, L. Saini, and G. Albrecht. Algebraic-trigonometric Pythagorean-Hodograph curves and their use for Hermite interpolation. *Advances in Computational Mathematics*, 40(5-6):977–1010, 2014.
- [21] I.J. Schoenberg. Contributions to the problem of approximation of equidistant data by analytic functions. *Quart. Appl. Math.*, 4:45–99 and 112–141, 1946.
- [22] D.J. Walton and D.S. Meek.  $G^2$  curve design with a pair of Pythagorean Hodograph quintic spiral segments. *Computer Aided Geometric Design*, 24:267–285, 2007.

## 8. Appendix

In this section we report some voluminous formulae of the preceding sections.

### Section 5

The weights and control points of the offset curves  $\mathbf{r}_h(t)$  of the clamped cubic PH B-Spline curves ( $n = 1$ ) from (52) in section 5.1 are given by:

$$\begin{aligned}\gamma_{5k} &= \sigma_{2k}, \quad k = 0, 1, \dots, m, \\ \gamma_{5k+1} &= \frac{3}{5}\sigma_{2k} + \frac{2}{5}\sigma_{2k+1}, \quad k = 0, 1, \dots, m-1, \\ \gamma_{5k+2} &= \frac{3}{10}\sigma_{2k} + \frac{3}{5}\sigma_{2k+1} + \frac{1}{10}\sigma_{2k+2}, \quad k = 0, 1, \dots, m-1, \\ \gamma_{5k+3} &= \frac{1}{10}\sigma_{2k} + \frac{3}{5}\sigma_{2k+1} + \frac{3}{10}\sigma_{2k+2}, \quad k = 0, 1, \dots, m-1, \\ \gamma_{5k+4} &= \frac{2}{5}\sigma_{2k+1} + \frac{3}{5}\sigma_{2k+2}, \quad k = 0, 1, \dots, m-1,\end{aligned}$$

and

$$\begin{aligned}\mathbf{q}_{5k} &= \left( \frac{d_{k+1}}{d_k+d_{k+1}}\mathbf{r}_{2k} + \frac{d_k}{d_k+d_{k+1}}\mathbf{r}_{2k+1} \right) \sigma_{2k} - i h \mathbf{p}_{2k}, \quad k = 0, 1, \dots, m, \\ \mathbf{q}_{5k+1} &= \frac{3}{5}\mathbf{r}_{2k+1}\sigma_{2k} + \frac{2}{5}\left( \frac{d_{k+1}}{d_k+d_{k+1}}\mathbf{r}_{2k} + \frac{d_k}{d_k+d_{k+1}}\mathbf{r}_{2k+1} \right) \sigma_{2k+1} \\ &\quad - i h \left( \frac{3}{5}\mathbf{p}_{2k} + \frac{2}{5}\mathbf{p}_{2k+1} \right), \quad k = 0, 1, \dots, m-1, \\ \mathbf{q}_{5k+2} &= \frac{3}{10}\mathbf{r}_{2k+2}\sigma_{2k} + \frac{3}{5}\mathbf{r}_{2k+1}\sigma_{2k+1} + \frac{1}{10}\left( \frac{d_{k+1}}{d_k+d_{k+1}}\mathbf{r}_{2k} + \frac{d_k}{d_k+d_{k+1}}\mathbf{r}_{2k+1} \right) \sigma_{2k+2} \\ &\quad - i h \left( \frac{3}{10}\mathbf{p}_{2k} + \frac{3}{5}\mathbf{p}_{2k+1} + \frac{1}{10}\mathbf{p}_{2k+2} \right), \quad k = 0, 1, \dots, m-1, \\ \mathbf{q}_{5k+3} &= \frac{1}{10}\left( \frac{d_{k+2}}{d_{k+1}+d_{k+2}}\mathbf{r}_{2k+2} + \frac{d_{k+1}}{d_{k+1}+d_{k+2}}\mathbf{r}_{2k+3} \right) \sigma_{2k} + \frac{3}{5}\mathbf{r}_{2k+2}\sigma_{2k+1} + \frac{3}{10}\mathbf{r}_{2k+1}\sigma_{2k+2} \\ &\quad - i h \left( \frac{1}{10}\mathbf{p}_{2k} + \frac{3}{5}\mathbf{p}_{2k+1} + \frac{3}{10}\mathbf{p}_{2k+2} \right), \quad k = 0, 1, \dots, m-1, \\ \mathbf{q}_{5k+4} &= \frac{2}{5}\left( \frac{d_{k+2}}{d_{k+1}+d_{k+2}}\mathbf{r}_{2k+2} + \frac{d_{k+1}}{d_{k+1}+d_{k+2}}\mathbf{r}_{2k+3} \right) \sigma_{2k+1} + \frac{3}{5}\mathbf{r}_{2k+2}\sigma_{2k+2} \\ &\quad - i h \left( \frac{2}{5}\mathbf{p}_{2k+1} + \frac{3}{5}\mathbf{p}_{2k+2} \right), \quad k = 0, 1, \dots, m-1,\end{aligned}$$

with  $d_0 := 0$  and  $d_{m+1} := 0$ .

The weights and control points of the offset curves  $\mathbf{r}_h(t)$  of the clamped quintic PH B-Spline curves ( $n = 2$ ) from (56) in section 5.2 are given by:

$$\begin{aligned}\gamma_{8k} &= \frac{4}{9}\sigma_{3k} + \frac{5}{9}\frac{\sigma_{3k+1}d_k + \sigma_{3k}d_{k+1}}{d_k+d_{k+1}}, \quad k = 0, 1, \dots, m-1, \\ \gamma_{8k+1} &= \frac{5}{9}\frac{\sigma_{3k+1}d_k + \sigma_{3k}d_{k+1}}{d_k+d_{k+1}} + \frac{4}{9}\sigma_{3k+1}, \quad k = 0, 1, \dots, m-1, \\ \gamma_{8k+2} &= \frac{5}{18}\frac{\sigma_{3k+1}d_k + \sigma_{3k}d_{k+1}}{d_k+d_{k+1}} + \frac{5}{9}\sigma_{3k+1} + \frac{1}{6}\sigma_{3k+2}, \quad k = 0, 1, \dots, m-2, \\ \gamma_{8k+3} &= \frac{5}{42}\frac{\sigma_{3k+1}d_k + \sigma_{3k}d_{k+1}}{d_k+d_{k+1}} + \frac{10}{21}\sigma_{3k+1} + \frac{5}{14}\sigma_{3k+2} + \frac{1}{21}\sigma_{3k+3}, \quad k = 0, 1, \dots, m-2, \\ \gamma_{8k+4} &= \frac{5}{126}\frac{\sigma_{3k+1}d_k + \sigma_{3k}d_{k+1}}{d_k+d_{k+1}} + \frac{20}{63}\sigma_{3k+1} + \frac{10}{21}\sigma_{3k+2} + \frac{10}{63}\sigma_{3k+3} + \frac{1}{126}\frac{\sigma_{3k+4}d_{k+1} + \sigma_{3k+3}d_{k+2}}{d_{k+1}+d_{k+2}}, \quad k = 0, 1, \dots, m-2, \\ \gamma_{8k+5} &= \frac{1}{126}\frac{\sigma_{3k+1}d_k + \sigma_{3k}d_{k+1}}{d_k+d_{k+1}} + \frac{10}{63}\sigma_{3k+1} + \frac{10}{21}\sigma_{3k+2} + \frac{20}{63}\sigma_{3k+3} + \frac{5}{126}\frac{\sigma_{3k+4}d_{k+1} + \sigma_{3k+3}d_{k+2}}{d_{k+1}+d_{k+2}}, \quad k = 0, 1, \dots, m-2, \\ \gamma_{8k+6} &= \frac{1}{21}\sigma_{3k+1} + \frac{5}{14}\sigma_{3k+2} + \frac{10}{21}\sigma_{3k+3} + \frac{5}{42}\frac{\sigma_{3k+4}d_{k+1} + \sigma_{3k+3}d_{k+2}}{d_{k+1}+d_{k+2}}, \quad k = 0, 1, \dots, m-2, \\ \gamma_{8k+7} &= \frac{1}{6}\sigma_{3k+2} + \frac{5}{9}\sigma_{3k+3} + \frac{5}{18}\frac{\sigma_{3k+4}d_{k+1} + \sigma_{3k+3}d_{k+2}}{d_{k+1}+d_{k+2}}, \quad k = 0, 1, \dots, m-2,\end{aligned}$$

and

$$\begin{aligned}\mathbf{q}_{8k} &= \frac{4}{9}\left( \frac{\mathbf{r}_{3k+2}d_k^2 + 2\mathbf{r}_{3k+1}d_k d_{k+1} + \mathbf{r}_{3k}d_{k+1}^2}{(d_k+d_{k+1})^2} \right) \sigma_{3k} + \frac{5}{9}\left( \frac{\mathbf{r}_{3k+1}d_k + \mathbf{r}_{3k}d_{k+1}}{d_k+d_{k+1}} \right) \left( \frac{\sigma_{3k+1}d_k + \sigma_{3k}d_{k+1}}{d_k+d_{k+1}} \right) \\ &\quad - i h \left( \frac{4}{9}\mathbf{p}_{3k} + \frac{5}{9}\left( \frac{\mathbf{p}_{3k+1}d_k + \mathbf{p}_{3k}d_{k+1}}{d_k+d_{k+1}} \right) \right), \quad k = 0, 1, \dots, m-1, \\ \mathbf{q}_{8k+1} &= \frac{5}{9}\left( \frac{\mathbf{r}_{3k+2}d_k + \mathbf{r}_{3k+1}d_{k+1}}{d_k+d_{k+1}} \right) \left( \frac{\sigma_{3k+1}d_k + \sigma_{3k}d_{k+1}}{d_k+d_{k+1}} \right) + \frac{4}{9}\left( \frac{\mathbf{r}_{3k+2}d_k^2 + 2\mathbf{r}_{3k+1}d_k d_{k+1} + \mathbf{r}_{3k}d_{k+1}^2}{(d_k+d_{k+1})^2} \right) \sigma_{3k+1} \\ &\quad - i h \left( \frac{4}{9}\mathbf{p}_{3k+1} + \frac{5}{9}\left( \frac{\mathbf{p}_{3k+1}d_k + \mathbf{p}_{3k}d_{k+1}}{d_k+d_{k+1}} \right) \right), \quad k = 0, 1, \dots, m-1,\end{aligned}$$

$$\begin{aligned}
\mathbf{q}_{8k+2} &= \frac{5}{18} \mathbf{r}_{3k+2} \left( \frac{\sigma_{3k+1} d_k + \sigma_{3k} d_{k+1}}{d_k + d_{k+1}} \right) + \frac{5}{9} \left( \frac{\mathbf{r}_{3k+2} d_k + \mathbf{r}_{3k+1} d_{k+1}}{d_k + d_{k+1}} \right) \sigma_{3k+1} \\
&+ \frac{1}{6} \left( \frac{\mathbf{r}_{3k+2} d_k^2 + 2\mathbf{r}_{3k+1} d_k d_{k+1} + \mathbf{r}_{3k} d_{k+1}^2}{(d_k + d_{k+1})^2} \right) \sigma_{3k+2} \\
&- i h \left( \frac{1}{6} \mathbf{p}_{3k+2} + \frac{5}{9} \mathbf{p}_{3k+1} + \frac{5}{18} \left( \frac{\mathbf{p}_{3k+1} d_k + \mathbf{p}_{3k} d_{k+1}}{d_k + d_{k+1}} \right) \right), \quad k = 0, 1, \dots, m-2, \\
\mathbf{q}_{8k+3} &= \frac{5}{42} \mathbf{r}_{3k+3} \left( \frac{\sigma_{3k+1} d_k + \sigma_{3k} d_{k+1}}{d_k + d_{k+1}} \right) + \frac{10}{21} \mathbf{r}_{3k+2} \sigma_{3k+1} + \frac{5}{14} \left( \frac{\mathbf{r}_{3k+2} d_k + \mathbf{r}_{3k+1} d_{k+1}}{d_k + d_{k+1}} \right) \sigma_{3k+2} \\
&+ \frac{1}{21} \left( \frac{\mathbf{r}_{3k+2} d_k^2 + 2\mathbf{r}_{3k+1} d_k d_{k+1} + \mathbf{r}_{3k} d_{k+1}^2}{(d_k + d_{k+1})^2} \right) \sigma_{3k+3} \\
&- i h \left( \frac{1}{21} \mathbf{p}_{3k+3} + \frac{5}{14} \mathbf{p}_{3k+2} + \frac{10}{21} \mathbf{p}_{3k+1} + \frac{5}{42} \left( \frac{\mathbf{p}_{3k+1} d_k + \mathbf{p}_{3k} d_{k+1}}{d_k + d_{k+1}} \right) \right), \quad k = 0, 1, \dots, m-2, \\
\mathbf{q}_{8k+4} &= \frac{5}{126} \left( \frac{\mathbf{r}_{3k+4} d_{k+1} + \mathbf{r}_{3k+3} d_{k+2}}{d_{k+1} + d_{k+2}} \right) \left( \frac{\sigma_{3k+1} d_k + \sigma_{3k} d_{k+1}}{d_k + d_{k+1}} \right) \\
&+ \frac{20}{63} \mathbf{r}_{3k+3} \sigma_{3k+1} + \frac{10}{21} \mathbf{r}_{3k+2} \sigma_{3k+2} + \frac{10}{63} \left( \frac{\mathbf{r}_{3k+2} d_k + \mathbf{r}_{3k+1} d_{k+1}}{d_k + d_{k+1}} \right) \sigma_{3k+3} \\
&+ \frac{1}{126} \left( \frac{\mathbf{r}_{3k+2} d_k^2 + 2\mathbf{r}_{3k+1} d_k d_{k+1} + \mathbf{r}_{3k} d_{k+1}^2}{(d_k + d_{k+1})^2} \right) \left( \frac{\sigma_{3k+4} d_{k+1} + \sigma_{3k+3} d_{k+2}}{d_{k+1} + d_{k+2}} \right) \\
&- i h \left( \frac{1}{126} \left( \frac{\mathbf{p}_{3k+4} d_{k+1} + \mathbf{p}_{3k+3} d_{k+2}}{d_{k+1} + d_{k+2}} \right) + \frac{10}{63} \mathbf{p}_{3k+3} + \frac{10}{21} \mathbf{p}_{3k+2} + \frac{20}{63} \mathbf{p}_{3k+1} + \frac{5}{126} \left( \frac{\mathbf{p}_{3k+1} d_k + \mathbf{p}_{3k} d_{k+1}}{d_k + d_{k+1}} \right) \right), \\
&k = 0, 1, \dots, m-2, \\
\mathbf{q}_{8k+5} &= \frac{1}{126} \left( \frac{\mathbf{r}_{3k+5} d_{k+1}^2 + 2\mathbf{r}_{3k+4} d_{k+1} d_{k+2} + \mathbf{r}_{3k+3} d_{k+2}^2}{(d_{k+1} + d_{k+2})^2} \right) \left( \frac{\sigma_{3k+1} d_k + \sigma_{3k} d_{k+1}}{d_k + d_{k+1}} \right) \\
&+ \frac{10}{63} \left( \frac{\mathbf{r}_{3k+4} d_{k+1} + \mathbf{r}_{3k+3} d_{k+2}}{d_{k+1} + d_{k+2}} \right) \sigma_{3k+1} + \frac{10}{21} \mathbf{r}_{3k+3} \sigma_{3k+2} + \frac{20}{63} \mathbf{r}_{3k+2} \sigma_{3k+3} \\
&+ \frac{5}{126} \left( \frac{\mathbf{r}_{3k+2} d_k + \mathbf{r}_{3k+1} d_{k+1}}{d_k + d_{k+1}} \right) \left( \frac{\sigma_{3k+4} d_{k+1} + \sigma_{3k+3} d_{k+2}}{d_{k+1} + d_{k+2}} \right) \\
&- i h \left( \frac{5}{126} \left( \frac{\mathbf{p}_{3k+4} d_{k+1} + \mathbf{p}_{3k+3} d_{k+2}}{d_{k+1} + d_{k+2}} \right) + \frac{20}{63} \mathbf{p}_{3k+3} + \frac{10}{21} \mathbf{p}_{3k+2} + \frac{10}{63} \mathbf{p}_{3k+1} + \frac{1}{126} \left( \frac{\mathbf{p}_{3k+1} d_k + \mathbf{p}_{3k} d_{k+1}}{d_k + d_{k+1}} \right) \right), \\
&k = 0, 1, \dots, m-2, \\
\mathbf{q}_{8k+6} &= \frac{1}{21} \left( \frac{\mathbf{r}_{3k+5} d_{k+1}^2 + 2\mathbf{r}_{3k+4} d_{k+1} d_{k+2} + \mathbf{r}_{3k+3} d_{k+2}^2}{(d_{k+1} + d_{k+2})^2} \right) \sigma_{3k+1} + \frac{5}{14} \left( \frac{\mathbf{r}_{3k+4} d_{k+1} + \mathbf{r}_{3k+3} d_{k+2}}{d_{k+1} + d_{k+2}} \right) \sigma_{3k+2} \\
&+ \frac{10}{21} \mathbf{r}_{3k+3} \sigma_{3k+3} + \frac{5}{42} \mathbf{r}_{3k+2} \left( \frac{\sigma_{3k+4} d_{k+1} + \sigma_{3k+3} d_{k+2}}{d_{k+1} + d_{k+2}} \right) \\
&- i h \left( \frac{5}{42} \left( \frac{\mathbf{p}_{3k+4} d_{k+1} + \mathbf{p}_{3k+3} d_{k+2}}{d_{k+1} + d_{k+2}} \right) + \frac{10}{21} \mathbf{p}_{3k+3} + \frac{5}{14} \mathbf{p}_{3k+2} + \frac{1}{21} \mathbf{p}_{3k+1} \right), \quad k = 0, 1, \dots, m-2, \\
\mathbf{q}_{8k+7} &= \frac{1}{6} \left( \frac{\mathbf{r}_{3k+5} d_{k+1}^2 + 2\mathbf{r}_{3k+4} d_{k+1} d_{k+2} + \mathbf{r}_{3k+3} d_{k+2}^2}{(d_{k+1} + d_{k+2})^2} \right) \sigma_{3k+2} + \frac{5}{9} \left( \frac{\mathbf{r}_{3k+4} d_{k+1} + \mathbf{r}_{3k+3} d_{k+2}}{d_{k+1} + d_{k+2}} \right) \sigma_{3k+3} \\
&+ \frac{5}{18} \mathbf{r}_{3k+3} \left( \frac{\sigma_{3k+4} d_{k+1} + \sigma_{3k+3} d_{k+2}}{d_{k+1} + d_{k+2}} \right) - i h \left( \frac{5}{18} \left( \frac{\mathbf{p}_{3k+4} d_{k+1} + \mathbf{p}_{3k+3} d_{k+2}}{d_{k+1} + d_{k+2}} \right) + \frac{5}{9} \mathbf{p}_{3k+3} + \frac{1}{6} \mathbf{p}_{3k+2} \right), \\
&k = 0, 1, \dots, m-2.
\end{aligned}$$

The weights and control points of the offset curves  $\mathbf{r}_h(t)$  of the closed cubic PH B-Spline curves ( $n = 1$ ) from (58) in section 5.3 are given by:

$$\begin{aligned}
\gamma_0 &= \gamma_1 = \gamma_2 = \gamma_3 = 0, \\
\gamma_4 &= \frac{d_0}{10(d_0 + d_1)} \sigma_1, \\
\gamma_5 &= \frac{3}{10} \sigma_1, \\
\gamma_6 &= \frac{3}{5} \sigma_1, \\
\gamma_{5k+7} &= \sigma_{2k+1}, \quad k = 0, 1, \dots, m+1, \\
\gamma_{5k+8} &= \frac{3}{5} \sigma_{2k+1} + \frac{2}{5} \sigma_{2k+2}, \quad k = 0, 1, \dots, m, \\
\gamma_{5k+9} &= \frac{3}{10} \sigma_{2k+1} + \frac{3}{5} \sigma_{2k+2} + \frac{1}{10} \sigma_{2k+3}, \quad k = 0, 1, \dots, m, \\
\gamma_{5k+10} &= \frac{1}{10} \sigma_{2k+1} + \frac{3}{5} \sigma_{2k+2} + \frac{3}{10} \sigma_{2k+3}, \quad k = 0, 1, \dots, m, \\
\gamma_{5k+11} &= \frac{2}{5} \sigma_{2k+2} + \frac{3}{5} \sigma_{2k+3}, \quad k = 0, 1, \dots, m, \\
\gamma_{5m+13} &= \frac{3}{5} \sigma_{2m+3}, \\
\gamma_{5m+14} &= \frac{3}{10} \sigma_{2m+3},
\end{aligned}$$

$$\begin{aligned}\gamma_{5m+15} &= \frac{d_{m+4}}{10(d_{m+3}+d_{m+4})} \sigma_{2m+3}, \\ \gamma_{5m+16} &= \gamma_{5m+17} = \gamma_{5m+18} = \gamma_{5m+19} = 0,\end{aligned}$$

and

$$\begin{aligned}\mathbf{q}_0 &= \mathbf{q}_1 = \mathbf{q}_2 = \mathbf{q}_3 = 0, \\ \mathbf{q}_4 &= \frac{d_0}{10(d_0+d_1)} (\mathbf{r}_0 \sigma_1 - i h \mathbf{p}_1), \\ \mathbf{q}_5 &= \frac{3}{10} (\mathbf{r}_0 \sigma_1 - i h \mathbf{p}_1), \\ \mathbf{q}_6 &= \frac{3}{5} (\mathbf{r}_1 \sigma_1 - i h \mathbf{p}_1), \\ \mathbf{q}_{5k+7} &= \left( \frac{d_{k+2}}{d_{k+1}+d_{k+2}} \mathbf{r}_{2k+1} + \frac{d_{k+1}}{d_{k+1}+d_{k+2}} \mathbf{r}_{2k+2} \right) \sigma_{2k+1} - i h \mathbf{p}_{2k+1}, \quad k = 0, 1, \dots, m+1 \\ \mathbf{q}_{5k+8} &= \frac{3}{5} \mathbf{r}_{2k+2} \sigma_{2k+1} + \frac{2}{5} \left( \frac{d_{k+2}}{d_{k+1}+d_{k+2}} \mathbf{r}_{2k+1} + \frac{d_{k+1}}{d_{k+1}+d_{k+2}} \mathbf{r}_{2k+2} \right) \sigma_{2k+2} \\ &\quad - i h \left( \frac{3}{5} \mathbf{p}_{2k+1} + \frac{2}{5} \mathbf{p}_{2k+2} \right), \quad k = 0, 1, \dots, m, \\ \mathbf{q}_{5k+9} &= \frac{3}{10} \mathbf{r}_{2k+3} \sigma_{2k+1} + \frac{3}{5} \mathbf{r}_{2k+2} \sigma_{2k+2} + \frac{1}{10} \left( \frac{d_{k+2}}{d_{k+1}+d_{k+2}} \mathbf{r}_{2k+1} + \frac{d_{k+1}}{d_{k+1}+d_{k+2}} \mathbf{r}_{2k+2} \right) \sigma_{2k+3} \\ &\quad - i h \left( \frac{3}{10} \mathbf{p}_{2k+1} + \frac{3}{5} \mathbf{p}_{2k+2} + \frac{1}{10} \mathbf{p}_{2k+3} \right), \quad k = 0, 1, \dots, m, \\ \mathbf{q}_{5k+10} &= \frac{1}{10} \left( \frac{d_{k+3}}{d_{k+2}+d_{k+3}} \mathbf{r}_{2k+3} + \frac{d_{k+2}}{d_{k+2}+d_{k+3}} \mathbf{r}_{2k+4} \right) \sigma_{2k+1} + \frac{3}{5} \mathbf{r}_{2k+3} \sigma_{2k+2} + \frac{3}{10} \mathbf{r}_{2k+2} \sigma_{2k+3} \\ &\quad - i h \left( \frac{1}{10} \mathbf{p}_{2k+1} + \frac{3}{5} \mathbf{p}_{2k+2} + \frac{3}{10} \mathbf{p}_{2k+3} \right), \quad k = 0, 1, \dots, m, \\ \mathbf{q}_{5k+11} &= \frac{2}{5} \left( \frac{d_{k+3}}{d_{k+2}+d_{k+3}} \mathbf{r}_{2k+3} + \frac{d_{k+2}}{d_{k+2}+d_{k+3}} \mathbf{r}_{2k+4} \right) \sigma_{2k+2} + \frac{3}{5} \mathbf{r}_{2k+3} \sigma_{2k+3} \\ &\quad - i h \left( \frac{2}{5} \mathbf{p}_{2k+2} + \frac{3}{5} \mathbf{p}_{2k+3} \right), \quad k = 0, 1, \dots, m, \\ \mathbf{q}_{5m+13} &= \frac{3}{5} (\mathbf{r}_{2m+4} \sigma_{2m+3} - i h \mathbf{p}_{2m+3}), \\ \mathbf{q}_{5m+14} &= \frac{3}{10} (\mathbf{r}_{2m+5} \sigma_{2m+3} - i h \mathbf{p}_{2m+3}), \\ \mathbf{q}_{5m+15} &= \frac{d_{m+4}}{10(d_{m+3}+d_{m+4})} (\mathbf{r}_{2m+5} \sigma_{2m+3} - i h \mathbf{p}_{2m+3}), \\ \mathbf{q}_{5m+16} &= \mathbf{q}_{5m+17} = \mathbf{q}_{5m+18} = \mathbf{q}_{5m+19} = 0.\end{aligned}$$

**Remark 9.** Since  $\sigma_0 = \sigma_{2m+4} = 0$  as well as  $\mathbf{p}_0 = \mathbf{p}_{2m+4} = 0$ , the values of  $\zeta_3^{0,0}$ ,  $\zeta_4^{0,0}$ ,  $\zeta_5^{1,0}$ ,  $\zeta_6^{1,0}$ ,  $\zeta_6^{2,0}$  and  $\zeta_{5m+13}^{2m+3,2m+4}$ ,  $\zeta_{5m+13}^{2m+4,2m+4}$ ,  $\zeta_{5m+14}^{2m+4,2m+4}$ ,  $\zeta_{5m+15}^{2m+5,2m+4}$ ,  $\zeta_{5m+16}^{2m+5,2m+4}$  are indeed not used to compute  $\gamma_k$  and  $\mathbf{q}_k$ ,  $k = 0, \dots, 5m+19$ .

The weights and control points of the offset curves  $\mathbf{r}_h(t)$  of the closed quintic PH B-Spline curves ( $n = 2$ ) from (60) in section 5.4 are given by:

$$\begin{aligned}\gamma_0 &= \gamma_1 = \gamma_2 = \gamma_3 = \gamma_4 = \gamma_5 = \gamma_6 = 0, \\ \gamma_7 &= \frac{1}{126} \left( \frac{d_0}{d_0+d_1} \right)^2 \left( \frac{d_1}{d_1+d_2} \right) \sigma_2, \\ \gamma_8 &= \frac{5}{126} \left( \frac{d_0}{d_0+d_1} \right) \left( \frac{d_1}{d_1+d_2} \right) \sigma_2, \\ \gamma_9 &= \frac{5}{42} \left( \frac{d_1}{d_1+d_2} \right) \sigma_2, \\ \gamma_{10} &= \frac{5}{18} \left( \frac{d_1}{d_1+d_2} \right) \sigma_2, \\ \gamma_{8k+11} &= \frac{4}{9} \sigma_{3k+1} + \frac{5}{9} \frac{\sigma_{3k+2} d_{k+1} + \sigma_{3k+1} d_{k+2}}{d_{k+1}+d_{k+2}}, \quad k = 0, \dots, m+3, \\ \gamma_{8k+12} &= \frac{5}{9} \frac{\sigma_{3k+2} d_{k+1} + \sigma_{3k+1} d_{k+2}}{d_{k+1}+d_{k+2}} + \frac{4}{9} \sigma_{3k+2}, \quad k = 0, \dots, m+3, \\ \gamma_{8k+13} &= \frac{5}{18} \frac{\sigma_{3k+2} d_{k+1} + \sigma_{3k+1} d_{k+2}}{d_{k+1}+d_{k+2}} + \frac{5}{9} \sigma_{3k+2} + \frac{1}{6} \sigma_{3k+3}, \quad k = 0, \dots, m+2, \\ \gamma_{8k+14} &= \frac{5}{42} \frac{\sigma_{3k+2} d_{k+1} + \sigma_{3k+1} d_{k+2}}{d_{k+1}+d_{k+2}} + \frac{10}{21} \sigma_{3k+2} + \frac{5}{14} \sigma_{3k+3} + \frac{1}{21} \sigma_{3k+4}, \quad k = 0, \dots, m+2, \\ \gamma_{8k+15} &= \frac{5}{126} \frac{\sigma_{3k+2} d_{k+1} + \sigma_{3k+1} d_{k+2}}{d_{k+1}+d_{k+2}} + \frac{20}{63} \sigma_{3k+2} + \frac{10}{21} \sigma_{3k+3} + \frac{10}{63} \sigma_{3k+4} + \frac{1}{126} \frac{\sigma_{3k+5} d_{k+2} + \sigma_{3k+4} d_{k+3}}{d_{k+2}+d_{k+3}}, \quad k = 0, \dots, m+2, \\ \gamma_{8k+16} &= \frac{1}{126} \frac{\sigma_{3k+2} d_{k+1} + \sigma_{3k+1} d_{k+2}}{d_{k+1}+d_{k+2}} + \frac{10}{63} \sigma_{3k+2} + \frac{10}{21} \sigma_{3k+3} + \frac{20}{63} \sigma_{3k+4} + \frac{5}{126} \frac{\sigma_{3k+5} d_{k+2} + \sigma_{3k+4} d_{k+3}}{d_{k+2}+d_{k+3}}, \quad k = 0, \dots, m+2, \\ \gamma_{8k+17} &= \frac{1}{21} \sigma_{3k+2} + \frac{5}{14} \sigma_{3k+3} + \frac{10}{21} \sigma_{3k+4} + \frac{5}{42} \frac{\sigma_{3k+5} d_{k+2} + \sigma_{3k+4} d_{k+3}}{d_{k+2}+d_{k+3}}, \quad k = 0, \dots, m+2, \\ \gamma_{8k+18} &= \frac{1}{6} \sigma_{3k+3} + \frac{5}{9} \sigma_{3k+4} + \frac{5}{18} \frac{\sigma_{3k+5} d_{k+2} + \sigma_{3k+4} d_{k+3}}{d_{k+2}+d_{k+3}}, \quad k = 0, \dots, m+2,\end{aligned}$$

$$\begin{aligned}
\gamma_{8m+37} &= \frac{5}{18} \left( \frac{d_{m+5}}{d_{m+4}+d_{m+5}} \right) \sigma_{3m+10}, \\
\gamma_{8m+38} &= \frac{5}{42} \left( \frac{d_{m+5}}{d_{m+4}+d_{m+5}} \right) \sigma_{3m+10}, \\
\gamma_{8m+39} &= \frac{5}{126} \left( \frac{d_{m+6}}{d_{m+5}+d_{m+6}} \right) \left( \frac{d_{m+5}}{d_{m+4}+d_{m+5}} \right) \sigma_{3m+10}, \\
\gamma_{8m+40} &= \frac{1}{126} \left( \frac{d_{m+6}}{d_{m+5}+d_{m+6}} \right)^2 \left( \frac{d_{m+5}}{d_{m+4}+d_{m+5}} \right) \sigma_{3m+10}, \\
\gamma_{8m+41} &= \gamma_{8m+42} = \gamma_{8m+43} = \gamma_{8m+44} = \gamma_{8m+45} = \gamma_{8m+46} = \gamma_{8m+47} = 0
\end{aligned}$$

and

$$\begin{aligned}
\mathbf{q}_0 &= \mathbf{q}_1 = \mathbf{q}_2 = \mathbf{q}_3 = \mathbf{q}_4 = \mathbf{q}_5 = \mathbf{q}_6 = 0, \\
\mathbf{q}_7 &= \frac{1}{126} \left( \frac{d_0}{d_0+d_1} \right)^2 \left( \frac{d_1}{d_1+d_2} \right) (\mathbf{r}_0 \sigma_2 - i h \mathbf{p}_2), \\
\mathbf{q}_8 &= \frac{5}{126} \left( \frac{d_0}{d_0+d_1} \right) \left( \frac{d_1}{d_1+d_2} \right) (\mathbf{r}_0 \sigma_2 - i h \mathbf{p}_2), \\
\mathbf{q}_9 &= \frac{5}{42} \left( \frac{d_1}{d_1+d_2} \right) (\mathbf{r}_0 \sigma_2 - i h \mathbf{p}_2), \\
\mathbf{q}_{10} &= \frac{5}{18} \left( \frac{d_1}{d_1+d_2} \right) (\mathbf{r}_1 \sigma_2 - i h \mathbf{p}_2), \\
\mathbf{q}_{8k+11} &= \frac{4}{9} \left( \frac{\mathbf{r}_{3k+3} d_{k+1}^2 + 2\mathbf{r}_{3k+2} d_{k+1} d_{k+2} + \mathbf{r}_{3k+1} d_{k+2}^2}{(d_{k+1}+d_{k+2})^2} \right) \sigma_{3k+1} + \frac{5}{9} \left( \frac{\mathbf{r}_{3k+2} d_{k+1} + \mathbf{r}_{3k+1} d_{k+2}}{d_{k+1}+d_{k+2}} \right) \left( \frac{\sigma_{3k+2} d_{k+1} + \sigma_{3k+1} d_{k+2}}{d_{k+1}+d_{k+2}} \right) \\
&\quad - i h \left( \frac{4}{9} \mathbf{p}_{3k+1} + \frac{5}{9} \left( \frac{\mathbf{p}_{3k+2} d_{k+1} + \mathbf{p}_{3k+1} d_{k+2}}{d_{k+1}+d_{k+2}} \right) \right), \quad k = 0, \dots, m+3, \\
\mathbf{q}_{8k+12} &= \frac{5}{9} \left( \frac{\mathbf{r}_{3k+3} d_{k+1} + \mathbf{r}_{3k+2} d_{k+2}}{d_{k+1}+d_{k+2}} \right) \left( \frac{\sigma_{3k+2} d_{k+1} + \sigma_{3k+1} d_{k+2}}{d_{k+1}+d_{k+2}} \right) + \frac{4}{9} \left( \frac{\mathbf{r}_{3k+3} d_{k+1}^2 + 2\mathbf{r}_{3k+2} d_{k+1} d_{k+2} + \mathbf{r}_{3k+1} d_{k+2}^2}{(d_{k+1}+d_{k+2})^2} \right) \sigma_{3k+2} \\
&\quad - i h \left( \frac{4}{9} \mathbf{p}_{3k+2} + \frac{5}{9} \left( \frac{\mathbf{p}_{3k+2} d_{k+1} + \mathbf{p}_{3k+1} d_{k+2}}{d_{k+1}+d_{k+2}} \right) \right), \quad k = 0, \dots, m+3, \\
\mathbf{q}_{8k+13} &= \frac{5}{18} \mathbf{r}_{3k+3} \left( \frac{\sigma_{3k+2} d_{k+1} + \sigma_{3k+1} d_{k+2}}{d_{k+1}+d_{k+2}} \right) + \frac{5}{9} \left( \frac{\mathbf{r}_{3k+3} d_{k+1} + \mathbf{r}_{3k+2} d_{k+2}}{d_{k+1}+d_{k+2}} \right) \sigma_{3k+2} \\
&\quad + \frac{1}{6} \left( \frac{\mathbf{r}_{3k+3} d_{k+1}^2 + 2\mathbf{r}_{3k+2} d_{k+1} d_{k+2} + \mathbf{r}_{3k+1} d_{k+2}^2}{(d_{k+1}+d_{k+2})^2} \right) \sigma_{3k+3} \\
&\quad - i h \left( \frac{1}{6} \mathbf{p}_{3k+3} + \frac{5}{9} \mathbf{p}_{3k+2} + \frac{5}{18} \left( \frac{\mathbf{p}_{3k+2} d_{k+1} + \mathbf{p}_{3k+1} d_{k+2}}{d_{k+1}+d_{k+2}} \right) \right), \quad k = 0, \dots, m+2, \\
\mathbf{q}_{8k+14} &= \frac{5}{42} \mathbf{r}_{3k+4} \left( \frac{\sigma_{3k+2} d_{k+1} + \sigma_{3k+1} d_{k+2}}{d_{k+1}+d_{k+2}} \right) + \frac{10}{21} \mathbf{r}_{3k+3} \sigma_{3k+2} + \frac{5}{14} \left( \frac{\mathbf{r}_{3k+3} d_{k+1} + \mathbf{r}_{3k+2} d_{k+2}}{d_{k+1}+d_{k+2}} \right) \sigma_{3k+3} \\
&\quad + \frac{1}{21} \left( \frac{\mathbf{r}_{3k+3} d_{k+1}^2 + 2\mathbf{r}_{3k+2} d_{k+1} d_{k+2} + \mathbf{r}_{3k+1} d_{k+2}^2}{(d_{k+1}+d_{k+2})^2} \right) \sigma_{3k+4} \\
&\quad - i h \left( \frac{1}{21} \mathbf{p}_{3k+4} + \frac{5}{14} \mathbf{p}_{3k+3} + \frac{10}{21} \mathbf{p}_{3k+2} + \frac{5}{42} \left( \frac{\mathbf{p}_{3k+2} d_{k+1} + \mathbf{p}_{3k+1} d_{k+2}}{d_{k+1}+d_{k+2}} \right) \right), \quad k = 0, \dots, m+2, \\
\mathbf{q}_{8k+15} &= \frac{5}{126} \left( \frac{\mathbf{r}_{3k+5} d_{k+2} + \mathbf{r}_{3k+4} d_{k+3}}{d_{k+2}+d_{k+3}} \right) \left( \frac{\sigma_{3k+2} d_{k+1} + \sigma_{3k+1} d_{k+2}}{d_{k+1}+d_{k+2}} \right) \\
&\quad + \frac{20}{63} \mathbf{r}_{3k+4} \sigma_{3k+2} + \frac{10}{21} \mathbf{r}_{3k+3} \sigma_{3k+3} + \frac{10}{63} \left( \frac{\mathbf{r}_{3k+3} d_{k+1} + \mathbf{r}_{3k+2} d_{k+2}}{d_{k+1}+d_{k+2}} \right) \sigma_{3k+4} \\
&\quad + \frac{1}{126} \left( \frac{\mathbf{r}_{3k+3} d_{k+1}^2 + 2\mathbf{r}_{3k+2} d_{k+1} d_{k+2} + \mathbf{r}_{3k+1} d_{k+2}^2}{(d_{k+1}+d_{k+2})^2} \right) \left( \frac{\sigma_{3k+5} d_{k+2} + \sigma_{3k+4} d_{k+3}}{d_{k+2}+d_{k+3}} \right) \\
&\quad - i h \left( \frac{1}{126} \left( \frac{\mathbf{p}_{3k+5} d_{k+2} + \mathbf{p}_{3k+4} d_{k+3}}{d_{k+2}+d_{k+3}} \right) + \frac{10}{63} \mathbf{p}_{3k+4} + \frac{10}{21} \mathbf{p}_{3k+3} + \frac{20}{63} \mathbf{p}_{3k+2} + \frac{5}{126} \left( \frac{\mathbf{p}_{3k+2} d_{k+1} + \mathbf{p}_{3k+1} d_{k+2}}{d_{k+1}+d_{k+2}} \right) \right), \\
&\quad k = 0, \dots, m+2, \\
\mathbf{q}_{8k+16} &= \frac{1}{126} \left( \frac{\mathbf{r}_{3k+6} d_{k+3}^2 + 2\mathbf{r}_{3k+5} d_{k+2} d_{k+3} + \mathbf{r}_{3k+4} d_{k+3}^2}{(d_{k+2}+d_{k+3})^2} \right) \left( \frac{\sigma_{3k+2} d_{k+1} + \sigma_{3k+1} d_{k+2}}{d_{k+1}+d_{k+2}} \right) \\
&\quad + \frac{10}{63} \left( \frac{\mathbf{r}_{3k+5} d_{k+2} + \mathbf{r}_{3k+4} d_{k+3}}{d_{k+2}+d_{k+3}} \right) \sigma_{3k+2} + \frac{10}{21} \mathbf{r}_{3k+4} \sigma_{3k+3} + \frac{20}{63} \mathbf{r}_{3k+3} \sigma_{3k+4} \\
&\quad + \frac{5}{126} \left( \frac{\mathbf{r}_{3k+3} d_{k+1} + \mathbf{r}_{3k+2} d_{k+2}}{d_{k+1}+d_{k+2}} \right) \left( \frac{\sigma_{3k+5} d_{k+2} + \sigma_{3k+4} d_{k+3}}{d_{k+2}+d_{k+3}} \right) \\
&\quad - i h \left( \frac{5}{126} \left( \frac{\mathbf{p}_{3k+5} d_{k+2} + \mathbf{p}_{3k+4} d_{k+3}}{d_{k+2}+d_{k+3}} \right) + \frac{20}{63} \mathbf{p}_{3k+4} + \frac{10}{21} \mathbf{p}_{3k+3} + \frac{10}{63} \mathbf{p}_{3k+2} + \frac{1}{126} \left( \frac{\mathbf{p}_{3k+2} d_{k+1} + \mathbf{p}_{3k+1} d_{k+2}}{d_{k+1}+d_{k+2}} \right) \right), \\
&\quad k = 0, \dots, m+2, \\
\mathbf{q}_{8k+17} &= \frac{1}{21} \left( \frac{\mathbf{r}_{3k+6} d_{k+3}^2 + 2\mathbf{r}_{3k+5} d_{k+2} d_{k+3} + \mathbf{r}_{3k+4} d_{k+3}^2}{(d_{k+2}+d_{k+3})^2} \right) \sigma_{3k+2} + \frac{5}{14} \left( \frac{\mathbf{r}_{3k+5} d_{k+2} + \mathbf{r}_{3k+4} d_{k+3}}{d_{k+2}+d_{k+3}} \right) \sigma_{3k+3} \\
&\quad + \frac{10}{21} \mathbf{r}_{3k+4} \sigma_{3k+4} + \frac{5}{42} \mathbf{r}_{3k+3} \left( \frac{\sigma_{3k+5} d_{k+2} + \sigma_{3k+4} d_{k+3}}{d_{k+2}+d_{k+3}} \right) \\
&\quad - i h \left( \frac{5}{42} \left( \frac{\mathbf{p}_{3k+5} d_{k+2} + \mathbf{p}_{3k+4} d_{k+3}}{d_{k+2}+d_{k+3}} \right) + \frac{10}{21} \mathbf{p}_{3k+4} + \frac{5}{14} \mathbf{p}_{3k+3} + \frac{1}{21} \mathbf{p}_{3k+2} \right), \quad k = 0, \dots, m+2,
\end{aligned}$$



$$\begin{aligned}
\mathbf{q}_{8k+18} &= \frac{1}{6} \left( \frac{\mathbf{r}_{3k+6}d_{k+2}^2 + 2\mathbf{r}_{3k+5}d_{k+2}d_{k+3} + \mathbf{r}_{3k+4}d_{k+3}^2}{(d_{k+2}+d_{k+3})^2} \right) \sigma_{3k+3} + \frac{5}{9} \left( \frac{\mathbf{r}_{3k+5}d_{k+2} + \mathbf{r}_{3k+4}d_{k+3}}{d_{k+2}+d_{k+3}} \right) \sigma_{3k+4} \\
&+ \frac{5}{18} \mathbf{r}_{3k+4} \left( \frac{\sigma_{3k+5}d_{k+2} + \sigma_{3k+4}d_{k+3}}{d_{k+2}+d_{k+3}} \right) - i\hbar \left( \frac{5}{18} \left( \frac{\mathbf{p}_{3k+5}d_{k+2} + \mathbf{p}_{3k+4}d_{k+3}}{d_{k+2}+d_{k+3}} \right) + \frac{5}{9} \mathbf{p}_{3k+4} + \frac{1}{6} \mathbf{p}_{3k+3} \right), \\
&k = 0, \dots, m+2, \\
\mathbf{q}_{8m+37} &= \frac{5}{18} \left( \frac{d_{m+5}}{d_{m+4}+d_{m+5}} \right) \left( \mathbf{r}_{3m+12} \sigma_{3m+10} - i\hbar \mathbf{p}_{3m+10} \right), \\
\mathbf{q}_{8m+38} &= \frac{5}{42} \left( \frac{d_{m+5}}{d_{m+4}+d_{m+5}} \right) \left( \mathbf{r}_{3m+13} \sigma_{3m+10} - i\hbar \mathbf{p}_{3m+10} \right), \\
\mathbf{q}_{8m+39} &= \frac{5}{126} \left( \frac{d_{m+6}}{d_{m+5}+d_{m+6}} \right) \left( \frac{d_{m+5}}{d_{m+4}+d_{m+5}} \right) \left( \mathbf{r}_{3m+13} \sigma_{3m+10} - i\hbar \mathbf{p}_{3m+10} \right), \\
\mathbf{q}_{8m+40} &= \frac{1}{126} \left( \frac{d_{m+6}}{d_{m+5}+d_{m+6}} \right)^2 \left( \frac{d_{m+5}}{d_{m+4}+d_{m+5}} \right) \left( \mathbf{r}_{3m+13} \sigma_{3m+10} - i\hbar \mathbf{p}_{3m+10} \right), \\
\mathbf{q}_{8m+41} &= \mathbf{q}_{8m+42} = \mathbf{q}_{8m+43} = \mathbf{q}_{8m+44} = \mathbf{q}_{8m+45} = \mathbf{q}_{8m+46} = \mathbf{q}_{8m+47} = 0.
\end{aligned}$$

**Remark 10.** Since  $\sigma_0 = \sigma_1 = \sigma_{3m+11} = \sigma_{3m+12} = 0$  as well as  $\mathbf{p}_0 = \mathbf{p}_1 = \mathbf{p}_{3m+11} = \mathbf{p}_{3m+12} = 0$ , the values of  $\zeta_5^{0,0}$ ,  $\zeta_6^{0,0}$ ,  $\zeta_6^{0,1}$ ,  $\zeta_7^{0,0}$ ,  $\zeta_7^{0,1}$ ,  $\zeta_8^{0,1}$ ,  $\zeta_8^{1,0}$ ,  $\zeta_9^{0,1}$ ,  $\zeta_9^{1,0}$ ,  $\zeta_9^{1,1}$ ,  $\zeta_9^{2,0}$ ,  $\zeta_{10}^{1,0}$ ,  $\zeta_{10}^{1,1}$ ,  $\zeta_{10}^{2,0}$ ,  $\zeta_{10}^{2,1}$ ,  $\zeta_{10}^{3,0}$  and  $\zeta_{8m+37}^{3m+10,3m+12}$ ,  $\zeta_{8m+37}^{3m+11,3m+11}$ ,  $\zeta_{8m+37}^{3m+11,3m+12}$ ,  $\zeta_{8m+37}^{3m+12,3m+11}$ ,  $\zeta_{8m+37}^{3m+12,3m+12}$ ,  $\zeta_{8m+37}^{3m+13,3m+11}$ ,  $\zeta_{8m+37}^{3m+13,3m+12}$ ,  $\zeta_{8m+37}^{3m+13,3m+11}$ ,  $\zeta_{8m+37}^{3m+13,3m+12}$ ,  $\zeta_{8m+37}^{3m+13,3m+11}$ ,  $\zeta_{8m+37}^{3m+13,3m+12}$ ,  $\zeta_{8m+37}^{3m+13,3m+11}$ ,  $\zeta_{8m+37}^{3m+13,3m+12}$ ,  $\zeta_{8m+37}^{3m+13,3m+11}$ ,  $\zeta_{8m+37}^{3m+13,3m+12}$  are indeed not used to compute  $\gamma_k$  and  $\mathbf{q}_k$ ,  $k = 0, \dots, 8m+47$ .

## Section 6

In section 6 the coefficients of the symmetric matrices  $A = (a_{i,j})_{i,j=0,1,2}$  and  $B = (b_{i,j})_{i,j=0,1,2}$  in equation (72) read as follows:

$$\begin{aligned}
a_{0,0} &= \mathbf{p}_{0,x}^* - \mathbf{p}_{1,x}^* + \frac{1}{5} (a \mathbf{d}_{0,x} + (1-a) \mathbf{d}_{1,x}) - \frac{1}{240u_0^2} \kappa_0^2 a^2 (3-a) (u_0^2 + v_0^2)^4 - \frac{1}{240u_3^2} \kappa_1^2 (1-a)^2 (2+a) (u_3^2 + v_3^2)^4 \\
&+ \frac{1}{80u_0u_3} \kappa_0 \kappa_1 a (1-a) (u_0^2 u_3^2 + v_0^2 v_3^2 + u_3^2 v_0^2 + u_0^2 v_3^2)^2 - \frac{1}{60u_0} \kappa_0 a (u_0^2 + v_0^2)^2 (a(4-a)v_0 + (1-a)^2 v_3) \\
&+ \frac{1}{60u_3} \kappa_1 (1-a) (u_3^2 + v_3^2)^2 (a^2 v_0 + (1-a)(3+a)v_3),
\end{aligned}$$

$$a_{0,1} = \frac{1}{10} \left[ \frac{1}{3u_0} (a(4-a)(u_0^2 - v_0^2) + (1-a)^2 (u_0 u_3 - v_0 v_3)) - \frac{1}{6u_0} \kappa_0 v_0 a (3-a) (u_0^2 + v_0^2)^2 + \frac{1}{4u_0u_3} \kappa_1 v_0 (1-a) (u_3^2 + v_3^2)^2 \right],$$

$$a_{0,2} = \frac{1}{10} \left[ \frac{1}{6u_3^2} \kappa_1 v_3 (a+2) (1-a) (u_3^2 + v_3^2)^2 - \frac{1}{4u_0u_3} \kappa_0 a v_3 (u_0^2 + v_0^2)^2 + \frac{1}{3u_3} (a^2 (u_0 u_3 - v_0 v_3) + (a+3) (1-a) (u_3^2 - v_3^2)) \right],$$

$$a_{1,1} = \frac{(u_0^2 - v_0^2)(3-a)}{15u_0^2}, \quad a_{1,2} = \frac{u_0 u_3 - v_0 v_3}{10u_0 u_3}, \quad a_{2,2} = \frac{(u_3^2 - v_3^2)(2+a)}{15u_3^2},$$

$$\begin{aligned}
b_{0,0} &= \mathbf{p}_{0,y}^* - \mathbf{p}_{1,y}^* + \frac{1}{5} (a \mathbf{d}_{0,y} + (1-a) \mathbf{d}_{1,y}) + \frac{1}{60u_0} \kappa_0 a (u_0^2 + v_0^2)^2 [a(4-a)u_0 + (1-a)^2 u_3] \\
&- \frac{1}{60u_3} \kappa_1 (1-a) (u_3^2 + v_3^2)^2 [u_3 (1-a)(3+a) + u_0 a^2],
\end{aligned}$$

$$b_{0,1} = \frac{1}{2} \left[ \frac{1}{30u_0} \kappa_0 a (3-a) (u_0^2 + v_0^2)^2 + \frac{1}{15u_0} (1-a)^2 (u_0 v_3 + u_3 v_0) + \frac{1}{15} 2a v_0 (4-a) - \frac{1}{20u_3} \kappa_1 (1-a) (u_3^2 + v_3^2)^2 \right],$$

$$b_{0,2} = \frac{1}{20} \left[ \frac{1}{3u_3} (2a^2 (u_3 v_0 + u_0 v_3) + 4u_3 v_3 (3+a) (1-a) - \kappa_1 (2+a) (1-a) (u_3^2 + v_3^2)^2) + \frac{1}{2u_0} \kappa_0 a (u_0^2 + v_0^2)^2 \right],$$

$$b_{1,1} = \frac{2v_0(3-a)}{15u_0}, \quad b_{1,2} = \frac{v_0 u_3 + u_0 v_3}{10u_0 u_3}, \quad b_{2,2} = \frac{2v_3(2+a)}{15u_3}.$$